DESIGN OF AN ALL OPTICAL CLOCK RECOVERY SYSTEM USING NON LINEAR OPTICAL LOOP MIRRORS

by

MAJOR KAMESH KUMAR

DEPARTMENT OF ELECTRICAL ENGINEERING

INDIAN INSTITUTE OF TECHNOLOGY KANPUR

March, 1999

DESIGN OF AN ALL OPTICAL CLOCK RECOVERY SYSTEM USING NON LINEAR OPTICAL LOOP MIRRORS

A Thesis Submitted

in Partial Fulfilment of the Requirements

for the Degree of

MASTER OF TECHNOLOGY

BY

MAJOR KAMESH KUMAR

to the

DEPARTMENT OF ELECTRICAL ENGINEERING

I.I.T KANPUR

MARCH 1999

CERTIFICATE

It is certified that the work contained in the thesis entitled "**DESIGN OF AN ALL OPTICAL CLOCK RECOVERY SYSTEM USING NON LINEAR OPTICAL LOOP MIRRORS**" by Major Kamesh Kumar, has been carried out under my supervision and this work has not been submitted elsewhere for a degree.

Dr Anjan K Ghosh
Professor
Department of Electrical Engineering
I.I.T Kanpur

ABSTRACT

Clock recovery is an important part of all communication system. To use the enormous bandwidth provided by optical fiber, and to meet requirement of high speed switching in the next generation of photonic networks, all optical processing is essential. All optical clock recovery system is an important part of all optical regeneration of signals to perform, both amplitude and timing restoration. All optical clock recovery is also required in other all optical processing for demultiplexing and wavelength translation.

Actively mode locked fiber lasers using Nonlinear optical loop mirror (NOLM) offer a novel method of all optical clock recovery with a high data rate in excess of Gbit/s. In this thesis we have studied all optical clock recovery using nonlinear optical loop mirror scheme proposed by British Telecom and derived the design equations (which were not disclosed by British Telecom group in their publication) with the aim of validating the experimental result and modeling the optical clock recovery circuit.

ACKNOWLEDGEMENT

I wish to express my sincere gratitude to my thesis supervisor, Dr AK Ghosh, for his esteemed guidance during the course of my thesis work. I am grateful to him to have given me an insight into the realm of Optical Communications. Inspite of his busy schedule, he was always available whenever I required help.

My sincere thanks are due Major T S Bains, Major S P Sira and Major Anurag Chandra with whom I had many a fruitful talk relating to my thesis work.

I am grateful to Shailesh Tiwari for his unstinting help during the writing of this thesis. I am deeply indebted to my wife Nisha and son Utkarsh, who stood by me and supported me all through the course.

I am indebted to my parents whose inspiration and upbringing have brought me to the portals of my present achievement.

Contents

LIST OF FIGURES

CHAPTER 1

INTRODUCTION

1.1 Requirement Of Clock Recovery

Any data sent over a communication channel, either in electronic or optical domain, is corrupted by noise, jitter, attenuation, and pulse spreading and inter-symbol interference [1.1].

The received pulses are processed in a receiver or regenerator to determine the original data sent. A regenerative repeater or a receiver performs three functions: equalization, timing and decision making. The equalizer shapes the received pulses to compensate for the effects of amplitude and phase distortions produced by transmission characteristics of channel. The timing circuitry generates a periodic pulse train i.e. the clock from the received pulses. The clock is used for sampling the equalized pulses at the instants of time where the eye pattern of the received pulses shows maximum opening [1.1]. The decision device is enabled at the sampling times determined by the timing circuitry.

Clock recovery is the process of generating a periodic train of pulses at the original bit rate from encoded data. The clock is used to correctly decode the data. Decoding of data implies getting back the original data pulse stream. To correctly decode the data the receiver should be synchronized to transmitter. Synchronization of bit, word and frame at the receiver is achieved by receiver clock by deciding bits at the time these have been sent. To use the transmission bandwidth available in a channel fully, data from various users such as, digital signals from computer, digitized voice signals and digitized facsimile and television signals are multiplexed into a single data stream at a high bit rate. Clock information is also required for both multiplexing and demultiplexing of channels.

1.2 Evolving Fiber Optic Communication and all optical processing

The optical carrier frequency in the range 10^{13} to 10^{16} Hz yields a far greater transmission bandwidth than metallic transmission lines. The entire bandwidth offered by optics has not been exploited due to limitation of electronics. Today's single mode fiber can provide a huge transmission bandwidth of the order of 25 THz. All optical processing technology fully exploits the enormous bandwidth of fibers and can support a processing speed in excess of 100 Gb/s [1.2-1.3].

In the present scenario of existing telecommunication network, fiber optics communication will be required in different fields of applications such as, high speed interconnection of computers in local area network or metropolitan area networks, or interconnection between telephone exchanges in wide area networks. These networks require technique for high speed packet routing and multiple access to provide a large traffic.

A concentration of telecommunication traffic occurs at switching nodes where multiplexing, demultiplexing and switching of channels take place. This happens because of switching in electronic domain and 'electronic bottleneck' i.e. the low speed of response upto a few 100 Mbit/s of electronic circuits and devices restricting the overall data rate. All optical switches which use optical signal processing and fiber link capable of carrying data at high data rate has to be used to overcome electronic bottleneck.

To exploit enormous bandwidth available in optical domain and to meet the requirement of the evolving fiber optics communication all optical processing has been resorted and processing speed upto 100 Gbit/s all optical signal processing is reported [1.4]. Optical processing or switching opens up possibilities for realizing fiber optics communication network with a high throughput.

To meet the evolving fiber optics communication data at more than 100 Gbit/s, response of few ps or even less for photonic devices are required. One of the important optical signal processing for lightwave communication system is all optical clock recovery, which does not use electronic devices and can generate clock at data rate upto 100Gbits/s [1.6].

To achieve all optical signal processing we need controlling light with light in a nonlinear optical medium. Nonlinear optical loop mirror (NOLM) is an optical fiber based all optical switch where one optical signal controls the other optical signal by non-linear cross phase modulation (XPM). These switches together with fiber optic long haul lines can provide a backbone for an all-optical communication system with as little electronics as possible. NOLM can be used in various devices such as Optical Demultiplexer, All optical Switch and in Clock recovery circuit using mode-locking phenomena of fiber laser [1.5-1.8]. NOLM based devices have advantages of high speed, low loss, large optical bandwidth and low polarization sensitivity.

1.3 Proposed All Optical clock recovery scheme

In 1992, British Telecom. Experimentally demonstrated an NOLM based all optical clock recovery system. The block diagram of the all-optical clock recovery circuit using NOLM is shown in fig 1.1 and 1.2 [1.9-1.10]. As shown in fig 1.1 and 1.2, an all-optical clock recovery consists of a laser cavity comprising of a non-linear optical modulator (NOM), filter, amplifier, isolator, and directional couplers. Active mode locking phenomenon was used to make a mode locked fiber laser that generated the clock pulses from a set of data pulse triggers. The clock pulses generated from Data pulses by British Telecom Experiment is shown in fig 1.3.

The laser cavity consists of a simple dispersion shifted fiber functioning as NOM. The laser cavity and transmission fiber share the NOM. Data pulses having high power are used to introduce a periodic phase modulation because of XPM. Thus active mode locking is achieved. The experiment demonstrated the mode-locked pulses obtained and measured its pulse width. These mode –locked pulses are clock pulses of data pulses.

In fig 1.2, the NOM consisted of a NOLM and a fiber grating and an Erbium Doped Amplifier (EDFA) to make a laser cavity. The NOLM introduces a periodic amplitude modulation on lasing signal. Data pulses introduce a nonlinear XPM on lasing signal as both the signals co-propagate in NOLM. NOLM has functioned here as an amplitude modulator and a reflector. The data pulses increase the reflectivity of NOLM. Due to amplitude modulation of lasing signal, the data mode locks the laser and hence

clock pulses are extracted. British Telecom experimented with three sequences 1111..., 1010..., and pseudo random bit sequence (PRBS) and extracted clock from these data sequences [1.7-1.9].

1.4 Overview of Workdone

In the schemes for all-optical clock recovery proposed by British Telecom, only a few experimental results were given but very little scientific information in the form of equation or working principle was revealed. As the schemes proposed seem promising, we have tried to analyze in order to derive basic design issues. We have analyzed transient phenomena of an active harmonically mode locked fiber ring laser to understand the basic method of extracting clock form the proposed scheme. We have also studied different components used in the scheme and its use in the schemes. We have also derived equations as regard to design issues such as spectral width, number of pulses required to modelock the laser, pulse width, peak power required and length of NOM. We have also suggested improvement such as inclusion of filters for removing the noise due to supermode competition. We surveyed other optical clock recovery schemes to compare the different phenomena for an optical clock recovery scheme.

1.5 Overview of thesis

In chapter 2 we have derived basic theory of NOLM, one of the design component of proposed clock recovery scheme. We have also carried out a detailed study of literature on NOLM and its application to various optical devices. The main advantages of NOLM have been brought out for its use in all optical processing.

In chapter 3 we have carried out a detailed study of Mode locking of laser including active and passive mode locking .We have also compared two schemes to bring out advantages of active mode locking.

In chapter 4 we have derived basic equation for an understanding of working principles of transient phenomena of active modelocking. Computer simulation has also been done to show evolution of mode locked pulses i.e. clock pulses from the scheme.

We have also derived equation related to spectral width, pulsewidth of extracted clock in stable mode of laser in proposed scheme. We have also derived basic condition to modelock the fiber laser and requirement of number of pulses and its power. We have also suggested including Fabry Perot filters for improving the performance of the scheme. We have also derived equation to show variation of pulse width of clock pulses with number of round trips of laser before stability condition is achieved.

In chapter 5, we conclude that British Telecom has suggested a novel all optical clock recovery scheme in which an optical data stream is used to mode lock a fiber laser and hence clock is recovered. We have derived basic equations regarding spectral width and pulse width of clock. We have also investigated into basic design issues of the scheme. We have observed that there exists a simple relationship between the repetition rate and cavity frequency for mode locking. The laser output forms a replica of any driving pattern and is thus optically programmed .The theory can be extended to evaluate the performance of optically programmablemode locked laser.

REFERENCES

1.1 Simon Haykin, "Introduction to analog and digital communication," John Wiley and Sons (SEA) Pte Ltd., Singapore.,1994.

1.2 A. Takada and M. Saruwatari, "100 Gbit/s optical signal generation by time division multiplication of modulated and compressed pulses from gain switched distributed feedback (DFB) laser diode, "Electron Lett., 24, pp. 1406-1408, Nov.1988.

1.3 H. Izadpanah, D. Chen, C. Lin, M.A. Saifi, W.I.Way, A.Yi-Yan, J.L.Gimlett, "Distortion free amplification of high speed test patterns upto 100 Gbit/s with erbium doped amplifiers, "Electron Lett., 27, pp. 196-198., Jan 1991.

1.4 Glesk, J. P. Sokoloff and P. R. Prucnal, "Demonstration of all optical demultiplexing of TDM data at 250 Gbit/s," Electron Lett., 30, pp.339-341, February 1994.

1.5 K. Suzuki, K.Iwatuski, S.Nishiand M.Saruwatari, "160 Gbit/s single polarisation subpicosecond transform limited pulse signal demultiplexing using ultrafast optical loop mirror including MQW travelling wave semiconductor laser amplifier, "Electron Lett., 30, pp. 660-661, April 1994.

1.6 S. Kawanishi, H. Takara, K.Uchiyama, M.Saruwatari and T. Kitoh, "Fully time division multiplexed 100 Gbit/s optical transmission experiment, " Electron Lett., 29 (25), pp. 2211-2212, December 1993.

1.7 A. D. Ellis, K. Smith and D.M.Patrick, "All optical clock recovery at bit rates upto 40 Gbit/s, "Electron Lett., 29, pp.1323-1324, July 1993.

1.8 J. K. Lucek and K.Smith, "All optical signal generator, "Opt. Lett., 18, pp. 1226-1228, August 1993.

1.9 E. J. Greer and K. Smith, "All optical FM mode –locking of fibre laser," Electron Lett., 28, pp. 1741-1743, August 1992.

1.10B. P. Nelson, K. Smith and K. J. Blow, "Mode-locked Erbium fiber laser using all-optical nonlinear loop modulator, "Electron Lett., 28, pp. 656-657, March 1992.

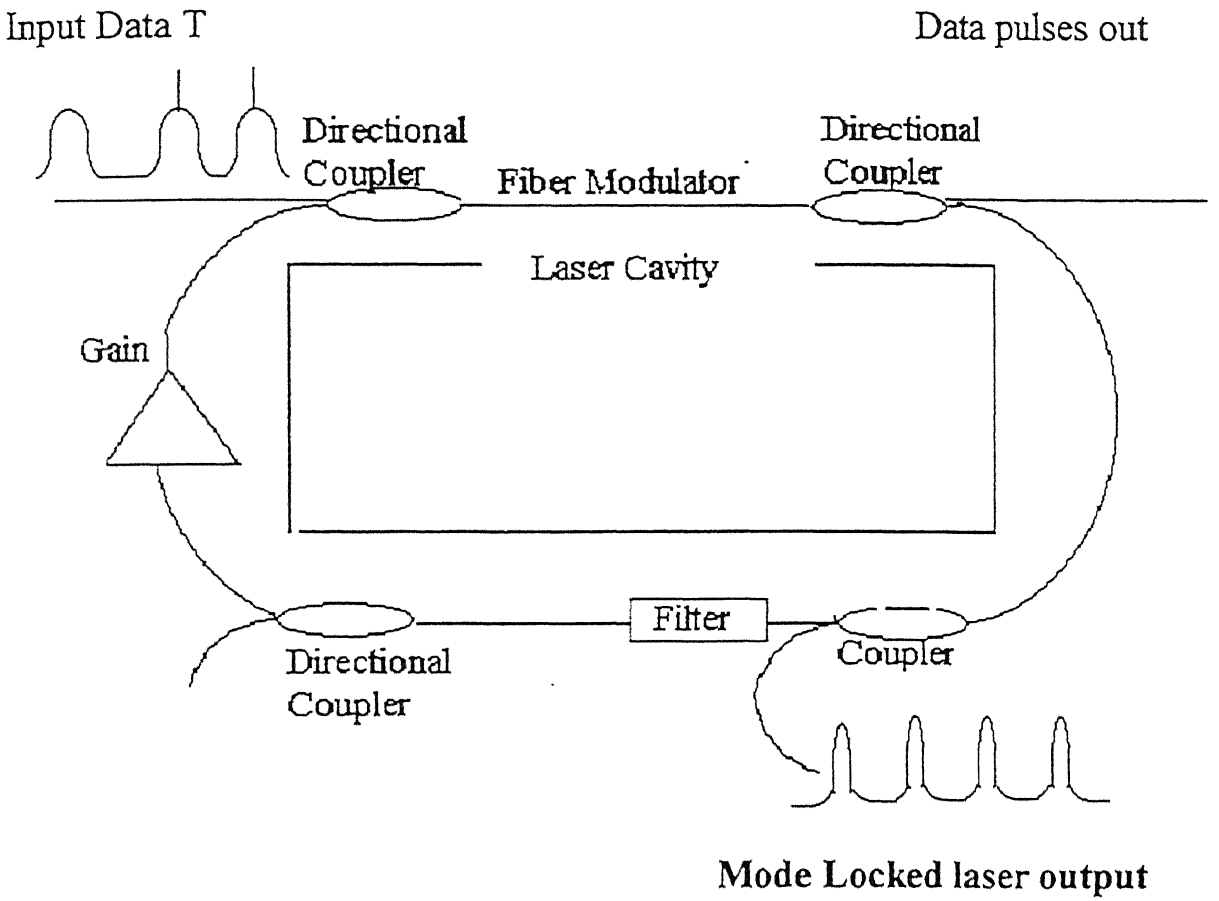

Fig 1.1 Experimental diagram of All Optical Clock Recovery Circuit [1.9]

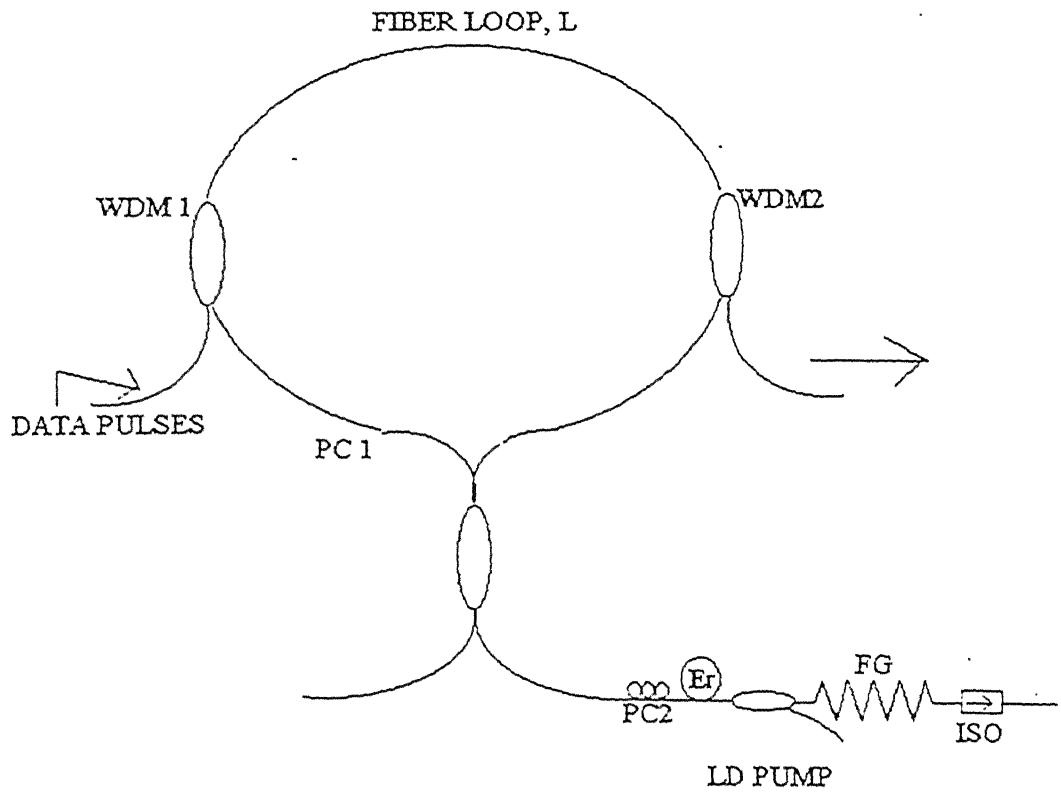

LEGEND	
PC	: POLARISATION CONTROLLER
FG	: FIBER GRATING
LD PUMP	: LASER DIODE PUMP
ISO	: ISOLATOR
Er	: ERBIUM DOPED FIBER

Fig 1.2 Experimental configuration of mode-locked erbium laser [1.10]

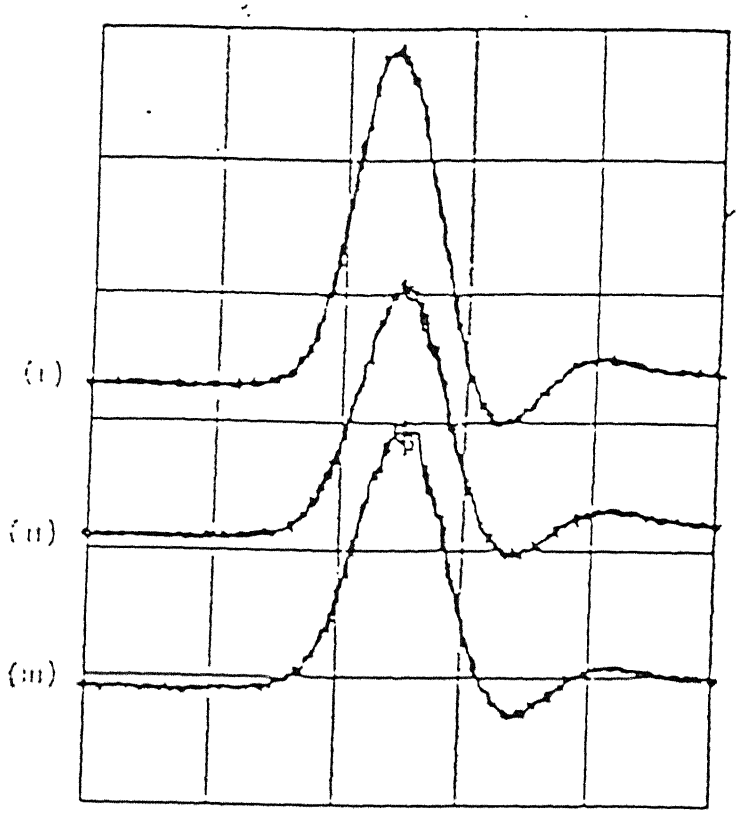

Fig 1.3 Output of experimental clock recovery circuit displayed on fast photodiode/sampling oscilloscope [1.9]

(i) 111... input

(ii) 1010.. input

(iii) PRBS input

Horizontal scale: 40 ps/division

NON LINEAR OPTICAL LOOP MIRROR (NOLM)

NOLM is a very promising all optical switching device. Optical networks of future generation requires all optical processing to avoid the electrical processing bottleneck. NOLM is used to carry out one of the most important function i.e. to regularize or regenerate multiplexed optical data stream in terms of their pulse period, pulse shape and wavelength in the optical domain. Unevenness in pulse period, shape and wavelength in the multiplexed optical data stream arise from two sources.

1. Passive multiplexing where original data stream consisting of optical short pulses that come from different points are combined using a passive optical coupler at the outport of the optical nodes [2.1].
2. Long distance fiber transmission where distortion, random modulation of pulse frequency shapes pulse (this results in increased pulse to pulse timing jitter).
3. The signal to noise ratio degradation occur due to Group Velocity Distribution (GVD) and spontaneous emission generated by the optical amplifier used.

To achieve all optical processing for data regeneration, NOLM switches were devised. NOLM is a complete all optical switch where one optical signal controls another optical signal using nonlinear response of the medium. These nonlinear effects are Kerr effect, self phase modulation (SPM), cross phase modulation (XPM). Kerr effect is due to a particular non-linearity where the refractive index of the medium depends on the intensity of the light propagating into it. Since the speed of the light in a medium depends on refractive index, hence phase velocity of the beam depends both on its own intensity and the intensity of any other beam present.

$n = n_0 + n_2 I$, where n represents the total refractive index of the medium , n_0 is the linear Part (i.e. RI in the absence of the light), n_2 is the Kerr coefficient and I is the intensity of light . In presence of the other beam present, the RI seen by one beam depends on I of a second beam. These two phenomena are known as SPM and XPM.

The change in RI and correspondingly change in phase is used in NOLM to produce output depending on phase shift of optical field. NOLM can be considered as folded Mach Zehnder Interferometer.

2.1 Basic Theory

First optical signal is applied by use of one of the polarization maintaining coupler 1(PMC 1) to a second PMC i.e. PMC2 as shown in fig 2.1. In PMC 1 and PMC2, polarization of input signal is maintained and couplers split power equally. PMC 2 splits the signal into two counter-propagating signals that travel on one of the fiber's axes of polarization. The two propagating signals normally traverse an identical path and destructively interfere at the Y outport of PMC 2. The loop thus functions as a mirror rather than as a loop with the applied signal reflected out of PMC1 [2.2, 2.3].

If a second optical signal (port B) were injected into the loop on the other polarization axis by means of a polarization beam splitter coupler (PBS1), then clockwise portion of interferometer signal would experience cross phase modulation (XPM) and travel ever so slightly slower than the counterclockwise propagating interferometer signal. With proper design the two portion of the interferometer signal can be made to interfere constructively, causing all of the signal to be transmitted out of Y outport. Thus device functions as a loop rather than a mirror with the applied power supply signal directed out of the other arm of the PMC1. Hence the input signal can be used to make the device function either as a mirror or as a loop and thus direct the optical power supply signal to one of two possible outports. Hence the device is called as a Non Linear Optical Loop Mirror. The brief mathematical analysis is reproduced from reference [2.4].

2.1.1 Mathematical Analysis

Coupler Model is taken as

$$\begin{pmatrix} E_3 \\ E_4 \end{pmatrix} = \sqrt{1-\gamma} \begin{pmatrix} \sqrt{1-\kappa} & j\sqrt{\kappa} \\ j\sqrt{\kappa} & \sqrt{1-\kappa} \end{pmatrix} \tag{2.1}$$

κ -coupling constant

γ -excess scattering loss of coupler

PMC1 and PMC 2 are assumed to be identical with parameters (0.5,0) and both PBS to be identical with (0.5,0). In PBS response depends upon polarization of incoming

signal. If signal is polarized along one axis, it will couple immediately but if it is polarized along the orthogonal axis then it won't couple. (i.e. κ=0). We take signal at port A is polarized along one axis such that it doesn't couple at all and signal at port B is polarized along orthogonal axis such that it couples completely. Polarization controllers (PC) adjust the proper polarization state of the signals immediately before entering PBS. So signal at port B enters the fiber loop via PBS1 and leaves the loop via PBS2. It doesn't come to port X or Y directly [2.3,2.4].

The signal at port A is split by PMC2 into two parts and they rotate in opposite direction along same PMBF and recombine in PMC2. If the signal at port B is absent, the phase change of counter rotating signal depends on length of fiber loop; RI and nonlinear effect like SPM.

Phase change is given by

$$\phi_c = \frac{2\pi}{\lambda}\left[n_0 + \frac{n_2}{A_{eff}} P_c\right] l \qquad (2.2)$$

$$\phi_a = \frac{2\pi}{\lambda}\left[n_0 + \frac{n_2}{A_{eff}} P_a\right] l \qquad (2.3)$$

ϕ_c - Phase change of clockwise rotating signal while travelling the loop

ϕ_a - Phase change of anticlockwise rotating signal while travelling the loop.

λ - Wavelength of the carrier signal

n_0 - refractive index in the absence of nonlinear effect

n_2 - nonlinear Kerr coefficient

l - length of fiber loop

A_{eff} - Effective core area of fiber.

P_c - Power of clockwise rotating signal $= \frac{P_A}{4}$

P_a - Power of anticlockwise rotating signal $= \frac{P_A}{4}$

Since PMCs split power equally κ_1 =1/2, $P_c = P_a$ hence ϕ_c and ϕ_a are equal and they interfere constructively at port Y and destructively at port X and all power comes through output port Y and no power at port X.

But if the signal at port B is present, XPM takes place. Signal at port B travels only with clockwise rotating signal and imparts asymmetric phase change to clockwise

rotating signal via XPM. But it doesn't affect anticlockwise rotating signal in the presence of signal at port B. Phase changes are given by

$$\phi_a = \frac{2\pi l}{\lambda}\left[n_o + \frac{n_2}{A_{eff}}\frac{P_A}{4}\right] \tag{2.4}$$

$$\phi_c = \frac{2\pi l}{\lambda}\left[n_o + \frac{n_2}{A_{eff}}\left(\frac{P_A}{4} + \frac{2}{3}P_B\right)\right] \tag{2.5}$$

P_B = power of signal at port B.

By manipulating different parameters such that difference between ϕ_c and ϕ_a becomes then constructive and destructive interference takes place and all power comes out through port X. Then it works as a NOLM. For a given setup we can achieve switching by varying power of signal at port B.

Taking the coupler model as described earlier, expressions for power at port X and Y are derived (Reference 2.4) as

$$P_X = P_A\left[1 - \cos^2\left(\frac{\phi_c - \phi_a}{2}\right)\right] \tag{2.6}$$

$$P_Y = \frac{P_A}{2}\cos^2\left(\frac{\phi_c - \phi_a}{2}\right) \tag{2.7}$$

$$\phi_a = \frac{2\pi l}{\lambda}\left[n_o + \frac{n_2}{A_{eff}}\frac{P_A}{4}\right] \tag{2.8}$$

$$\phi_c = \frac{2\pi l}{\lambda}\left[n_o + \frac{n_2}{A_{eff}}\left(\frac{P_A}{2} + \frac{2}{3}P_B\right)\right] \tag{2.9}$$

$$\frac{\phi_c - \phi_a}{2} = \frac{\pi l}{\lambda}\frac{n_2}{A_{eff}}\frac{2}{3}P_B \tag{2.10}$$

Condition for switching is given by

$$\frac{2}{3}P_B = \frac{\lambda}{2n_2 l}A_{eff} \tag{2.11}$$

If the fiber is linear, then expressions get simplified as

$$P_X = 0$$

$$P_Y = \frac{P_A}{2} \tag{2.12}$$

Hence all power comes out through port Y and device works as a mirror.

For κ_1=0 and κ_2=1, all power comes out through port X and NOLM works as a loop.

2.1.2 Ideal behaviour of NOLM

In ideal case for port A signal and for port B signal, all couplers have zero excess loss. Under these assumption power at port X in terms of power at port A and port B for different values of copling constantsof PBS1varies. We find that power at port X and Y vary sinusoidally with power at port B. For larger values of κ_1, min power required for switching decreases. For κ_1 =0.5, P_X or P_Y is a linear function of for P_A for a fixed P_B. With κ_1 =0.5 min power requirement of power at port B becomes independent of P_A and equation becomes

$$\frac{2}{3}P_B = \frac{\lambda}{2n_2 l}A_{eff} \qquad (2.14)$$

With this the value of power at port X becomes exactly zero when X=0. So contrast ratio is defined as

$$\text{Contrast ratio} = \frac{\text{power at port X when X} = 1}{\text{power at port X when X} = 0} \text{ becomes infinite.}$$

2.1.3 Effect of Bireferingence

A nonlinear fiber with zero bireferingence is difficult to find. Because of bireferingence present in fiber, signals polarized along orthogonal axes travel with different velocities. As a result of bireferingence one signal catches up other signal and slips away. The effect of bireferingence in Non linear Fiber Sagnac Interferometer (NSIS) as a special class of NOLM is taken for investigation. The NSIS realizes all optical signal regeneration including timing and amplitude regularizing by switching clock pulses with amplified input signal using a walk off induced wide, square switching window and the sinusoidal power dependent transmittaance [2.3].

The scheme of regenerative repeater is taken as shown in fig 2.2. In regenerative repeater, locally generated optically clock pulses are launched at port A. Clock pulses are stream of pulses of the same shape as original signal pulses. We have used following assumptions:

1. Clock and signal pulses are orthogonally polarized.
2. Loss and group velocity dispersion (GVD) of fiber loop can be neglected
3. Intensity of clock pulse is too small to cause XPM in signal pulse

4. Signal pulses after travelling a long distance may have irregular time lag between signal and clock pulses.

5. Signal pulses may also have uneven pulse period shape and wavelength and have a degraded SNR. Such inconveniences may arise from passive multiplexing at an optical node and long distance fiber transmission using linear optical amplifiers.

6. Signal and clock pulses are Gaussian pulses.

Since clock pulse is always 1, port X varies according to pulse at port B. But the pulse shape is governed by clock pulse which is locally generated and ideal gaussian. So regenerated signal pulse is available at port X.Clock pulse propagating with amplified signal pulses suffer from signal induced XPM. With signal clock walk off clock pulse is modulated by data the input signal pulse carries i.e. regenerated signal pulse only inherits the data, not the unevenness of different pulse parameters.

2.1.4.1 Mathematical Analysis without noise

The detailed analysis is presented in Appendix A. Here only main results are shown. Multiplexed optical data stream is given by

$$P_s(t) = P_s \sum_{-\infty}^{\infty} x_n \exp\left\{-\left(\frac{t-nT}{t_s}\right)^2\right\} \tag{2.15}$$

where $x_n = \{0,1\}$

T = slot width of the data stream

t_s = rms width of gaussian pulse

P_s = signal pulse peak power

$$\phi_c(t) = \begin{cases} M\frac{\sqrt{\pi}}{3} P_s L \frac{t_s}{t_w} \sum_{-\infty}^{\infty} x_n \left\{ erf\left(\frac{t+t_w-nT}{t_s}\right) - erf\left(\frac{t-nT}{t_s}\right)\right\} & t_w \neq 0 \\ M\frac{2}{3} P_s L \left\{ \exp\left(\frac{t-nT}{t_s}\right)^2 \right\} & t_w = 0 \end{cases} \tag{2.16}$$

where ϕ_c = phase change of clockwise signal

$$M = \frac{2\pi n_2}{\lambda A_{eff}} \tag{2.17}$$

$$t_w = \frac{l}{V_s} - \frac{l}{V_c} \tag{2.18}$$

V_s = velocity of signal pulse; V_c = velocity of clock pulse

$$\phi_c(t) = \begin{pmatrix} M\frac{\sqrt{\pi}}{3} P_s L \frac{t_s}{t_w} \\ M\frac{2}{3} P_s L \end{pmatrix} \tag{2.19}$$

when walk off =0 (i.e. $t_w = 0$). ϕ_c has some gaussian profile as signal pulse. But as t_w increases ϕ_c becomes more and more squarer than gaussian profile. For $t_w >> t_s$, a flat plateau of height given by equation is obtained.

If the time slot width T is much smaller than twice the loop transient time (T<<2Ln/c) the signal induced nonlinear phase shift of anticlockwise rotating pulse is constant and proportional to the averaged pump power rather than instantaneous, It is given by

$$\phi_a = M\frac{2\sqrt{\pi}}{3} P_s L \frac{m t_s}{T} \tag{2.20}$$

m=fraction of '1' in data stream $0 \le m \le 1$

Electric field and power equations for regenerated signal pulse are given as

$$\left.\begin{aligned} E_{reg}(t) &= \frac{E_c}{\sqrt{2}} e^{\frac{j(\phi_c+\phi_a)}{2}} \sin\left(\frac{\phi_c - \phi_q}{2}\right) e^{j\left(\frac{\pi}{2}+\delta_l\right)} \\ P_{reg}(t) &= \frac{P_c(t)}{2}\left\{1 - \cos^2\left(\frac{\phi_c - \phi_q}{2}\right)\right\} \end{aligned}\right\} \tag{2.21}$$

2.2 APPLICATION OF NOLM BASED DEVICES AND REVIEW OF PAPERS

NOLM has been used for various applications. We have surveyed some of the applications of NOLM in telecommunication, which are outlined as below.

2.2.1 All optical demultiplexing with NOLM

Figure 2.3 illustrates a typical configuration of two wavelengths NOLM. The NOLM comprises of a 3db coupler for data signal light, a wavelength division multiplexing (WDM) coupler; a polarization controller and dispersion shifted fiber. The optical signal enters the loop through a 3 db coupler and is then split into two equal beams. The control pulses are amplified by using an erbium doped amplifier (EDFA) before they are launched into the loop through a WDM coupler. A polarization controller is inserted into the loop, and it is adjusted such that NOLM acts as a perfect mirror in the absence of the control (clock) signal i.e. the data signal is reflected back to the input port [1.8,2.2,2.4]. However the loop would be also biased with this polarization controller to fully transmit the data signal if no control signal is present. Therefore this biasing condition is equivalent to the loop behaving as a half wave plate [2.5].

In the reflecting mode, if a strong control pulse is present, only the copropagating portion of the weak signal pulse coinciding with the control pulse acquires a nonlinear phase shift through cross phase modulation [2.5] where as the counter propagating portion does not suffer from this control induced phase shift. Thus the recombined signal pulse, overlapping the control pulse at the NOLM input, is switched to the NOLM output. However in the absence of a control pulse, the equal amplitude clockwise and anticlockwise signal beams are recombined in the loop coupler and are reflected to the input port of the NOLM, because both beams exactly experience the same propagation length and result in an identical phase delay. In the transmitting mode, only the signal pulse coinciding with the strong pulse is reflected. Therefore, such a signal pulse is now removed from the output port of the NOLM, and then the complimentary output is obtained [2.5].

The exact nonlinear phase change imposed on the signal is dependent on the control pulsewidth and power as well as the group delay difference (i.e. walk off) between two wavelengths. In order to achieve a pi (π) phase shift in the NOLM due to

XPM, the required peak power for the control pulses (assuming no walk off) is given by P = $k\lambda A_{eff}/n_2 L$ where k ranges from 0.25 to 0.75 depending upon the relative state of polarization between the signal and the control pulse; λ is the wavelength; A_{eff} is the effective fiber mode area; n_2 is the nonlinear coefficient and L is the fiber length.

One of the major problems associated with this device is the walk off between two wavelength light. Increasing the loop length can reduce the switching power but it results in larger walk off which in turn limits the switching speed of a two wavelength NOLM.

To reduce the walk off, the signal and clock wavelength should be chosen to straddle the zero dispersion wavelength of the loop fiber. Moreover the use of two lasers with close wavelengths can further alleviate walk-off. For example when both lasers operate at ~1.53 μm with a 3 nm separation, the walk off is about 2 ps in a14 km dispersion shifted fiber of zero dispersion wavelength at 1.532 μm and this NOLM can demultiplex 62 Gbits/s optical TDM signal stream to the 4 Gbit/s channel data with a penalty of 2.2 db.

2.2.2 Gigabits per second switching using a NOLM -drop and insert

The two wavelengths NOLM as discussed in Sec 2.2.1 has proved to be extremely successful in all optical switching. The switching of 20 Gbit/s pulse train at 2.5Gbit/s has been demonstrated. The schematic diagram of the experiment is shown in fig 2.4.

6.4 km of length of dispersion shifted fiber was used as loop fiber such that the 1.53 μm switching source (a gain switched DFB laser operating at 2.5 GHz) and the 1.56 μm signal source (a 10 GHz mode locked semiconductor laser interleaved to 20 GHz) straddle the dispersion minimum (at 1.545 μm) to minimize the group delay difference between the two wavelengths. With this loop the peak power for complete switching was ~ 160 mW. The gain switched DFB laser pulses were compressed to ~ 16 ps (via the 700 m length of negative group delay dispersion fiber) and amplified to a maximum mean power of ~ 20 mW. The two wavelengths were then combined using a WDM coupler and launched into the loop. The loop was constructed from a coupler, which had a 50:50 coupling ratio for the 1.56 μm and 100:0 for the 1.53 μm switching signal. Polarization controllers provided an adjustable phase bias between the counterpropagating signal

beams and thereby allowed the operation of loop in 'reflecting ' or 'transmitting mode [2.6, 2.7]. In the 'reflecting ' mode the output of the loop was zero in the absence of switching pulses i.e. the whole signal was reflected back. The injection of switching pulses served to switch the signal pulses to the output. In the transmitting mode the situation was reversed and the switched pulses were reflected.

Fig 2.5 shows the 20 GHz interleaved mode locked 1.56 μ m train of pulses incident on the loop mirror .Fig 2.6 shows the switched output with the loop in reflecting mode i.e. only signal pulses are transmitted (every eighth pulse). Fig 2.7 shows the loop biased in transmitting mode and shows every eighth pulse switched out. The loop mirror can be demonstrated as drop and insert function [2.6, 2.7].

2.2.3 Optical Soliton Memory

To achieve speed in al optical processing, rapid access to a high capacity relatively short-term memory is required. For a variety of all optical processing functions, the memory is required to be effectively linked with ultrafast switching elements. Fig 2.8 shows a basic architecture, which permits the memory to be addressed and updated directly via the ultrafast NOLM device [2.8].

A 25 km length of single mode fiber and a single EDFA constitute the linear fiber delay line, which is sandwitched between the two loop -mirror switches (LM 1 and LM 2). The loop mirrors are both operated in two wavelength mode. The loop mirror fiber coupler is chosen to have a coupling ratio of 50:50 at the signal wavelength. the pump pulses are introduced into the loop -mirror via the seperate WDM. Both loop -mirrors are setup in reflecting mode through adjustment of the polarization controllers (PC). Therefore the incoming data (signal pulse) to LM1 is only transmitted through the loop mirror (and into the delay line) when a pump pulse is coincident. the, first loop -mirror can also be used to modulate the incoming data for storage in the delay line . The signal is gated into the delay line (for a time upto round trip time of the delay fiber) by gating the pump pulses. When the data has been admitted to the delay line, multiple pass circulation is achieved between the LM1 and LM2 reflectors. Ultimately the stored data is degraded through pulse jitter effects, which accumulate over the thousands of km of effective length propagation. This may limit the total storage time .The accumulated effects of amplified spontaneous emission and the associated jitter tends to limit the storage time of

the memories. However the memory degradation may be suppressed by the use of signal regeneration techniques within the optical delay line. In this case, one can store data rates well into the tens of gigabits range for times in excess of ~ 10s.

2.2.4 All optical signal regularizing /regeneration using a nonlinear fiber Sagnac interferometer switch with signal clock walk off

Nonlinear Sagnac interferometer switch (NSIS) is a special class of switch. The NSIS realizes all optical signal regeneration, including timing and amplitude regularizing, by switching clock pulses using a walk-off induced, via, square switching window and intensity dependent transmittance of the device. If clock pulses are within the square switching window obtained with signal clock walk off, the clock pulses can be modulated according to data that the input signals carry and retain their temporal and spectral profiles. If clock pulses are prepared to meet the system requirements, which has been discussed in section 2.1, the NSIS can convert input signals that may not satisfy system requirements into high quality output signals [2.3, 2.9].

Two possible applications of NSIS based all optical signal regularizing /regeneration is

1. An all optical demultiplexer with an optical clock as shown in Fig 2.9.
2. An all optical regenerative repeater as shown in fig 2.10.

2.2.5 Sagnac fiber logic gates

The Sagnac fiber logic gate is an ultrafast all-optical fiber three terminal device, which is a special class of NOLM switch. It is based on a fiber sagnac interferometer as shown in fig 2.1. It consists of two polarizations preserving 3 db couplers, two polarization beam splitting couplers and same polarization maintaining fiber. The basic theory of these switches has already been discussed in section 2.1.

The basic functionality of the switch is shown in fig 2.11. The physical layout is shown in fig, The device can be viewed as a mirror that behaves as a loop, given the presence of an optical control pulse. From a switching perspective this device can be viewed as a single pole double throw switch. Given no optical input at B, the signal entering at A will emerge at Y. Given an optical input at B, the signal entering at A will

emerge at X.From a logic perspective this device can be viewed as an AND gate with an input A, an input B and an output X [2.9].

There are differences between sagnac gates and electronic gates. The sagnac gate has a built-in jitter tolerance. Electronic logic gates do not have a similar capability. This feature is very useful in high speed applications.

2.2.6 NOLM oscillator and its injection locking technique for timing clock extraction and demultiplexing

NOLM has been used as a new self oscillatory circuit with an electro optical feedback circuit as shown in fig 2.12 .The oscillator has regenerative and harmonic mode locking chracteristics and generates a picosecond pulse train. By applying an injection locking technique to the laser i.e. by coupling a data signal to the input port of the NOLM opto -electric oscillator 10 GHz clock can be extracted and 80 Gbits /s soliton has been demultiplexed to 10 Gbit/s [2.10].

The NOLM consists of a NOLM and an electro-optical feedback circuit, which has a clock extraction circuit at 10 GHz and an optical control pulse unit. Part of the optical signal transmitted through the NOLM is detected with a high speed photodiode and a 10GHz clock signal is extracted from the harmonic cavity modes using a high Q electrical filter. The sinusoidal clock signal drives a 1.533 micro m DFB LD under a gain switching condition and the generated optical pulse is converted to a 9 ps transform limited pulse with a combination of spectral filtering and linear compression techniques. The 9 ps pulse train at 10 GHz is then amplified and fed back to part of the loop terminal of the NOLM as a feed back optical control pulse. The NOLM consisted of a 6 km long polarization maintained fiber, where the polarization axis of the fiber is rotated by 90 degree and spliced to remove the polarization mode dispersion. The control pulse forms an incident angle of 45 degree with the polarization axis of the NOLM fiber, in order to maintain an equal linear phase shift in both the axes.

2.2.7 All optical, all -fiber circulating shift register with an inverter

Fiber Sagnac interferometer switches has been demonstrated into number of different formats and at extremely high speeds. To build an optical three -terminal device, a control beam must be used that is isolated from a separate signal beam. Two distinct

wavelengths can be used in which case lossless combination and separation of the control and signal can be effected using wavelength -dependent couplers or filters. While the use of different wavelength is an elegant scheme, the complexity grows as the system grows in size since identical device of this type cannot be cascaded. If polarization is used to distinguish the control beam from the signal beam, then stable interferometry can be achieved by controlling the polarization rather than wavelength to discriminate the two signals.

In order to configure the Sagnac loop as a three terminal switch, a control beam is split into the loop, so as to travel in one direction only. The signal beam is split into two equal parts, which traverse the Sagnac loop in both the directions and recombine interferometrically. The signal beam is held in a single linearly polarized state in the loop and the control beam is introduced in an orthogonal state by using a polarization combining coupler. When the control beam is absent, the recombining signal beams interfere at the coupler so that the pulse is reflected back into the input port of the interferometer. With the control beam present, a nonlinear phase shift on the half of the signal beam with which it travels causes the pulse to be transmitted rather than reflected. The reflected output of a Sagnac loop switch is amplified and fed back to provide the control beam after a time delay. This configuration implements the circulating shift register with inverter as shown in fig 2.13. The length of the shift register is determined by the time between pulses and it takes the light to traverse the entire circuit. The clock in this case is provided by pulsed laser, and the power supply is provided by the erbium doped fiber amplifier [2.11].

2.2.8 Ultrafast mode locked laser sources

Using NOLM we can generate ultrafast pulse streams at repetition rates into gigahertz region by using active laser mode locking. In active laser mode locking a periodic (amplitude or phase) perturbation of a laser cavity acts to couple the cavity modes and thereby force the laser to produce a continuous train of ultra-short optical pulses. Fig 1.1 and 1.2 show two types of active mode locked laser as described in chapter1.

2.2.9 Clock Recovery circuit

Actively mode locked laser using NOLM functioning either as an amplitude or phase modulator to ensure active mode locking can be utilized to extract clock as shown in fig 1.1 and 1.2. Mode locking is achieved by using a stream of optical pulses propagated along either a simple length of fiber or in NOLM to provide a periodic phase perturbation or amplitude modulation and clock is extracted. The scheme is discussed in detail in chapter 5.

2.3 Advantage of NOLM

1. Stability with respect to environmental effects-Since in a NOLM both signals experience the same optical path hence it is suitable for demonstrating nonlinear interaction and it is also stable.
2. Temperature sensitivity-Polarization state of both clockwise and anticlockwise rotating signals are maintained in the loop and they travel along the same physical fiber, thus any change in ambient condition affect both the signals equally.
3. Cascadability -Identical devices with polarization discriminated inputs can be cascaded because polarization can be maintained. That is the reason polarization instead of wavelength is used to isolate input and control signal inside the loop.
4. Jitter tolerance-Due to high birefringence two signal travel at different velocities along two orthogonal axes. Birefringence and loop length define an effective integration time at the device input and make it sensitive to timing error within that margin. The control-signals walk off can be used to effectively reduce the effect of timing jitter on the bit error rate of receivers.
5. Low Cost Implementation- NOLM require the use of commercial available devices /components and hence it results in low cost implementation.
6. Ultrafast speed Operation of a mode locked laser using Sagnac scheme as one of the end mirrors at 1.6THz is reported. Moreover all optical time demultiplexer have an ultrafast response time of a few seconds and a potentially low switching power.

REFERENCES

2.1 R.S.Tucker, G.Eisentein, and S.K. Koroty, "Optical time division multiplexing for very high bit rate transmission ,"J.Lightwave Technol.,Vol.6,pp.1737-1749,1988.

2.2 K.J.Blow ,N.J.Doran ,B.K.Nayar , and B.P.Nelson , "Two wavelenth operation of nonlinear fiber loop mirror,"Opt. Lett .15(4) ,pp. 248-250, February 1990.

2.3 M.Jinno,"All optical Siganl regularizing/regeneration using a nonlinear fiber sagnac interferometer switch with signal-clock walk off, "J Lightwave Technol, vol.12., No.9.,pp.1648-1658 September 1994.

2.4 Prosenjit Pal,"Performance analysis of alloptical sagnac logic gates", M.Tech Thesis, I.I.T, Kanpur ., 1997.

2.5 P.A.Andrekson, N.A.Olsson , J.R.Simpson, D.J.Digiovanni, P.A.Morton,et al, "64 Gbit/s all optical demultiplexing with the of nonlinear optical loop mirror,"IEEE Photon. Technol.Lett., 4(6), pp.646-647, June 1992.

2.6 B.P.Nelson, K.J.Blow, P.D.Constantine, N.J.Doran, J.K.Lucek, Marshall I Wet al.," Alloptical Gbit/s switching using nonlinear fiber optical loop mirror," Electron.Lett., 27,pp.704, 1991.

2.7 B.P.Nelson,K.J.Blow ,P.D.Constantine ,N.J.Doran,J.K.Lucek et al.,"All optical Gbit/s switching using nonlinear fiber optical loop mirror," Electron.Lett., 28(11), pp.1035-1037,May 1992.

2.8 K J Blow and K Smith ,"Nonlinear loop mirror devices and applicatios "., Academic Press, 1993.

2.9 Anan Huang, Norman Whitaker, H. Avramopoulos, P.French et.al ," Sagnac fiber logic gates and their possible application: a system perspective ," App. Optics., Vol.33, No.26., September 1994.

2.10 M. Nakazawa, K. Suzukiand E. Yamada, "NOLM oscillator and its injection locking technique for timing clock extraction and demultiplexing", Electron.Lett., Vol. 32, No. 12, June 1996.

2.11 Anan Huang, Norman Whitaker, H. Avramopoulos, M. C. Gabriel," All-optical, all-fiber circulating shift register with an inverter", Opt. Lett., Vol. 16, No. 24, December 1991.

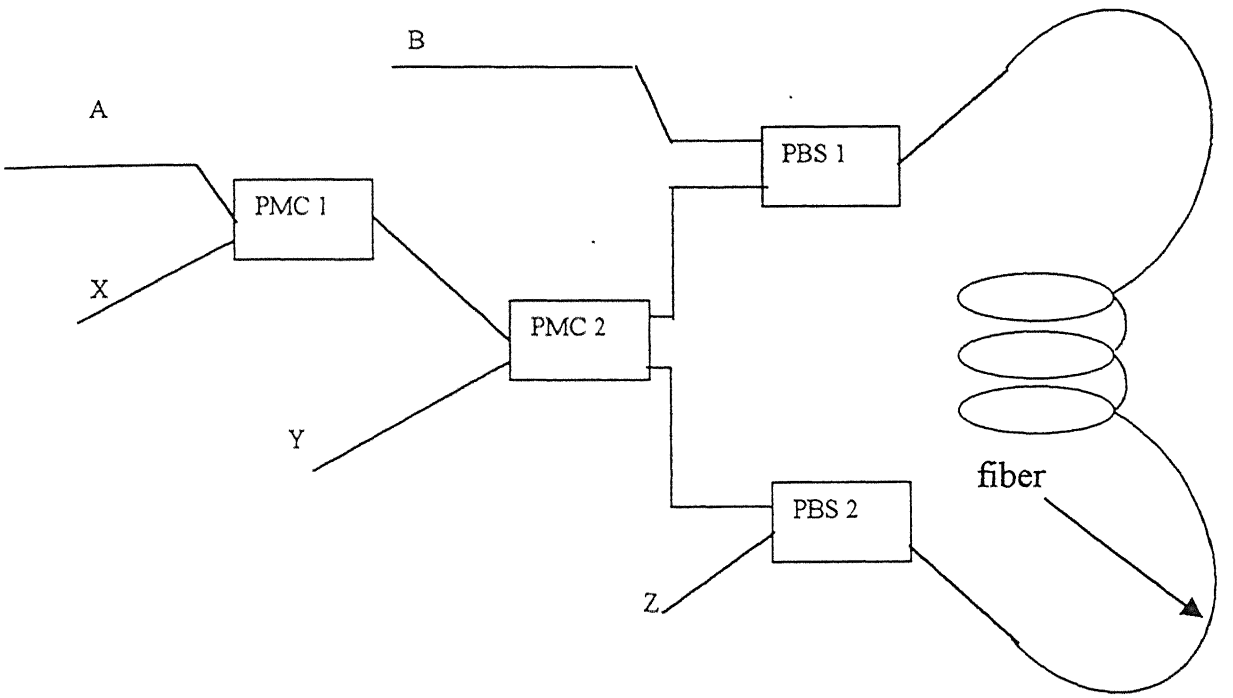

Fig 2.1 Basic configuration of Non Linear Optical Loop Mirror (NOLM) [2.3, 2.4]

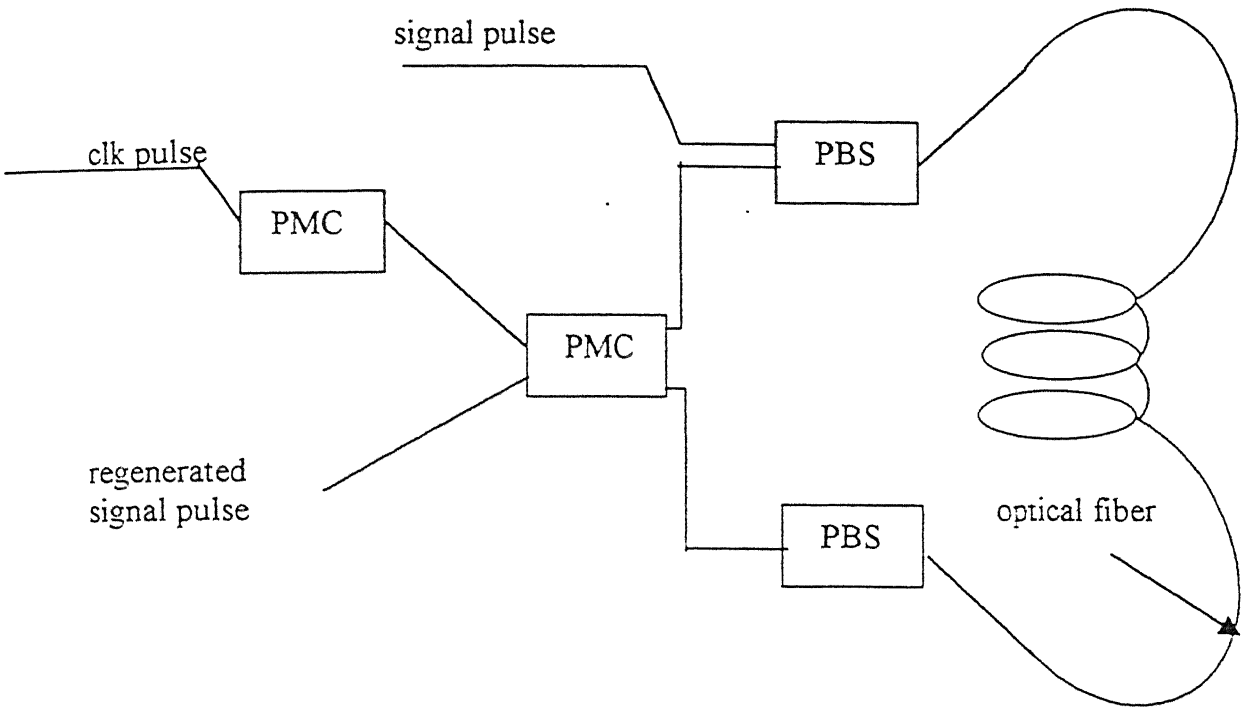

Fig 2.2 regenerative repeater scheme [2.3]

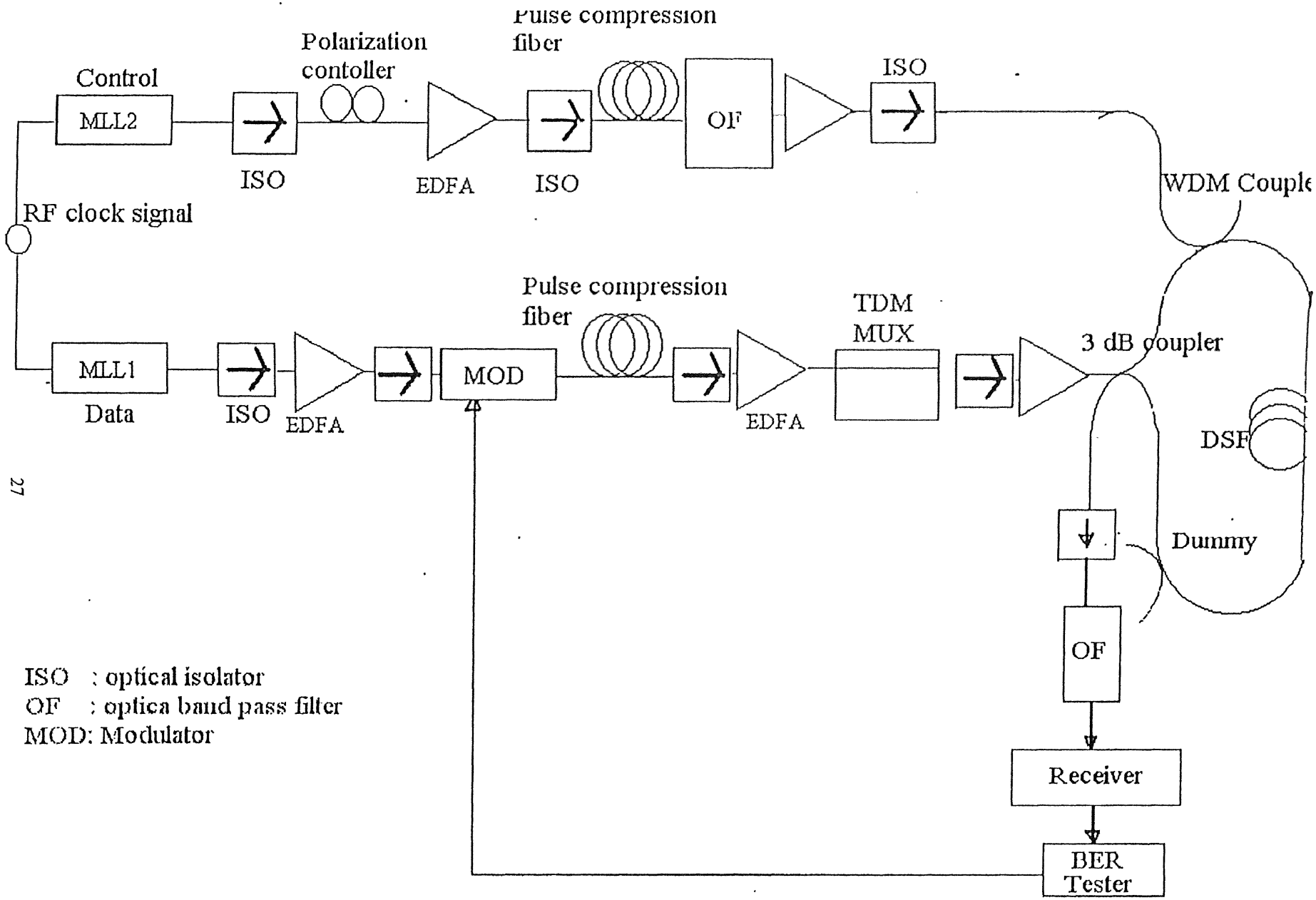

Fig 2.3 Configuration of a two wavelength NOLM [2.5]

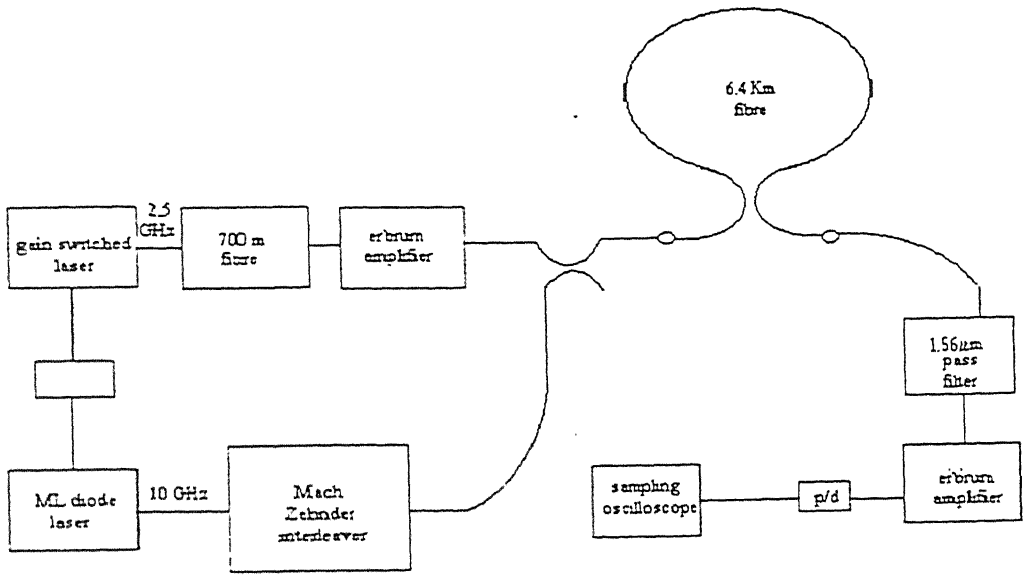

Fig 2.4 Schematic diagram of an all-optical switching experiment [2.6, 2.7]

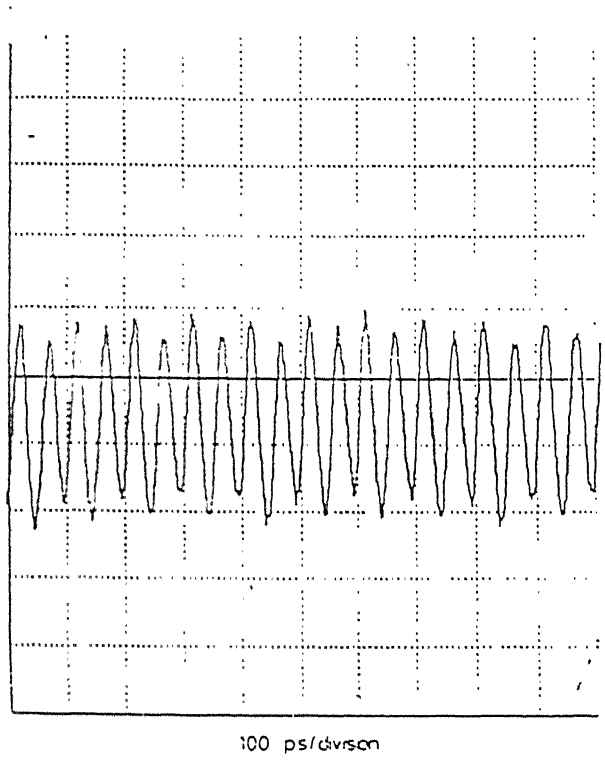

Fig 2.5 Signal pulse train used in experiment [2.6, 2.7]

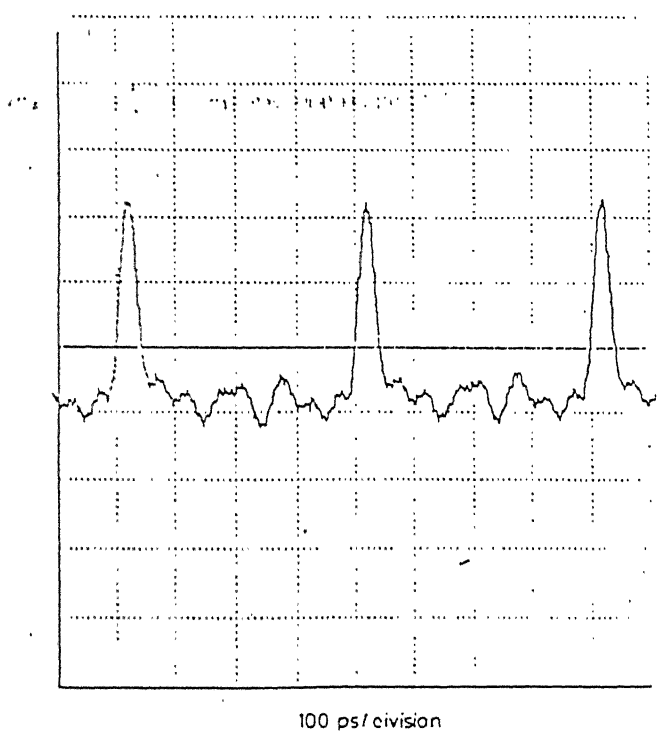

Fig 2.6 Reflected mode switched output [2.6, 2.7]

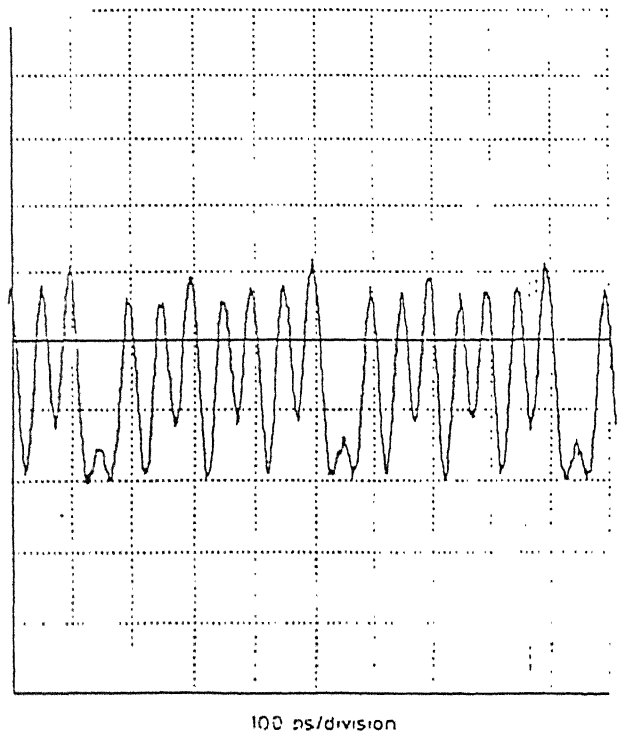

Fig 2.7 Transmitted mode switched output [2.6, 2.7]

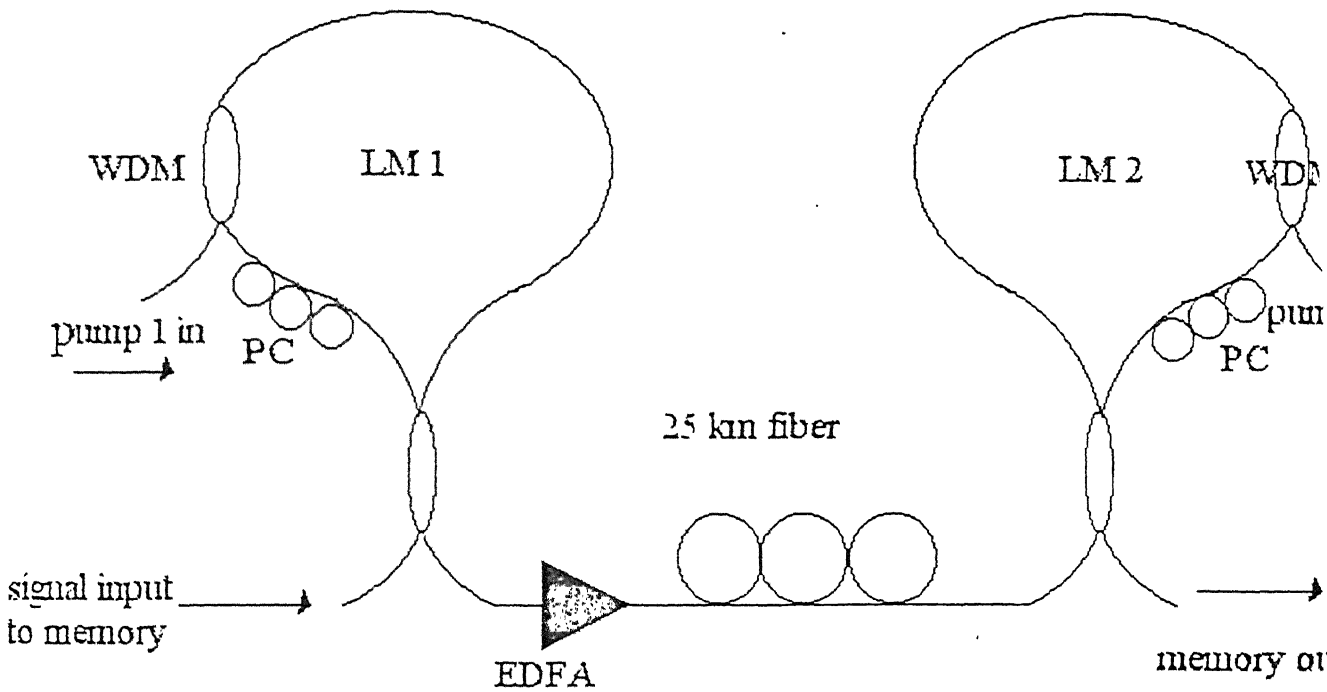

Fig 2.8 Soliton memory configuration[2.8]

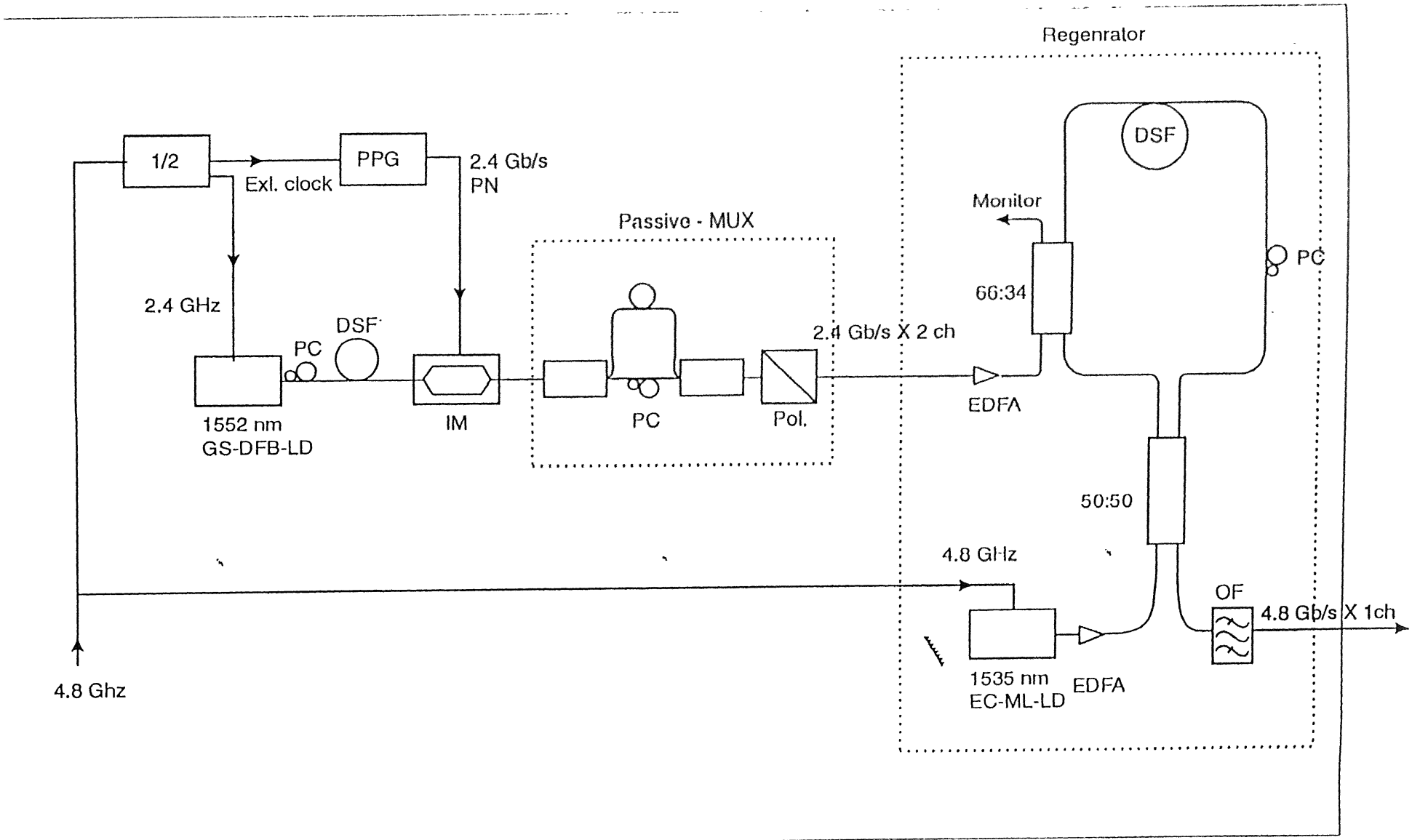

GS-DFB-LD : gain-switched distributed-feedback laser diode, PC : polarization controller
EC-ML-LD : external-cavity mode-locked laser diode, OF : optical filter, Pol : polarizer

Fig : 2.9 Experimental Setup for Testing all Optical Multiplexer

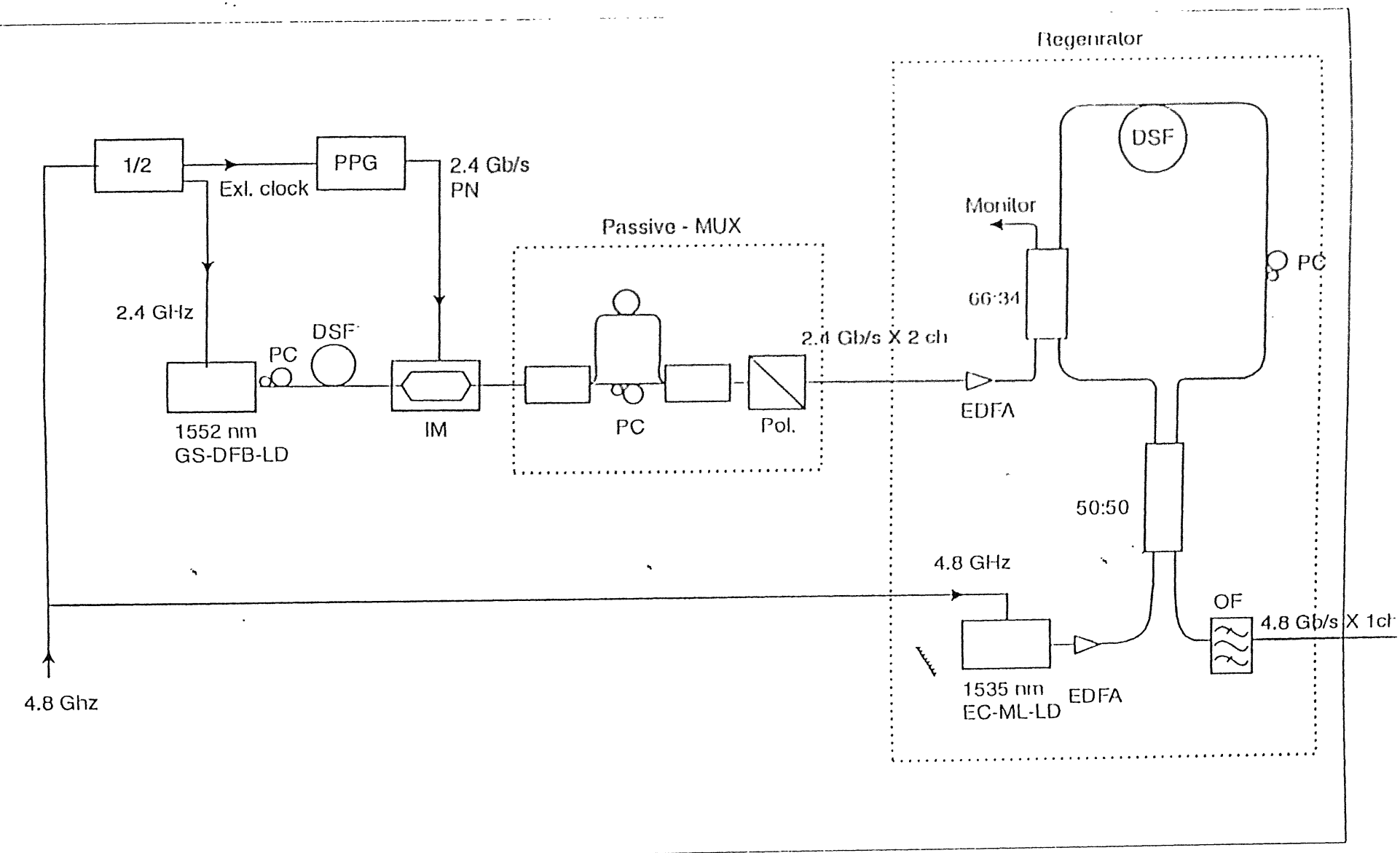

GS-DFB-LD : gain-switched distributed-feedback laser diode, PC : polarization controller
EC-ML-LD : external-cavity mode-locked laser diode, OF : optical filter, Pol : polarizer

Fig : 2.9 Experimental Setup for Testing all Optical Multiplexer[12-16]

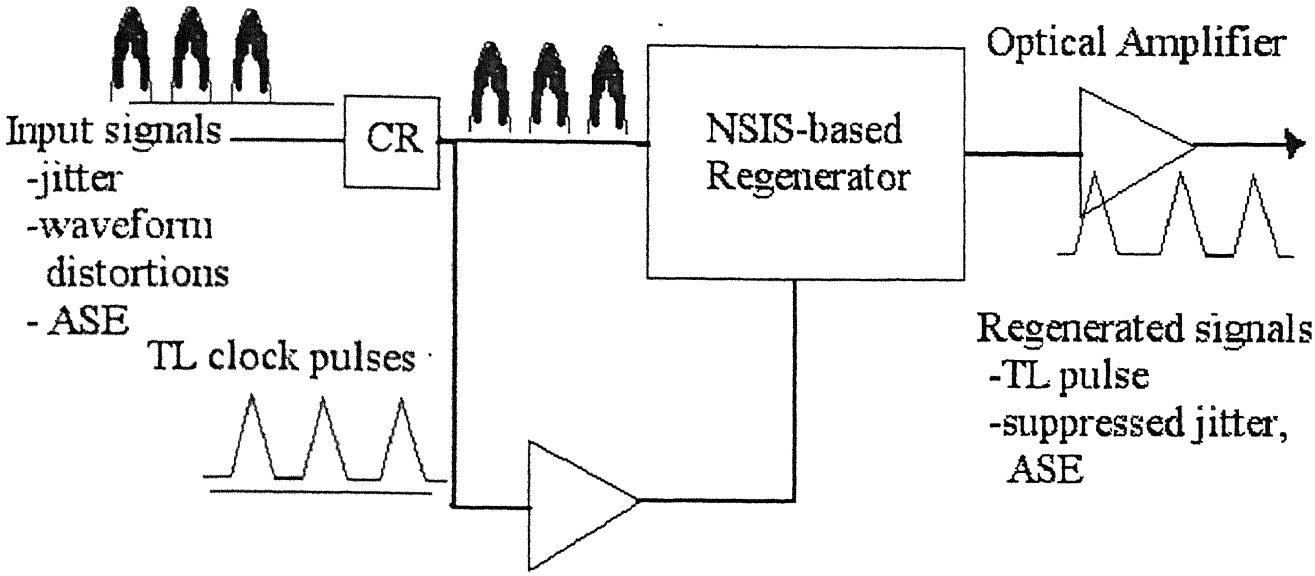

CR-all optical clock recovery circuit

Fig 2.10 Possible configuration of all optical regenerative repeater [2.3,2.10]

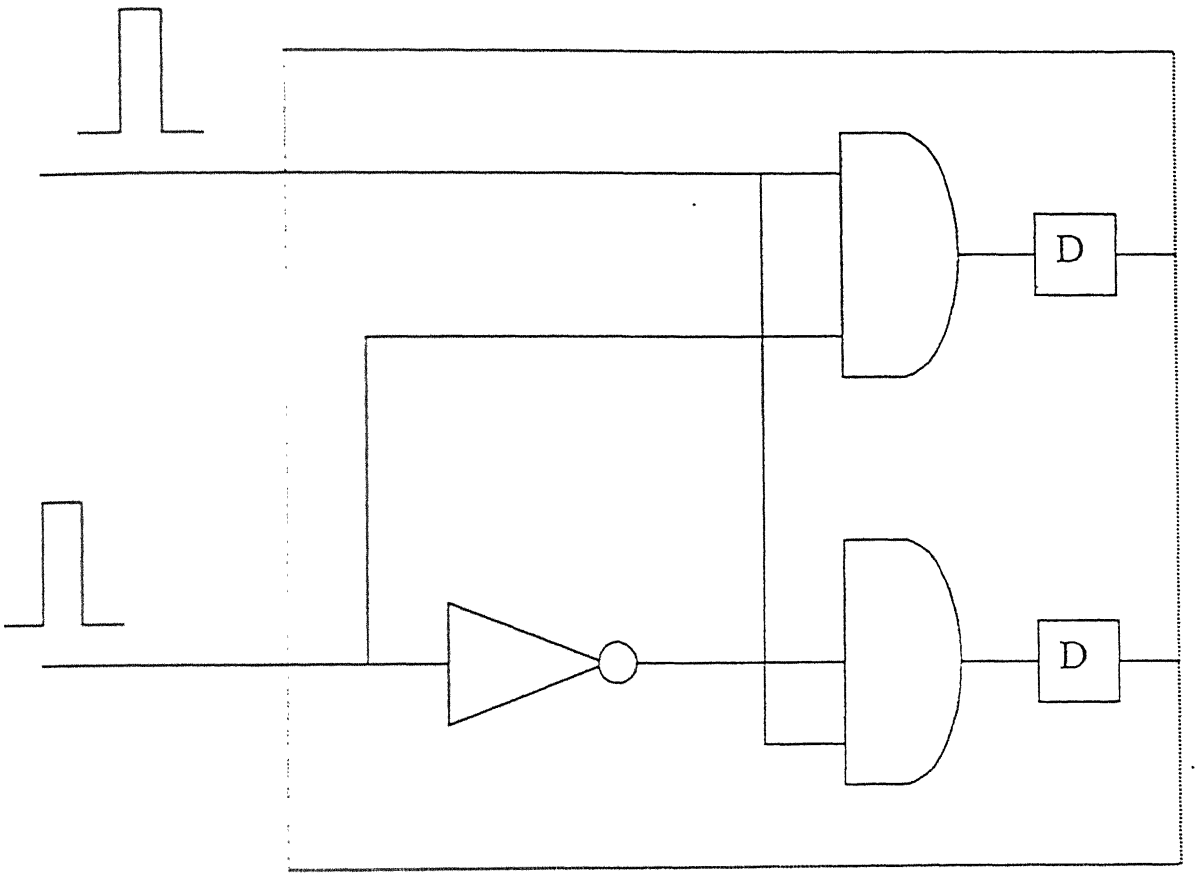

Fig 2.11 Logical Implementation of all optical switch using a Sagnac Interferometer [2.10]

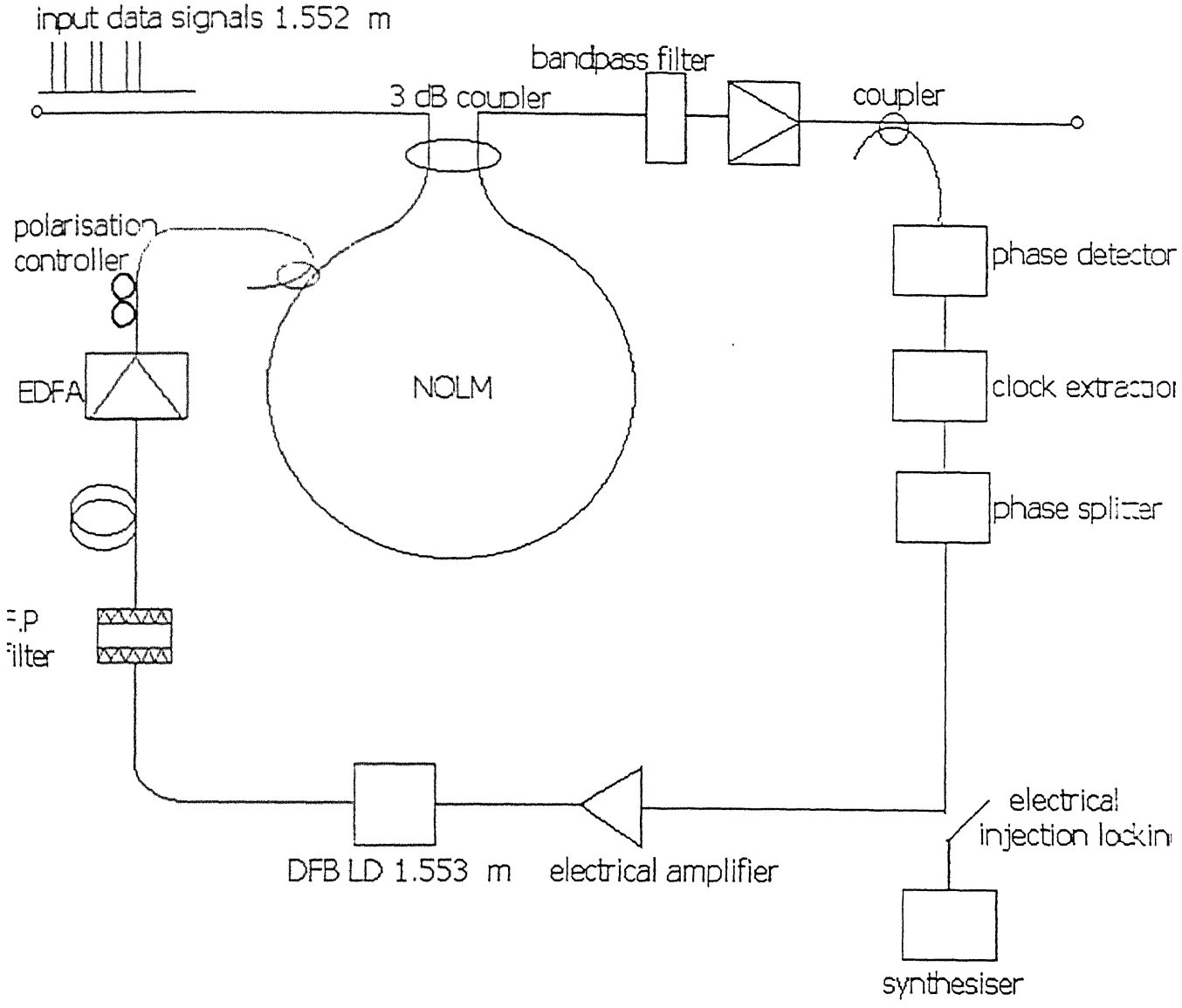

Fig 2.12 Regeneratively and harmonically mode locked NOLM laser [2.10]

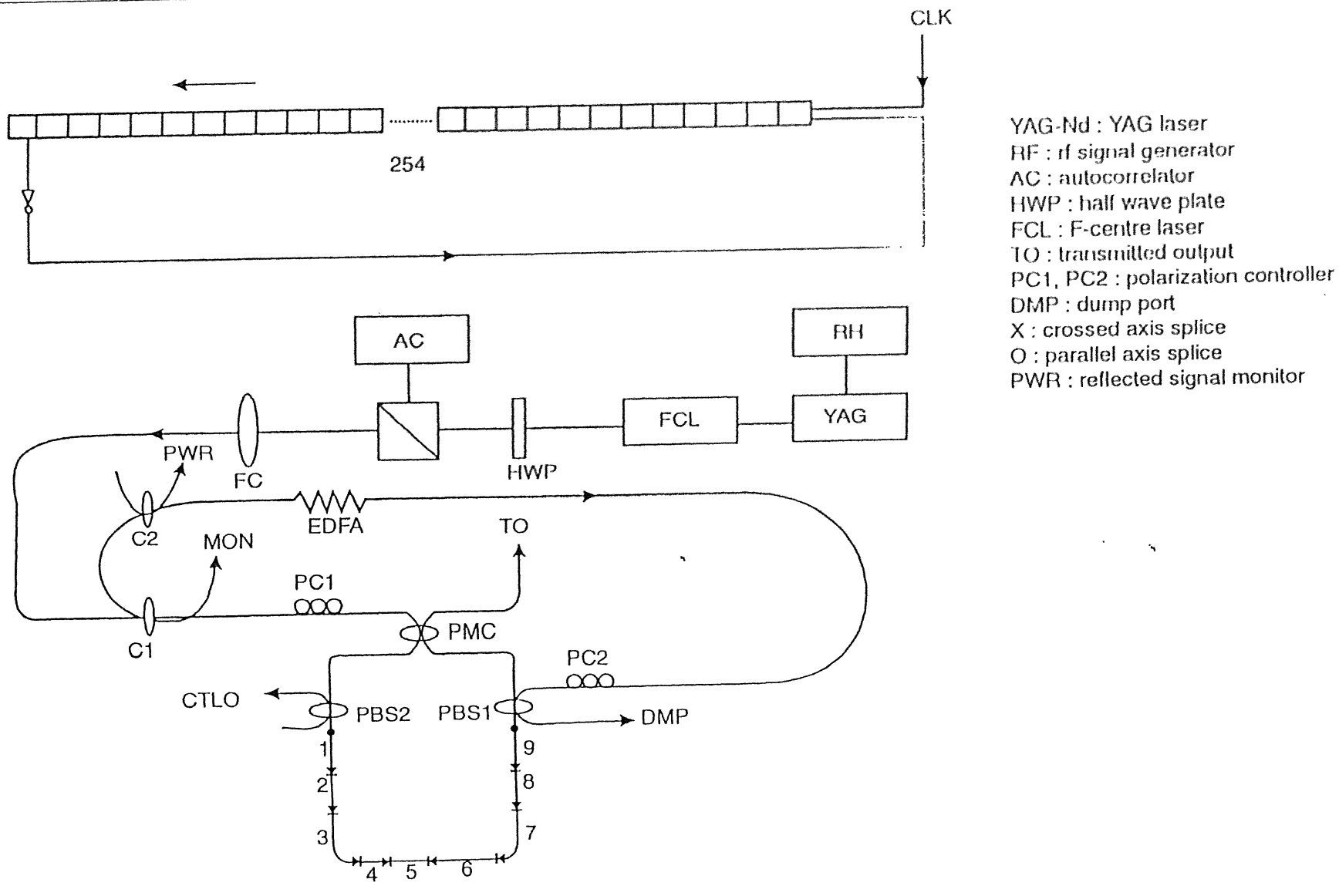

Fig : 2.13 **All optical, all -fiber circulating shift register with an inverter [2.11]**

CHAPTER 3

MODE LOCKING OF LASER

A mode of a resonator can be defined as a field configuration, supported by the resonator through a process of constructive interference. Fig 3.1 illustrates a typical laser output spectrum with a number of longitudinal resonator modes. Each frequency in the figure corresponds to a different longitudinal mode number. For each longitudinal mode number, there exists a set of different energy distribution in a plane transverse to the resonator axis called transverse modes.

3.1 Mode Locking

Mode locking has been defined as the process of fixing the frequency separation and phase differences of the excited modes. Mode locking is also used to couple various longitudinal modes present in a resonator to obtain short pulses of high energy [3.1].

Many laser or all optical processing operations require short pulses with a pulse width upto the order of few pico second. Q-switching which is also an excellent method of generating high-powered pulses is able to produce pulses with duration of approximately 10 ns. Mode locking technique usually covers the range from a nanosecond to a picosecond pulse.

One of the conditions of perfect longitudinal mode is to have only one transverse mode oscillating. In order to obtain single mode excitation, it is necessary to use some device, which will give high losses to all transverse mode but the desired one. When the laser oscillates naturally, the phase of each mode is a random parameter. When the phase of one mode changes, it does so without coordination with the other modes of the cavity. Thus even if every mode is coherent, it may interfere only with itself to form a standing wave and cannot interfere with other modes. To induce multimode interference, the phases of all modes must be locked together. That is, at a given time t=0, the phases of all modes are fixed to the same value.

Constructive interference can occur only at prescribed times when all modes are at the same phase thereby resulting in a laser pulse with an amplitude that exceeds the amplitude of any individual mode. At other times the modes interfere with each other destructively, thereby resulting in no emission. For each of the longitudinal modes, the time for one round trip in the cavity is $T_c = 2L/c$ where L is the length of resonating cavity and c is the velocity of light. Hence any event that requires simultaneous participation of the phases of these modes must be periodic with a period of T_c. Once condition for constructive interference is established, new pulses are emitted at regular interval of T_c. These pulses are much shorter than Q switched pulses. This technique of coupling the longitudinal modes together with the objective of generating a train of short pulses is called mode locking.

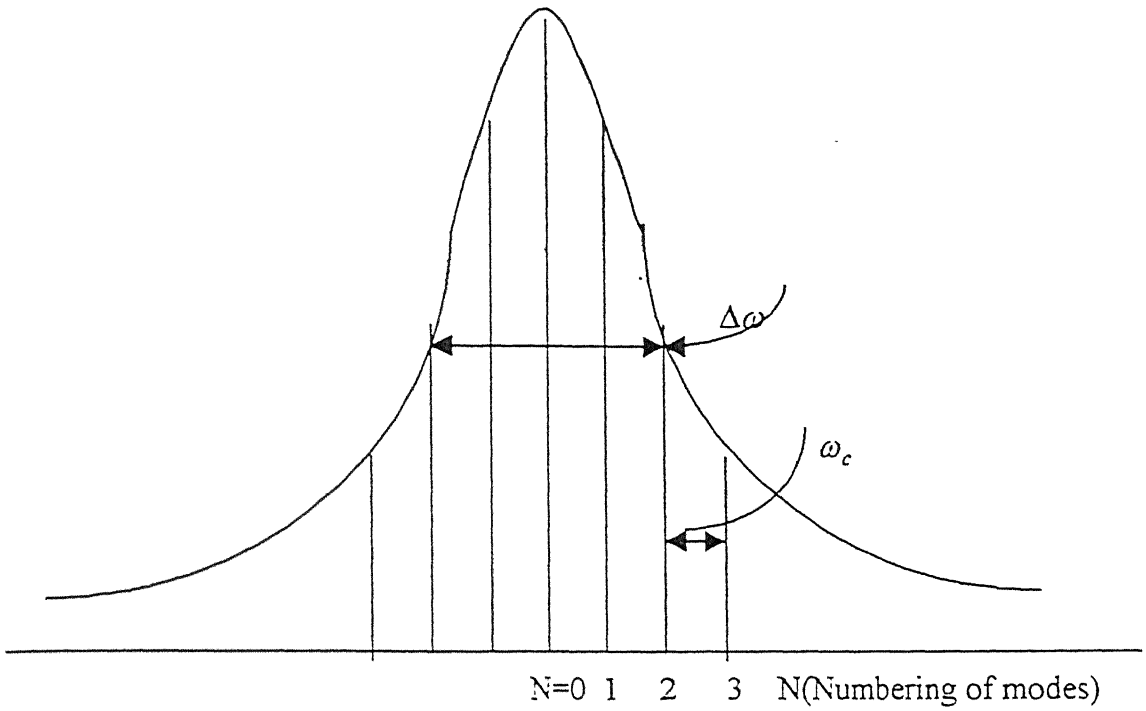

Fig 3.1 Longitudinal mode spectrum of a resonating cavity

In fig 3.1, the longitudinal modes are shown by vertical lines and are separated by a frequency $\omega_c = \frac{2\pi}{T_c}$.

The idea of locking of longitudinal modes can be explained by phasors. The electric field of longitudinal modes can be represented by phasors. Each cavity mode is represented by an arrow of length of unity. As the phase of mode revolves, phase angle of n^{th} mode is given by

$$\theta_n = \omega_n t + \phi_n \tag{3.1}$$

where θ_n is the total angle of n^{th} mode as represented in phasor plane.

ω_n is the frequency of n^{th} mode.

ϕ_n is the initial phase of n^{th} mode.

We have assumed amplitude of electric field to be same. We have also assumed the initial phase of all the cavity modes ϕ_n=0. The phasor of a mode can be viewed as vector in time domain. The phase angle of $(n-1)^{th}$ mode is given by

$$\theta_{n-1} = \omega_{n-1} t + \phi_{n-1} \tag{3.2}$$

Subtracting equation (3.2) from equation (3.1)

$$\theta_n - \theta_{n-1} = \omega_c t \tag{3.3}$$

as $\phi_n = \phi_{n-1} = \ldots = \phi_{n-N} \ldots = 0$

where ω_c is the separation between any two consecutive cavity mode

We have shown 8 cavity modes represented as phasors in fig 3.2(a), 3.2(b), 3.2(c) and 3.2(d). The same analysis can be extended to N cavity modes.

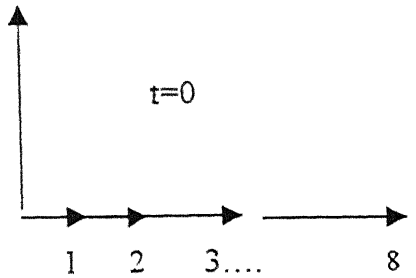

Fig 3.2(a) Phasors of cavity modes at t = 0

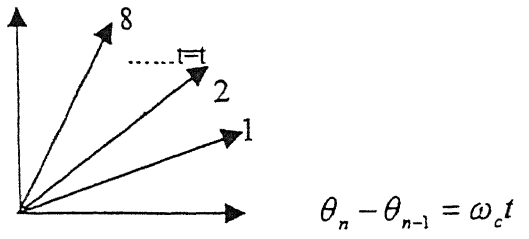

Fig 3.2(b) Phasors of cavity modes at t = t

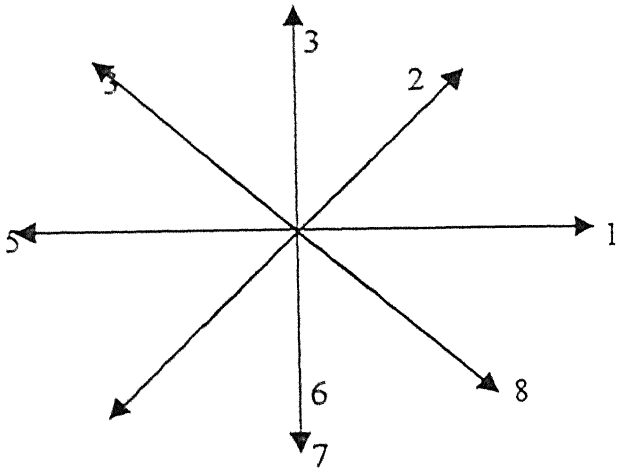

Fig 3.2(c) Phasors of cavity modes at $t = \Delta t$

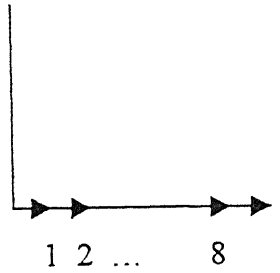

Fig 3.2(d) Phasors of cavity modes at $t = \frac{2\pi}{\omega_c}$

In fig 3.2(a), at t=0, ϕ_n=0, phasors of all N cavity modes point in the same direction and hence resultant is N times the amplitude of an individual mode. Angle between two adjacent modes is given by

$$\theta_n - \theta_{n-1} = \omega_c t \qquad (3.4)$$

As the angle between the phasors increases, the amplitude of their resultant decreases until a time Δt, when each phasor is aligned with another phasor that points exactly in the opposite direction, there by cancelling each other out, hence

$$\theta_n - \theta_{n-1} = \frac{2\pi}{N} \tag{3.5}$$

$$\Rightarrow \quad \frac{2\pi}{N} = \omega_c t$$

$$\Rightarrow \quad \Delta t = \frac{2\pi}{N\omega_c} \tag{3.6}$$

As the angle between each phasor increases, the combined electric field increases slightly and then declines again several times until the angle between two successive modes is

$$\theta_n - \theta_{n-1} = 2\pi \tag{3.7}$$

When the angle between two successive modes is 2π, then the phasors representing electric field of different cavity modes align in same direction and hence add up.
Time between two successive such event is given by

$\omega_c t = 2\pi$

$$\Rightarrow t = \frac{2\pi}{\omega_c} \tag{3.8}$$

which is in agreement with heuristic argument.

The peak power of each of the pulses increases quadratically with the field. Since the field of N mode when constructively interfering with each other is N times larger than the field of an individual mode, the power of each pulse is N times larger than power of a single mode.
The primary objective of the mode locking technique is to achieve a pulse with short possible duration.

3.1.1 Brief Mathematical Analysis

The resultant electric field of N cavity modes is given by

$$E = E_0 e^{-j\omega_0 t} \sum_{-(N-1)/2}^{N-1/2} e^{-jn\omega_c t} \tag{3.9}$$

where ω_0 is the optical frequency of laser pulses.
Assuming initial phases of all modes to be zero and their polarization to be identical

$$E(t) = E_0 e^{-j\omega_0 t} \frac{\sin(N\omega_c t/2)}{\sin(\omega_c t/2)} \tag{3.10}$$

ω_0 is the optical frequency and ω_c is the separation between two adjacent cavity modes
Peak occurs at periods when $\sin(\omega_c t/2) = 0$

i.e. when $t = \frac{2\pi N}{\omega_c}$ when N is an integer

Pulse power is $P(t) = I_0 \frac{\sin^2(N\omega_c t/2)}{\sin^2(\omega_c t/2)}$ (3.11)

I_0 is the average power of a single mode.

3.2 Types of Mode locking

Mode locking can be achieved in a controlled manner by employing two different methods

1. Passive mode locking
2. Active mode locking
3. A third type of mode locking called self-locking is also possible. In self-locking, ultrashort pulses can be obtained spontaneously without employing an external modulator or other mode locking elements. However, due to somewhat unstable and uncontrollable nature of self-locking, this method is very rarely used.

3.3.1 Passive Mode Locking

Passive mode locking is achieved by saturating a nonlinear element called absorber placed inside a laser cavity so that the absorber differentiates between the high and low intensity pulses inside laser. The three essential element for passive mode locking are the optical cavity, laser rod and the dye cell containing the nonlinear absorber. The arrangement required for passive mode locking in two-mirror laser cavity is shown in the fig 3.3. Saturable absorber has an optical absorption that is constant at low intensities, but the absorption coefficient saturates and decreases to lower values as the laser intensity increases.

In a laser cavity under stimulated condition different longitudinal modes in resonator oscillate with different amplitudes and random phases. The amplitudes of different modes oscillating in the cavity are constant but its phases vary randomly. Hence the resultant field in the cavity before mode locking takes place is in the form of a fluctuating waveform due to the random phases of the individual modes.

When the laser pumping process is first turned on, the absorption may even be larger than the laser gain, so that no signal can build up in the laser cavity. As the laser gain continues to increase because of continued laser pumping, the round trip gain begins to exceed the total saturable and non-saturable losses in the laser cavity and an initially weak laser oscillation gradually begins to build up from the noise. The initial noise distribution, i.e., the initial intensity distribution because of random nature of phases of individual modes, contain one particular noise spike that has larger intensity than the other noise spikes within the round trip times the laser oscillation continues to build up. This particular noise spike grows to an intensity level where it begins to saturate the loss it encounters in the saturable absorber.

When this begins to happen, the absorber starts to act in a nonlinear fashion by discriminating between the high intensity and low intensity pulses. This particular noise spike will begin to experience less loss per round trip rather than the other weaker noise

spikes that has not yet reached the absorber 's saturation levels. Thus low intensity pulses get absorbed since they fail to saturate dye.

For effective discrimination, the saturable dye must have a shorter relaxation time than the fluctuation pulse width, so that after a high intensity pulse saturates it and pass unabsorbed, the absorber must quickly relax back to its initial unsaturated state in order to be able to absorb a lower intensity pulse which may follow the larger pulse. The pulses pass through the absorber repetitively as they make consecutive round trips between the mirrors of the cavity. Therefore after a large number of round trips the discrimination between the initial largest pulse and smaller pulses can become enormous and in the end only one pulse remains in the cavity with the other pulse completely annihilated.This single pulse generates an output in the form of a mode –locked train of pulses, as a fraction of it escapes from the cavity through the partial reflecting mirror at each round trip. This process is also called burning through the saturable absorber.

3.3.2 Active Mode Locking

Active mode locking is achieved by placing in a laser cavity a device, which periodically modulates the loss of the resonator. The process is called 'active' mode locking because the modulator is driven by an externally controlled source and hence its response is independent of the radiation intensity. Active mode locking is used in a cw or pulsed laser whereas passive mode locking is inherently a transient process i.e. it is almost always accompanied by Q-switching in solid lasers. Active mode locking can be achieved either with an amplitude modulator or a phase modulator. The basic aim of this device is to periodically modulate the loss of the cavity.

If an amplitude modulator is placed inside the laser cavity as shown in fig 3.4, the noise like field goes through the amplitude modulator. The degree of loss suffered by field at any time is governed by modulating function. The frequency of this modulating function is adjusted so as to be equal to the inverse of the round trip time T_c, the same part of the field pass through the modulator every time the modulator is in its low loss state. Consequently, this particular portion of the field grows in intensity while the rest of field is attenuated and eventually a well-defined pulse is formed inside the cavity. The fluctuating pulse, which happens to arrive at the modulator when its transmission is maximum, passes through the modulator unattenuated and eventually builds into the mode-locked pulses. If a phase modulator is inserted inside the cavity then the pulse circulating inside the cavity experiences maximum transmission at two extremes of the phase variation. In harmonic mode locking the modulator transmission function reaches its transmission function maximum at N times where the round trip time is equal to N times modulating period. Hence there are N pulses circulating inside the cavity.

The modulator driven at the half or multiples of the mode spacing frequency creates side bands for each oscillating mode; this leads to spectral broadening (pulse compression in time domain) while the action of band limited gain of the active medium has the opposite effect i.e. pulse broadening. A mode locked condition is reached when these processes reach a balance in c.w. lasers. Although the modulator directly affects the field amplitude, the phases of the oscillating axial modes are also indirectly influenced by the modulator. The actual shape of the pulse depends not only on the mode amplitude but

also on the mode phases. The output is more coherent from a mode-locked laser as compared with a free running laser is due to the fact that the random phase variations of the modes caused by the presence of noise are damped by the influence of the modulator. A fully mode locked pulse is determined from its phase spectra.

3.3 Comparison of Active Mode Locking With Passive Mode Locking

1. In passive mode locking, the duration of the generated pulse is limited by the lifetime of the upper absorber level. The shorter the lifetime, the shorter the duration of the mode locked pulses. But there is a lower limit for this lifetime. In active mode locking the pulse duration is determined by the combined action of the modulator and amplifying medium.

2. Passive mode locking is inherently a probabilistic event in which the fluctuating intensity profile eventually survives. Active mode locking is not a statistical process. The pulse, which finally survives, need not be pulse, which initially has the maximum intensity. Parasitic pulses may also occur in passive mode locking whereas active mode locking is free from this kind of accidental and undesired double pulse generation.

3. In passive mode locking synchronization is not needed. There can be no detrimental effects due to detuning. Active mode locking loses its value due to synchronization problem because detuning and dispersion can never be avoided completely.

4. Active mode locking has two distinct superiorities over the passive process. Firstly the number of pulses to be generated per round trip period can easily be adjusted to any integer value. Secondly, active means of mode locking can be employed in lasers for which suitable saturable absorbers are not available In passive mode locking, only one pulse per round trip is usual, except when the saturable absorber is placed exactly at the center of the cavity in which case intentional double pulse generation is possible, with the train of pulses at the output being equidistant from each other. .

5. With the advent of nonlinear optics active mode locking has been able to generate sub picosecond pulses by mode locking of fiber laser .To meet the futuristic optics environment all optical clock recovery has been achieved at a repetition rate upto 100Gbit/s using mode locked laser whereas passive mode locking can not achieve this.

REFERENCE

3.1 Joseph T. Verdeyn, " Laser Electronics", Prentice –Hall of India Private Limited, New Delhi, 1993.

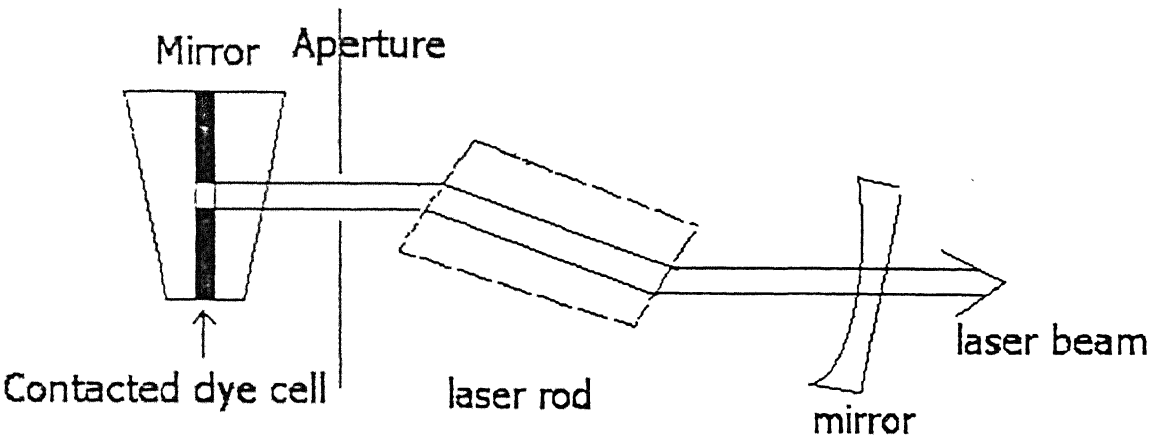

Fig 3.3 Configuration of two-mirror laser cavity [3.1]

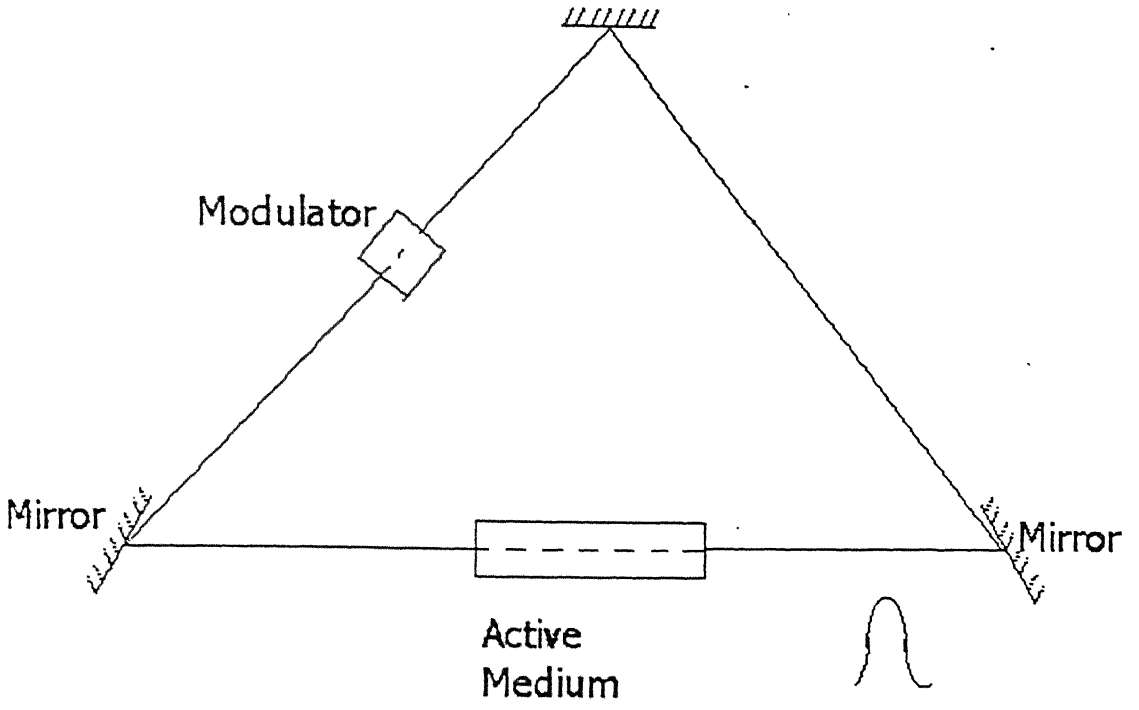

Fig 3.4 Model for Mode locked laser
Ring type cavity [3.1]

CHAPTER 4

Theoretical Analysis of clock recovery circuit

In this chapter, we analyze the extraction of clock from the configuration proposed by British Telecom in 1992. We have considered one of the two schemes, they proposed. We analyze scheme in which dispersion shifted fiber as nonlinear optical modulator (NOM). We also discuss the design issues such as requirement of power of input data pulse, length of fiber modulator, repetition rate and minimum number of pulses required for mode locking in the proposed system. We have also derived spectral width and pulse width of extracted clock.

We have also suggested improvements in clock recovery circuit by including two Fabry –Perot filters apart from the angle-tuned filter given in the circuit.

4.1 Resonant optical cavity

We survey the basic configuration of an optical cavity and the basic mechanism involved in oscillation of laser at cavity resonance before we carry out theoretical analysis of scheme under consideration. The clock recovery system has been configured as fiber laser.

We consider the excitation of the cavity as shown in fig 4.1. We consider all waves, incident on the cavity from the left, inside the cavity, or transmitted through it to the right to be uniform plane waves of limited spatial extent transverse to the direction of propagation.

We consider a wave as it bounces back and forth between two mirrors. E_0 is the initial field at the plane to the right of M_1. It propagates to M_2 and back to the starting plane and experience an amplitude change of $\rho_1.\rho_2$ and a phase factor of exp[-jk2d] as it travels that round trip and thus generates the field labeled E_1^+ which in turn generates E_2^+ and so on. We assume the reference phase of E_0 as 0^o. At every point along the path from M_1 to M_2, the fields E_1^+, E_2^+ and so on are added to E_0. The phasorial addition is shown in fig 4.2. Hence the total round phase shift

$$2\theta = 2kd = q2\pi - \phi \qquad (4.1)$$

where

k-propagation vector
d-length of optical cavity
ϕ-initial lagging phase angle

The total field E_T is many times the initial value E_0 if $\rho_{1,2}$ are close to1 and $\phi = 0$. The characteristics of resonance are defined by

$$2kd = q2\pi$$

$$\Rightarrow d = \frac{q\lambda}{2} \qquad (4.2)$$

Hence there has to be an integral number of half wavelengths between the two mirrors for resonance.

If we use frequency in place of wavelength, then we get from equation

$$\nu = q.\frac{c}{2nd}$$

Because q is restricted to integer values, there are only discrete frequencies, which obey the resonance condition. The separation between those frequencies is given by

$$\nu_{q+1} - \nu_q = \frac{c}{2nd} \tag{4.3}$$

The above equation gives the cavity modes occurring in resonant cavity. The sharpness of the resonance and condition of resonance is derived as below.

The total field propagating to the right is given by

$$E_T^+ = \sum_0^\infty E_n^+ = E_0\left[1 + \rho_1\rho_2 e^{-jk2d} + \left(\rho_1\rho_2 e^{-jk2d}\right)^2 + \left(\rho_1\rho_2 e^{-jk2d}\right)^3 + etc\right] \tag{4.4}$$

$$= \frac{E_0}{1 - \rho_1\rho_2 e^{-j2\theta}} \tag{4.5}$$

where θ = electric length of cavity = $\omega nd/c$

The field returning from M_2 is just ρ_2 times the round -trip phase factor, exp [-jk2d], multiplying the wave going to the right.

$$E_T^- = \sum E_n^- = \rho_2 e^{-j2\theta}.E_T^+$$

$$= E_0\left[\frac{\rho_2 e^{-j2\theta}}{1 - \rho_1\rho_2 e^{-j2\theta}}\right] \tag{4.6}$$

Taking external source exciting the system in Fig 4.1, and using the scattering matrix formalism, scattering matrix for each of the mirrors:

$$\begin{bmatrix} E_r \\ \sum E_n^+ \end{bmatrix} = \begin{bmatrix} \rho_1 & jt_1 \\ jt_1 & \rho_1 \end{bmatrix}\begin{bmatrix} E_i \\ \sum E_n^- \end{bmatrix} \tag{4.7}$$

where, for an assumed lossless mirror, we have the conservation of energy equation

$$\rho^2 + t^2 = 1$$

or (4.8)

$$R + T = 1;\ R = |\rho|^2;\ T = |t|^2$$

where

ρ is the reflection coefficient of mirror.

t is the transmission coefficient of mirror.

The summations in the equation (4.7) represent the waves impinging on and receding from the right side of M_1. Actually, the reflected wave E_r is also a summation of the partial transmission through the mirror from the right to the left. The bottom line of this matrix equation yields a relation between the field E_0 and that from the external source:

$$\sum E_n^+ = jt_1 E_i + \rho_1 \sum E_n^- \tag{4.9}$$

Combining equations (4.4) and (4.5) with equation (4.9)
we find E_0:

$$E_0 = j_1 E_i \tag{4.10}$$

The total field reflected from the cavity can be found from the top line of equation 4.7:

$$E_r = \rho_1 E_i + jt_1 \sum E_n^- \tag{4.11}$$

Using $E_0 = jt_1 E_i$ by equation (4.9), we find the reflected field is given by

$$\frac{E_r}{E_i} = \frac{\rho_1 - \rho_2 e^{-j2\theta}}{1 - \rho_1 \rho_2 e^{-j2\theta}} \tag{4.12}$$

To find the field transmitted through M_2 we propagate $\sum E^+$ from M_1 to M_2 by the normal propagator, exp[-jkd]

$$\frac{E_t}{E_i} = jt_2 e^{-j\theta} \cdot \frac{\sum E_n^-}{E_i} = \frac{-t_1 t_2 e^{-j\theta}}{1 - \rho_1 \rho_2 e^{-j2\theta}} \tag{4.13}$$

the power transmission coefficient through both mirrors is obtained by multiplying equation 10 by its complex conjugate

$$T = \left|\frac{E_t}{E_i}\right|^2 = \frac{t_1^2 t_2^2}{1 - 2\rho_1\rho_2\left[\frac{e^{j2\theta} - e^{-j2\theta}}{2}\right] + \rho^2{}_1\rho^2{}_2} \tag{4.14}$$

Now $\cos 2\theta = 1 - 2\mathrm{Sin}^2\theta$ and $1 - 2\rho_1\rho_2 + (\rho_1\rho_2)^2 = \left[1 - \sqrt{R_1 R_2}\right]^2$

where

the power reflectivity $R = \rho^2$ and $|t|^2 = 1 - R$:

$$T = \frac{(1-R_1)(1-R_2)}{\left(1 - \sqrt{R_1 R_2}\right)^2 + 4\sqrt{R_1 R_2}\,\mathrm{Sin}^2\theta} \tag{4.15}$$

The power reflection coefficient of the cavity $\left|E_r/E_i\right|^2$ is given by

$$R_{net} = \left[\frac{E_r}{E_i}\right]^2 = \frac{\left(\sqrt{R_1} - \sqrt{R_2}\right)^2 + 4\sqrt{R_1 R_2}\,\mathrm{Sin}^2\theta}{\left(1 - \sqrt{R_1 R_2}\right)^2 + 4\sqrt{R_1 R_2}\,\mathrm{Sin}^2\theta} \qquad (4.16)$$

We plot this transmission coefficient as a function of the electric length $\theta = \omega nd/c$ as in figure 4.3. We observe that the transmission peaks at resonance $\theta = q\pi$ as predicted by equation 2, with a maximum value of

$$T_{max} = \frac{(1-R_1)(1-R_2)}{(1-\sqrt{R_1 R_2})^2} \qquad (4.17)$$

$$T_{min} = \left[\frac{1-R}{1+R}\right]^2 \qquad (4.18)$$

4.2 Transient Phenomenon of modulation for Active Mode Locking

In the proposed configuration, the laser cavity consists of a dispersion shifted fiber based NOLM functioning as a non linear optical modulator (NOM), a filter for tuning wavelength, an EDFA as an amplifier and three directional couplers[4.1, 4.2]. Length of dispersion shifted fiber or fiber loop in NOLM as considered in British Telecom Experiment is of the order of few km. The scheme has been basically configured as fiber laser.

We have analyzed that in a mode locked laser such as mode locked solid state laser, the cavity round trip time is smaller than the bit period of data pulses forcing mode locking to occur within one bit period. But in the proposed scheme, the cavity round trip time is very large (43000 ns in experimentally demonstrated scheme) as compared to other lasers. Locking of cavity modes occur within one cavity round trip time due to large number of pulses N(any integer >1). N mode locked pulses are generated due to phenomenon of active harmonic mode locking.

Active harmonic mode locking occurs, if modulation frequency of either amplitude modulator or phase modulator is an integral multiple of cavity mode spacing. This analysis leads to the condition of mode locking for the proposed scheme.

In fiber lasers, the effective gain curve invariably extends over a large number of cavity modes. The irregular profile of the laser output caused by intensity fluctuation can then be improved only by establishing a fixed phase relationship between the oscillating modes. Fixed phase between oscillating modes can be achieved by placing an amplitude or phase modulator inside laser cavity.

We have considered an active harmonic mode locked laser in which

$$\omega_m = N\omega_s \qquad (4.19)$$

where ω_m = modulation frequency of modulator and

ω_s = cavity mode frequency spacing between cavity modes

When an Amplitude or phase modulator, when modulates the electric field of different modes, side bands are generated. If we modulate the fundamental mode, then these side bands are N modes away from the modulated fundamental mode. The N th modes away from fundamental mode on both sides also produce side bands. One of these sidebands correspond to the fundamental mode, hence electric field of fundamental mode is modified. A cavity mode is not locked to its nearest neighbour but to those that are N axial modes apart on each side. All the modes within the line-width of the emission are thus grouped into N sets or into N so called supermodes. Each supermode forms a separate mode locking solution and satisfies all the modulation and lasing conditions. As a result, all these supermodes can oscillate at the same time and compete against each other unless one of them suppresses the other. The energy shift among this supermode and the relative phase slides between them readily leads to pulse amplitude fluctuation. If only one supermode oscillate then stable operation of such lasers takes place. We will prove formulation of supermodes mathematically. Selection of one supermode with the help of filters leads to formation of N pulses in a cavity round trip time.

We have assumed that few resonator modes are present initially when modulator is turned on. We have considered generalized equation for

(a) Amplitude Modulator

(b) Phase Modulator

and derived equation for transient analysis of modulation process for active mode locking to show generation of N pulses in one cavity round trip time.

In a laser cavity the electric field belonging to the n th mode can be written as

$$E_n(t) = A_n(t) \exp j \{ \omega_n t + \phi_n(t) \} \qquad (4.20)$$

Above threshold due to increasing dominance of stimulated emission the mode amplitudes will gradually cease to vary in a random fashion and will only exhibit small and quite slow fluctuation. The total radiation field of the axial modes at any one point inside the resonator will then be the sum of the individual modes.

$$E_T = \sum_{n=1}^{K} A_n(t) \exp j \{ \omega_n t + \phi_n(t) \} \qquad (4.21)$$

where

$A_n(t)$ - Amplitude of the electric field of n th cavity mode

$\phi_n(t)$ - Phase of the electric field of n th cavity mode

E_T - Total electric field assumed to be stationery during a single round trip time and is constant in single round trip time because the deterministic time variation of mode phase are very slow above threshold, so that random fluctuation $A_n(t)$ and $\phi_n(t)$ are reduced to A_n and ϕ_n constant in round trip time T_c.

K -Total number of excited modes

Thus

$$E_T = \sum_{n=1}^{K} A_n(t) \cos(\omega_n t + \phi_n) \qquad (4.22)$$

By neglecting the effect of spontaneous emission on the phases, the frequency spectrum of laser output can be expressed as

$$E(w) = \sum_n A_n \exp(j\phi_n)\delta(w - w_n) \qquad (4.23)$$

where

$E(\omega)$ = Fourier transform of the electric field E_T

$\delta(\omega)$ = Impulse ocuring at frequency ω

We have assumed that width of spectral density of all cavity modes existing in laser cavity is much smaller than the optical frequency ω_0.

First we consider the use of an amplitude modulator in the cavity. We assume the amplitude transmission characteristics of the amplitude modulator is given by(derived in Appendix B)

$$\Gamma(t) = \cos(\beta \sin \theta_m t) = a + b\cos N\omega_s t \qquad (4.24)$$

β - Modulation depth

a, b- depth of modulation related to value of β

θ_m - modulation frequency of the modulator which can be accousto-optic, electro-optic or nonlinear fiber modulator

We assume that K modes are oscillating .We investigate the modulation process for three modes i.e. nth, (n-N)th and (n+N)th modes. The integer n represents any mode within the laser cavity and varies from 1 to K. All the modes generate side-bands when modulated with modulation frequency $\theta_m = N\omega_s$. The n th mode generates (n+N)th and (n-N)th modes as side bands. Similarly (n+N)th mode generates nth and (n+2N)th mode as side bands. The (n-N)th mode generates n and (n-2N)th mode side bands. Hence electric field of nth mode is modified. The resultant electric field of n th mode is given by field due to nth mode itself and side bands generated from (n-N)th mode and (n+N)th mode.

The electric field $E_n(t)$ of the nth mode when modulated by the amplitude modulator produces an electric field

$$E_n(t)\Gamma(t) = A_n(t)\cos(\omega_n t + \phi_n(t))(a + b\cos N\omega_s t) \qquad (4.25)$$

Similarly when the electric field of (n-N)th mode and (n+N)th mode are modulated by the same amplitude modulator . We obtain modified electric field is given as

$$\left.\begin{aligned} E_{n+N}(t)\Gamma(t) &= A_{n+N}(t)\cos(\omega_{n+N} t + \phi_{n+N}(t))(a + b\cos N\omega_s t) \\ E_{n-N}(t)\Gamma(t) &= A_{n-N}(t)\cos(\omega_{n-N} t + \phi_{n-N}(t))(a + b\cos N\omega_s t) \end{aligned}\right\}$$

The side bands generated at ω_n due to(n-N)th and (n+N)th mode modify field at nth mode. The expressions showing generation of side bands are derived in Appendix E. The resultant field of nth mode can be expressed as

$$E_n'(t) = aA_n(t)\cos(\omega_n t + \phi_n(t)) + b/2\, A_{n+N}(t)\cos(\omega_n t + \phi_{n+N}(t)) + b/2\, A_{n-N}(t)\cos(\omega_n t + \phi_{n-N}(t))$$

Hence the field of the nth mode can be written as (derived in Appendix B)

$$E_n'(t) = A_n'(t)\cos(\omega_n t + \phi_n'(t)) \qquad (4.26)$$

$$A_n'(t) = \left[\begin{array}{l} a^2 A_n^2(t) + \frac{b^2}{4}\left\{A_{n+N}^2(t) + A_{n-N}^2(t)\right\} + \frac{b^2}{4}A_n^2(t)A_n^2(t)\cos\left\{\phi_n(t) - \phi_{n+N}(t)\right\} \\ + abA_n(t)A_{n+N}(t)\cos\left\{\phi_n(t) - \phi_{n+N}(t)\right\} + abA_n(t)A_{n-N}(t)\cos\left\{\phi_n(t) - \phi_{n-N}(t)\right\} \end{array}\right]$$

$$\text{and } \phi_n' = \tan^{-1}\left[\frac{aA_n(t)\sin\left\{\phi_n(t)\right\} - \frac{b}{2}A_{n+N}(t)\sin\left\{\phi_{n+N}(t)\right\} + \frac{b}{2}A_{n-N}(t)\sin\left\{\phi_{n-N}(t)\right\}}{aA_n(t)\cos\left\{\phi_n(t)\right\} - \frac{b}{2}A_{n+N}(t)\cos\left\{\phi_{n+N}(t)\right\} + \frac{b}{2}A_{n-N}(t)\cos\left\{\phi_{n-N}(t)\right\}}\right]$$

We observe that both the amplitude and phases of each oscillating modes are slightly altered at each pass of the laser field through the modulator .The degree of change is dependent upon the depth of modulation (~a and ~b) and the relative amplitude and phase values of the modes.

If we use a phase modulator with a transfer chracteristics

$$\Gamma_p(t) = \exp\left\{j\delta_\phi \sin(\theta_m t)\right\} = \sum_{p=-\infty}^{\infty} J_p(\delta_\phi)\exp[jp\theta_m t]$$

where δ_ϕ is a constant.

If $\delta_\phi << 1$ the $\Gamma_p(t)$ can also be approximated as $\Gamma_p(t) = a_1 + b_1\cos\theta_m t$

and results similar to above will be obtained (derived in Appendix C).

From equation (4.26), we observe that amplitude and phase of electric field of oscillating modes are changed on each pass through the amplitude or phase modulator. We assume that initially the phases of oscillating modes are uniformly distributed between $-\pi$ to π .Depending upon depth of modulation the phases of each mode keeps changing on successive passes till the following condition is reached.

$\phi_{n+N} - \phi_n = \phi_n - \phi_{n-N} = \pi$ then

$$\phi_n' = \tan^{-1}\left[\frac{aA_n(t)\sin\{\phi_n(t)\} + \frac{b}{2}A_{n+N}(t)\sin\{\phi_n(t)+\pi\} + \frac{b}{2}A_{n-N}(t)\sin\{\phi_n(t)-\pi\}}{aA_n(t)\cos\{\phi_n(t)\} + \frac{b}{2}A_{n+N}(t)\cos\{\phi_n(t)+\pi\} + \frac{b}{2}A_{n-N}(t)\cos\{\phi_n(t)-\pi\}}\right]$$

$$\phi_n' = \tan^{-1}\left[\frac{\sin\phi_n(t)\left\{aA_n(t) + \frac{b}{2}A_{n+N}(t) + \frac{b}{2}A_{n-N}(t)\right\}}{\cos\phi_n(t)\left\{aA_n(t) + \frac{b}{2}A_{n+N}(t) + \frac{b}{2}A_{n-N}(t)\right\}}\right] = \phi_n(t) \qquad (4.27)$$

We observe that once the above condition is reached, then the phases of oscillating modes do not change and remain constant. Hence modulation gradually enforces a fixed phase relationship between nth, (n-N)th and (n-N)th mode. The difference between phases of nth mode and (n-N)th or (n+N)th mode is equal to π .Hence nth mode is locked to (n-N)th and (n+N)th mode.

Now we consider the creation of N mode locked pulses within one cavity round trip time. We can use the above result to show graphically that N supermodes are created. Every supermode locks the modes with N modes apart. Each supermode satifies the mode locking condition. Selection of one supermode results into generation of N mode locked pulses.

We consider N=5. The fig 4.4 shows that cavity modes numbered with N=0 is mode locked to N=5. Similarily mode with N=1 is mode locked to N=6 and so on until N=4.The cavity mode N=5 is further mode locked to N=10 and whole process is repeated. Hence the supermode with N=0 will have modes N=5, 10,15 and so on. Hence total five super modes are created.

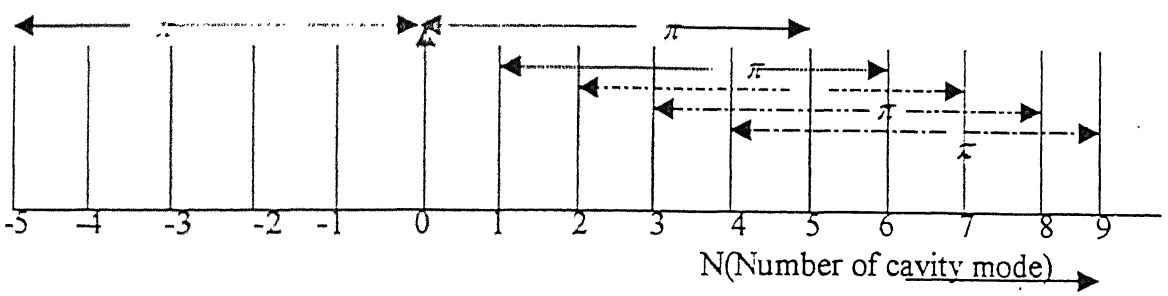

Fig 4.4 Graphical representation of creation of supermodes

The condition for creation of supermode is given as

$$\left.\begin{aligned}&\left|\phi_q - \phi_{q+1}\right| = \alpha;\left|\phi_{q+1} - \phi_{q+2}\right| = \beta;\left|\phi_{q+2} - \phi_{q+3}\right| = \xi;\left|\phi_{q+3} - \phi_{q+4}\right| = \zeta\\ &\text{and}\\ &\left|\phi_{q+4} - \phi_{q+5}\right| = \pi - (\alpha+\beta+\xi+\zeta)\end{aligned}\right\} \qquad (4.28)$$

If N=5 then

Five supermodes will be created. Every supermode will lock the modes with the mode N modes apart.

If $\left|\phi_q - \phi_{q+1}\right| = \left|\phi_{q+1} - \phi_{q+2}\right| = \cdots\cdots \left|\phi_{q+N-2} - \phi_{q+N-1}\right| = \alpha \Rightarrow \left|\phi_{q+N-1} - \phi_{q+N}\right| = \frac{N-1}{N}\alpha$ As shown graphically ,we observe that N supermodes are generated. Every mode is locked to N^{th} mode away from it. We have assumed that the amplitude of the modes to be gaussianly distributed after a large number of round trips in laser cavity.

The mode spacing between locked modes of a supermode is equal to

$$\omega_n - \omega_{n+N} = N\omega_s = \frac{2\pi N}{T_c} \qquad (4.29)$$

In time domain pulses with time period of T_c/N will be generated and in a cavity round trip time T ,the number of pulses generated will be equal to N. We have supported the above statement mathematically and simulated also.

4.2.1 Simulation of Mode locking Theory

We have tried to simulate the behaviour of an actively harmonically mode locked to show that N pulses are produced if modulation frequency of an amplitude or phase modulator is an integral multiple (N) of cavity mode spacing.

We assume that 51 cavity modes are oscillating, the phases of which are randomly assigned with a uniform distribution between $-\pi$ to $+\pi$. We also assume that amplitudes of electric field of these modes are initially random. We have tried to demonstrate that the changes forced upon the highly irregular intensity of laser field as it passes through the modulator generates a perfectly formed pulse per cavity round trip. The number of pulses depends upon N.

The simulation result for N=3 is shown for various iterations, i.e., the successive passes through the modulator in fig (4.5) . We have taken electric field for 51 equally spaced modes as given by equation. $A_n(t)$ has been taken as randomly distributed initially. We have taken 1024 samples of the electric field. The electric field is modified by the transfer chracteristics of amplitude modulator given by equation. The modulation frequency θ_m is equal to an integral multiple of cavity mode spacing. The frequency spectrum of modified field is stored and the intensity of the electric field after each pass is stored. We observe that number of pulses generated is equal to N. With increase in number of iteration, the pulse width of pulse reduces and pulse take the shape of gaussian pulse.

4.2.2 Analysis of generation of N pulses

We observe that input with sinusoidal modulation frequency equal to N(integeral multiple) of cavity mode spacing enforces mode locking and generates N mode locked

pulses. But in actual, data will consist of discrete pulses with different format such as RZ, NRZ and Manchester. The data pulses can have different shapes such as rectangular, gaussian or raised cosine pulses. These data pulses can have different sequences such as 111..., 1010..., pseudo random bit sequence(PRBS).

For easy mathematical understanding, we consider sequence 1010.., of NRZ and RZ pulses. The spectrum of NRZ pulses consists of infinite number of discrete frequencies with fundamental, third , fifth harmonics and so on. The fundamental impulse has got the value of 0.637. The amplitude of other harmonicss gets smaller by 1/n. The second harmonic of NRZ pulses has got the value of 0.2 and third harmonic has value of 0.12. The spatial frequency difference between harmonics is inverse of twice of bit period. For RZ pulses, the fundamental, first harmonic and second harmonic has got the valu 0.45, 0.3 and 0.15 respectively.

We observe that spectrum of data pulses contains fundamental relatively stronger than other harmonics present in the spectrum. Hence we can assume that data pulses at the input port of directional coupler 1(fig 1.1) behaves like sinusoidal input and enforces modulation of fiber modulator. We consider a periodic train of pulses having two pulses in time T. These pulses has got repetition rate of T. We obtain its frequency spectrum. We can show that these pulses behave like sinusoidal input and frequency spectrum of these pulse is similar to fig 4 We consider a periodic train of pulses as shown below

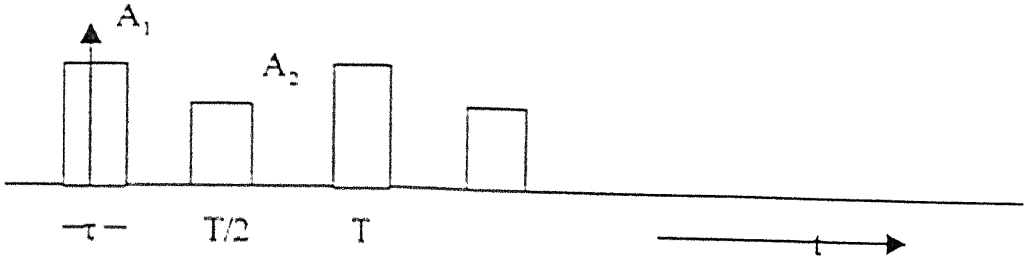

Fig 4.6 Periodic train of pulses

The periodic train of pulses can be represented as

$$g_p(t) = \begin{cases} A_1 & -\tau/2 \le t \le \tau/2 \\ 0 & \tau/2 \le t \le (T-\tau)/2 \\ A_2 & (T-\tau)/2 \le t \le (T+\tau)/2 \\ 0 & (T+\tau)/2 \le t \le T-\tau/2 \end{cases} \qquad (4.30)$$

The periodic train of pulses consists of two pulses with a repetition frequency of 1/T. The fourier series of $g_p(t)$ has been shown to be

$$g_p(t) = \sum_{n=-\infty}^{\infty} \left[A_1 \tau \sin c\left(\frac{\omega_n \tau}{2}\right)' + A_2 \tau \sin c\left(\frac{\omega_n \tau}{2}\right) \cos n\pi \right] \exp(j\omega_n t) \qquad (4.31)$$

$$\omega_n = \frac{2\pi n}{T}; n = 0, 1, 2...$$

derived in Appendix D

The frequency spectrum of the periodic train of pulses is shown below.

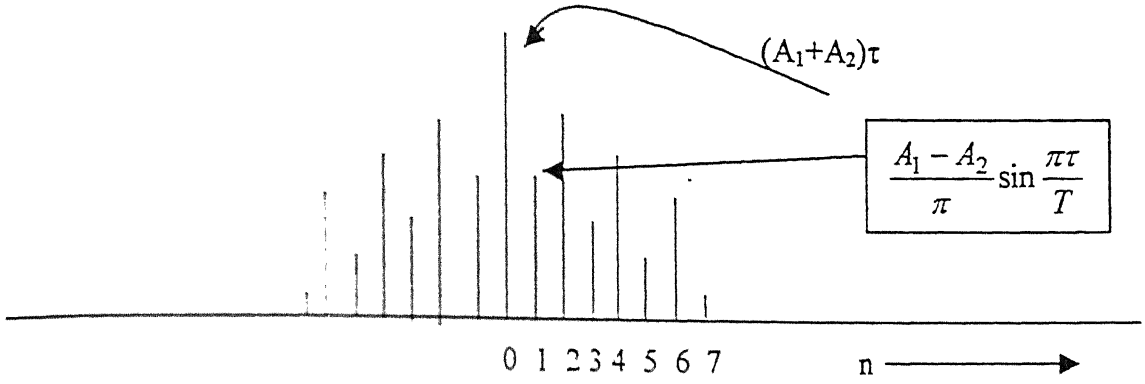

Fig 4.7 Frequency spectrum of periodic train of pulses having two pulse in time T

From the frequency spectrum of the periodic train of pulses, we observe that two amplitude spectrum are interlaced. The amplitude of electric field of cavity modes frequencies at n=0, 2,4, ... represent one set of amplitude spectrum and n=1, 3, 5, ... represent another set of amplitude spectrum. Hence we conclude that two interlaced amplitude spectrum represents two pulses occuring in time period T. If we compare this spectrum with figure by extending this analysis to N pulses, then amplitude spectrum of the mode locked laser with input as sinusoidal modulation frequency looks similar. Hence we conclude that modulation frequency equal to N times cavity mode spacing generates N mode locked pulses in time domain in one cavity round trip time.

4.2.3 Condition to mode lock

We have consider the input data pulses consisting of periodic train of pulses of RZ format with data rate B bits/s. The bit rate of the data is related to the fundamental frequency of the pulse and various harmonics present in data pulses. The content of fundamental and harmonics does not depend upon the pulse width, but it depends upon the repetition rate of pulse. We have analyzed the spectrum of RZ pulses of sequence 111...,1010... of rectangular shape and gaussian pulse shape. We observe that the frequency spectrum of RZ pulses of rectangular shape contains fundamental B=1/T, third, fifth ....harmonics for sequence 1111...,. The frequency spectrum for sequence 1010..., contains 1/2T, 1/T, 3/2T, 5/2T, 3/T, 7/2T,.. and so on We also observe that for input as data pulses, fundamental harmonic is predominant for modelocking. For active harmonic mode locking, modulation frequency or bit rate of modulator should be a harmonic multiple of cavity mode spacing. The repetition rate of data pulses for any sequence can replace fundamental frequency. Hence this condition can be further extended to the clock recovery scheme under consideration. Hence with data pulses modulating the modes through an amplitude or phase modulator, the condition to mode lock becomes as

$$\left.\begin{aligned} \omega_m &= N\omega_s && \text{for sinusoidal input data pulses} \\ B &= \frac{N\omega_s}{2\pi} && \text{for any input digtal data pulses} \end{aligned}\right\} \qquad (4.32)$$

where
B =data rate of input pulse (in bits/s)
N =harmonic integer of cavity mode spacing

where
f_s is cavity mode spacing and is related to the length of fiber modulator by a simple relationship

$$f_s \equiv \left(\frac{Ln_f}{c}\right)^{-1} \qquad (4.33)$$

where
L is the length of fiber modulator and c is the velocity of light.
n_f is the refractive index of the core of the fiber.

The condition to mode lock can be further modified to generate the clock at multiples m(harmonic integer of data rate) with the same cavity by changing the length of fiber. We consider an example by taking RZ sequence 1111..., 10101..., . The frequency spectrum contains terms at $\frac{1}{T}, \frac{2}{T}, \frac{3}{T}, \ldots$ for sequence111...and $\frac{1}{2T}, \frac{1}{T}, \frac{3}{2T}, \frac{5}{2T}, \frac{3}{T}, \frac{7}{2T}$ for sequence 1010. .,
The fundamental frequency of sequence 101010..., is 1/2T, whereas the fundamental frequency of sequence 1111..., for RZ pulse is 1/T. If the laser is mode locked at on an 'odd' order ring cavity mode, then when the driving pattern is switched to 1010.., the laser output remains at B Hz stream. The first harmonic of the 1010.. pattern (at B/2 Hz) falls between ring cavity modes. We show graphically that the above condition generates the output at both sequences 1111.., 10101....

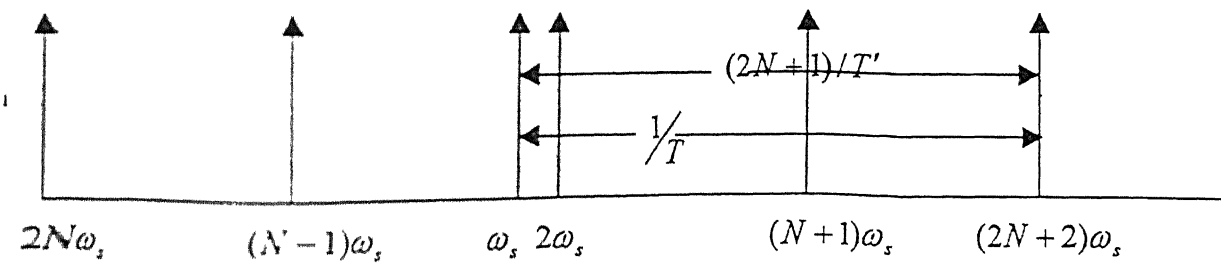

Fig 4.8 Graphical representation of modified condition to mode lock

hence if the sequence is changed from 1010..., to 1111..., then N pulses will be produced at a repetition rate of 1/T. Depending upon data rate of the input data pulses and the length of fiber modulator , the harmonic integer N can be fixed. The relation between bit

rate of sequence 111... and 1010.. is related by m=2. The conditon to modelock can be modified as

$$B = \left(N + \frac{1}{2}\right) f_s \Rightarrow 2B = (2N+1) f_s$$

$$\Rightarrow \frac{2}{T} = (2N+1)\frac{1}{T'}$$

Hence the clock pulse can be generated at multiples (m) of data rate B bits/s, if length of fiber modulator is tuned such that

$$B = \left(N + \frac{1}{m}\right) f_s \qquad (4.34)$$

The condition to mode lock can be defined as if modulation takes place with a base period (T) equal to (or a sub-multiple of) laser round trip time mode locking of laser follows It generates a continuous pulse stream produced by laser at a repetition rate of 1/T.

4.3 Design Issues

We have analyzed the mode locking requirements in subsection 5.2. Based on the condition of mode locking we have analyzed basic design parameters such as

1. Length of fiber modulator
2. Input data power

4.3.1 Length of fiber modulator

Unlike a solid state laser, where the laser cavity has got length in the range of few cm, the length of fiber modulator is in the range of few km. The length of fiber modulator is governed by following reasons:

(a) The laser cavity is configured as a ring type cavity. The cavity mode spacing ω_s is related to length of the cavity, i.e., length of dispersion shifted fiber and active medium, i.e., EDFA. For a given data rate B, harmonic integer N of cavity mode spacing and m(multiple of data rate), we find from equation that L is given by

$$L = \frac{c\left(N + \frac{1}{m}\right)}{Bn_f} \qquad (4.35)$$

Hence by tuning the length of fiber we can obtain clock pulses for both the sequence 1111..., and 1010...By using experimental data as B=1 Gbits/s,

N=43000 and m=2, we get L= 8.6 km, which matches with the test fiber used in experiment.

(b) The length of fiber can be reduced by selecting a large harmonic integer N, but minimum length will be decided by following two factors:

(i) Phase shift required to mode lock depends on a simple relationship derived later in this chapter. Phase shift is proportional to length of modulator and power of input data pulses. Hence this requirement imposes a limit on the minimum length of fiber modulator.

(ii) The solution of nonlinear schrodinger equation gives equation for region of predominance of group velocity dispersion (GVD) and nonlinearity. The expressions are:

$$L_D = \frac{T_0^2}{|\beta_2|}, L_{NL} = \frac{1}{\gamma P_0} \qquad (4.36)$$

where

L_D = Dispersion length

β_2 = GVD parameter

T_0 = Initial pulse width

L_{NL} = Nonlinear length

P_0 = Power of data pulses

γ = Nonlinearity coefficient

for a normal optical fiber $L_D = 20 W^{-1} km^{-1}, |\beta_2| = 20 ps^2 / km$

We have considered the region where nonlinearity predominates.

For nonlinearity to predominate the requirement is

$L << L_D$ and $L \geq L_{NL}$.

We have taken the data used in experiment of proposed scheme to evaluate the value of L_D and L_{NL}.

If we take $T_0 = 20\, ps$ and $P_0 = 4\, mw$

then

$$L_D = \frac{20^2}{20} = 20km, L_{NL} = \frac{1}{20x4x10^{-3}} = 12.5km \text{ and } \frac{L_D}{L_{NL}} > 1 \qquad (4.37)$$

Hence the calculated length as given by equation 8.8 km satisfies the condition for nonlinearity to predominate. Hence the length of fiber modulator has to satisfy the following condition

$$\frac{L_D}{L_{NL}} = \frac{\gamma P_0 T_0^2}{|\beta_2|} >> 1$$

$$\Rightarrow P_0 >> \frac{|\beta_2|}{\gamma P_0 T_0^2} \qquad (4.38)$$

For a system to work for clock recovery, the length of fiber modulator should satisfy

4.3.2 Input Data Power

The input power of data pulses depends on the input data pulse width to operate in nonlinear region. The power of the data pulses required to mode lock the laser is the minimum power required to induce π phase shift in all modes present in laser cavity. Though the laser modes will be having different phase, but the minimum power will be able to increase the phases of modes to same value π.
The phase shift in a simple fiber due to cross phase modulation is given by is given by following equation

$$\phi_s(t) = \frac{\omega_s z n_2}{c} \frac{P_p}{A_{eff}}; \qquad (4.39)$$

where $\Delta\phi_s(t)$ = Phase shift introduced in lasing signal at λ_s

ω_s = Angular frequency of signal

z = length of fiber

n_2 = Kerr – coefficient

A_{eff} = Effective Area of core

E_s = electric field of lasing signal

E_p = electric field of data pulses

$|E_s|^2$ = Signal power

$|E_p|^2$ = Data i.e pump power

We assume that data signal has more power than the lasing signal and data pulse is strong enough to induce cross phase modulation but vice versa is not true.
Now taking

$$L = 7.2km; A_{eff} = 50\mu m^2; \lambda_s = 1.56\mu m$$

$$\Rightarrow P_p = 84.6mw$$

Hence power required to give a phase change is dependent on length of fiber, wavelength of the lasing pulses and effective area of fiber.

Where $x_n \in (0,1)$

T – Time slot width of the multiplexed stream

t_p – Half width at 1/e point of the data pulse

$$t_p = \frac{T_p}{2\sqrt{\ln 2}} \tag{4.43}$$

T_p = Width of the pulse

$$\phi_s(t) = 2M\int_0^L P_p(t)dl$$

$$= 2MP_pL\sum_{-\infty}^{\infty} x_n \exp\left\{-\left(\frac{t-nT}{t_s}\right)^2\right\} \tag{4.44}$$

$$\phi_s(t)_{\max} = 2MP_pL \tag{4.45}$$

We observe that the maximum amount of phase induced is given by equation (4.45) . As we have already derived in Appendix that the pulses of rectangular for sequences 111.., 1010.., will have fundamental frequency, hence the NOM can be modeled as phase modulator. The excess phase shift introduced by the phase modulator will be given by

$t_m(t) = \exp\left[-j\delta_\phi \cos\omega_m t\right]$

where $\delta_\phi = 2MP_pL$ (4.46)

$$\phi_s(t) = 2MP_pL\sum_{0}^{N} x_n \exp\left\{-\left(\frac{t-nT}{t_s}\right)^2\right\}$$

$$= 2MP_pL\left[x_0 \exp\left\{-\left(\frac{t}{t_s}\right)^2\right\} + x_1 \exp\left\{-\left(\frac{t-T}{t_s}\right)^2\right\} + ... + x_N \exp\left\{-\left(\frac{t-NT}{t_s}\right)^2\right\}\right]$$

We consider $t = NT$

$$\phi_s(NT) = 2MP_pL\left[x_0 \exp\left\{-\left(\frac{NT}{t_s}\right)^2\right\} + x_1 \exp\left\{-\left(\frac{(N-1)T}{t_s}\right)^2\right\} + ... + x_N \exp\{0\}\right] \tag{4.47}$$

Since T/T_p is very large

for example $T = 100ps$ for B = 1GHz $t_p = 20ps$, $T/T_p = 50$

Now we know that $\exp\{-5\} \cong 0$, hence all terms containing $\left(T/T_p\right)^2$ in exponential term goes to zero.

$\Rightarrow \phi_s(NT) = 2MP_pLx_N$

$If x_0, x_1, ..., x_N = 1$ each i.e. continuous modulation

$t = 0 \Rightarrow \phi_s(0) = 2MP_pLx_0$

$t = T \Rightarrow \phi_s(T) = 2MP_pLx_1$

$t = NT \Rightarrow \phi_s(NT) = 2MP_pLx_N$

Hence total phase through single pass $\phi_s(NT) = 2MP_pL\sum_0^N x_n$ (4.48)

4.4.2 Derivation of expressions of active harmonically mode locked pulse

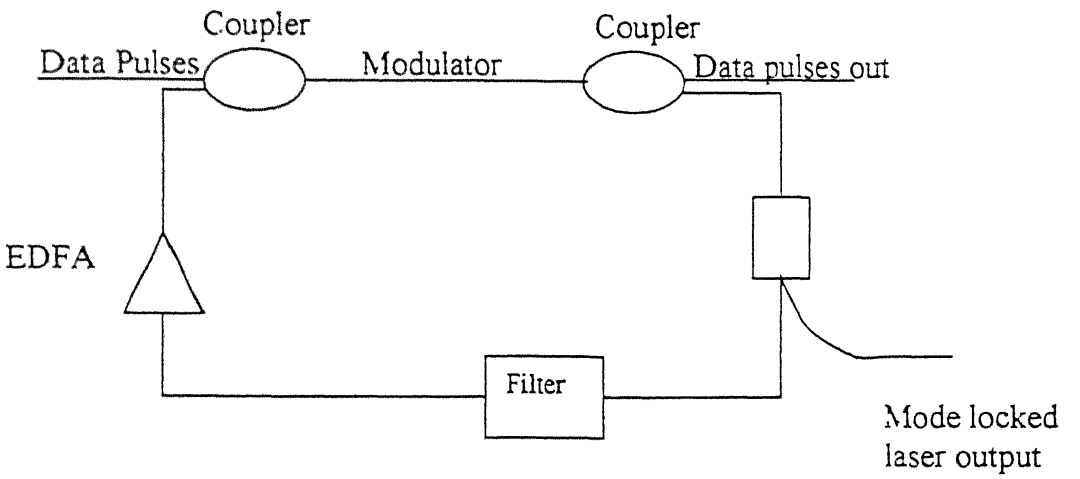

Fig 4.9 Basic clock recovery circuit under consideration

We have assumed an electric field entering the EDFA to be a Gaussian pulse given by

$$e_1(t) = A\exp\left[-2\ln 2\left(\frac{t}{t_p}\right)^2\right]e^{j\omega_s t} = Ae^{-at^2}e^{j\omega_s t} \quad (4.49)$$

where $\omega_s = \frac{2\pi c}{\lambda_s}$, (4.50)

$a = \frac{2\ln 2}{t_p{}^2}$

a determines the envelope of pulse .

The excess phase shift introduced by the modulation can be expressed as

$t_m(t) = \exp\left[-j\delta_\phi \cos\omega_m(t)\right]$

where δ_ϕ = Maximum phase excursion or single peak pass phase retardation

$\delta_\phi = 2MP_pL\sum x_n$

ω_m = Modulation frequency

Expanding into Taylor series

$$t_m(t) = \exp\left[-j\delta_\phi\left\{1-\frac{\omega_m{}^2t^2}{2}+\ldots\right\}\right] = \exp\left[-j\left\{\delta_\phi-\frac{\delta_\phi\omega_m{}^2t^2}{2}+\ldots\right\}\right]$$

Hence modulator introduces a time varying phase and thus pulse may have chirp, hence taking into account of a chirp parameter

$$e_1(t) = Ae^{-at^2}\exp\left[j\left\{\omega_s+\frac{\Delta\omega t}{T}\right\}t\right] \qquad (4.51)$$

where $b = \frac{\Delta\omega}{T}$ chirp parameter

Hence frequency at any time

$$\omega(t) = \left\{\omega_s+\frac{\Delta\omega t}{T}\right\}t = \omega_s + bt$$

Intensity $I_1(t) = |A_1|^2\exp\left\{-2(a-jb)t^2\right\}$ (4.52)

Taking fourier transform of

$$E_1(\omega) = A\exp\left[\left(\frac{\pi}{a-jb}\right)^{1/2}\exp\left\{-\frac{(\omega-\omega_s)^2}{4(a-jb)}\right\}\right] \qquad (4.53)$$

The bandwidth or spectral width Δf_s is defined as the frequency between half power points of the pulse spectrum

$$\Delta f_s = \frac{1}{\pi}\sqrt{2\ln 2\left[\frac{a^2+b^2}{a}\right]} \qquad (4.54)$$

$$t_s = \sqrt{\frac{2\ln 2}{a}}$$

$$\Rightarrow \Delta f_s t_s = \frac{2\ln 2}{\pi}\sqrt{1+\frac{b^2}{a^2}} \qquad (4.55)$$

Transfer function of EDFA

We have taken into account of the long wave guide structure for an EDFA . If $\Delta\omega$ is the spontaneous emission bandwidth then the saturated lineshape is of Lorentzian nature. Complex gain coefficient of EDFA is given by

$$g_E(\omega) = \exp\left\{\frac{g_0}{1 + j\left(\frac{\omega - \omega_E}{\Delta\omega/2}\right)}\right\} \tag{4.56}$$

where g_0 is the saturated amplitude gain through EDFA at line center (ω_E) for its length through the fiber,

L_E=Active medium length =Length of EDFA

$\Delta\omega$=FWHM of the gain coefficient

The single pass transfer function through EDFA is given by (derived in Appendix E)

$$T_g(\omega) = \exp\left[-jkl + g_0\left(1 - j\left(\frac{\omega - \omega_s}{\Delta\omega/2}\right) - \left(\frac{\omega - \omega_s}{\Delta\omega/2}\right)^2\right)\right] \tag{4.57}$$

where l is the length of fiber.

We know that the group velocity of a wave is related by equation

$$\frac{\partial\beta}{\partial g} \triangleq \frac{1}{v_g} = \frac{1}{c'} + \frac{g_0}{l}\frac{1}{\Delta\omega/2}$$

$$\tau_{RT} = \frac{l}{v_g} = \frac{l}{c'} + \frac{g_0}{\Delta\omega/2}$$

i.e. in $t_m(t) = \exp\left[-j\delta_\phi \cos\omega_m(t)\right]$

$$\omega_m t = m\pi \Rightarrow \omega_m \tau_{RT} = m\pi$$

$$\Rightarrow 2\pi f_m \tau_{RT} = m\pi \Rightarrow f_m = \frac{m}{2\tau_{RT}} = \frac{m}{2}\frac{1}{\frac{l}{c'} + \frac{g_0}{\Delta\omega/2}} \tag{4.58}$$

Hence we observe that modulation frequency have to be chosen correctly to allow passage of pulse when transmission coefficient is at maximum.

we know that $\Delta\nu_c = \frac{c}{l}$[cavity intermode spacing]

$$f_m = \frac{m}{2}\left[\frac{1}{\frac{1}{\Delta\nu_c} + \frac{g_0}{\pi\Delta\nu}}\right] = \frac{m\Delta\nu_c}{2\left(1+\frac{g_0\Delta\nu_c}{\pi\Delta\nu}\right)} \qquad (4.59)$$

Hence modulation frequency should be a multiple of cavity intermode spacing.

Fourier transform of pulse coming out of EDFA

The laser pulse circulating inside the cavity passes through EDFA. The fourier transform of the pulse coming out of EDFA is given by

$$E_2(\omega) = T_g(\omega)E_1(\omega) = A\exp\left[\left(\frac{\pi}{a-jb}\right)^{1/2}\exp\left\{-\frac{(\omega-\omega_s)^2}{4(a-jb)}\right\}\right]$$

$$*\exp\left[-jkl + g_0\left(1 - j\left(\frac{\omega-\omega_s}{\Delta\omega/2}\right) - \left(\frac{\omega-\omega_s}{\Delta\omega/2}\right)^2\right)\right] \qquad (4.60)$$

$$= AG\sqrt{\frac{\pi}{\gamma}}\exp\left[-(\omega-\omega_s)^2\left\{\frac{1}{4\gamma}+\frac{4g_0}{\Delta\omega^2}\right\}\right] * \exp\left[-j\frac{2g_0}{\Delta\omega}(\omega-\omega_s) - jkl\right]$$

$$= AG\sqrt{\frac{\pi}{\gamma}}\exp\left[-P(\omega-\omega_s)^2\right] * \exp\left[-jQ(\omega-\omega_s) - jkl\right] \qquad (4.61)$$

$$\left.\begin{aligned} &\text{where } \gamma = a - jb \\ &P = \left\{\frac{1}{4\gamma}+\frac{4g_0}{\Delta\omega^2}\right\} \\ &Q = \frac{2g_0}{\Delta\omega} \end{aligned}\right\} \qquad (4.62)$$

Thee total round trip linear phase delay of passive cavity are k.l. The imaginary term in equation correspond to group delay of the pulse for a round trip.

$$k = \frac{\omega}{c'} = \frac{\omega_0}{c'} + \frac{\omega-\omega_0}{c'}$$

$$kl + g_0\left(\frac{\omega-\omega_0}{\Delta\omega/2}\right) = \frac{\omega_0}{c'}l + \left(\frac{\omega-\omega_0}{c'}\right)l \div g_0\left(\frac{\omega-\omega_0}{\Delta\omega/2}\right) \hat{=} \left[\beta_0 + \frac{\partial\beta}{\partial\omega}(\omega-\omega_0)\right]l$$

{By Taylor series expansion of phase delay}

Transforming equation into time domain

$$e_2(t) = \frac{AG}{4\sqrt{\gamma P}} e^{-\left[\frac{(t-Q)^2}{4P}\right]} e^{(j\omega_s t)} \qquad (4.63)$$

Effect of Non Linear Fiber Modulator (NOM)

The transmission function of NOM is given by

$$t_m(t) = \exp[-j\phi_s(t)]$$

$$= \exp[-j\delta_\phi \cos\omega_m(t)] m t_m(t) = \exp\left[-j\delta_\phi + \frac{\delta_\phi \omega_m{}^2 t^2}{2}\right] \qquad (4.64)$$

δ_φ describes the modulation index . We have assumed that the fundamental harmonic of data pulses is equal to modulation frequency. The required expression of the pulse width of clock will be obtained by substituting modulation frequency by bit rate.

We note that there can exist two possible solutions for FM case , one for each extreme of the phase variation.

The peak of the pulse goes through t=0, hence pulse coming out of the modulator is

$$E_3(t) = E_2(t)\exp[-j\delta_\phi \omega_m{}^2 (t-B)^2] \qquad (4.65)$$

Finally pulse after one round trip is given by

$$E_3(t - \frac{L_F}{c}) \qquad (4.66)$$

To obtain a self-consistent solution ,the envelope of the pulse must go through the modulation at the same modulation phase every time . Hence total round trip time for pulse is T_m where $T_m = 2\pi/\omega_m$ for phase modulator

Self consistency requirement

$$E_1(t - T_m)e^{-j\phi} = E_3(t - \frac{L_F}{c}) \qquad (4.67)$$

By solving self-consistency condition ,we have derived the expression of spectral width Δf_s and pulse width τ_s of mode locked laser (derived in Appendix F).

$$\tau_s = \sqrt{\frac{2\ln 2}{a}} = \sqrt{2\ln 2}.\frac{1}{\pi}\left(\frac{g_0}{MP_pL\sum x_n}\right)^{1/4}\left(\frac{1}{f_m \Delta f}\right)^{1/2}$$

$$\Delta f_s = \frac{1}{\pi}\sqrt{2\ln 2\left[\frac{a^2+b^2}{a}\right]} = \sqrt{2\ln 2}.\left(\frac{MP_pL\sum x_n}{g_0}\right)^{1/4}(f_m \Delta f)^{1/2}$$

By replacing the modulation frequency with bit rate we obtain modified expressions of pulse width and spectral width

$$\left.\begin{aligned}\tau_S &= \sqrt{\frac{2\ln 2}{a}} = \sqrt{2\ln 2}.\frac{1}{\pi}\left(\frac{g_0}{MP_pL\sum x_n}\right)^{1/4}\left(\frac{1}{B\Delta f}\right)^{1/2}\\ \Delta f_s &= \frac{1}{\pi}\sqrt{2\ln 2\left[\frac{a^2+b^2}{a}\right]} = \sqrt{2\ln 2}.\left(\frac{MP_pL\sum x_n}{g_0}\right)^{1/4}(B\Delta f)^{1/2}\end{aligned}\right\} \quad (4.68)$$

The plot of pulse width showing dependence on input data power is shown in fig 4.10.

4.5 EFFECT OF FILTER

Though, tunable filter in range of (1.5-1.57 μm) is used to tune to the lasing wavelength as proposed in experiment by BT Laboratories. We have suggested inclusion of two more filters to improve the performance of the clock recovery scheme. When the modulation frequency of input data pulses is equal to harmonic multiple of cavity mode spacing, a number of supermodes are generated. Because of large number of supermode present in cavity, unwanted noise is generated. The requirement is to select only one supermode. By using a narrowband repetition rate Fabry Perot filter and Broadband Fabry Perot etalon in laser cavity unwanted supermodes can be suppressed and hence the stability of harmonic mode locking can be ensured. The mode spacing of this filter should be equal to an integral multiple of the fundamental cavity mode spacing. We have analyzed the effect of inclusion of these filters on the performance of clock recovery circuits in terms of improved regenerative properties of extracted clock.

4.5.1 Mathematical Analysis of Broadband Fabry Perot etalon

The electric field transfer function of a Fabry Perot etalon and its gaussian approximation is given by

$$T_{BB}(\omega) = \frac{T_{BB}\exp\left(jl_{BB}\frac{\omega}{c}\right)}{1-R_{BB}\exp\left(2jl_{BB}\frac{\omega}{c}\right)}$$

$$\cong \left|\frac{T_{BB}\exp\left(jl_{BB}\frac{\omega}{c}\right)}{1-R_{BB}\exp\left(2jl_{BB}\frac{\omega}{c}\right)}\right|\exp\left(\frac{2jR_{BB}}{1-R_{BB}}\frac{l_{BB}\omega}{c}\right) \quad (4.69)$$

$$g_{BB}(\omega) = \exp\left[-2\ln 2\left(\frac{\omega-\omega_0}{4\omega_{BB}}\right)^2\right]\exp\left[2j\sqrt{2\ln 2}\frac{\omega-\omega_0}{\Delta\omega_{BB}}\right]$$

$$\Delta\omega_{BB} = \sqrt{2\ln 2}\frac{c}{l_{BB}}\frac{1-R_{BB}}{\sqrt{R_{BB}}} \quad (4.70)$$

R_{BB} = Mirror Reflectivity

ω_0 = Optical frequency

l_{BB} = Fabry Perot length

$\Delta\omega_{BB}$ = FWHM of a pass band

4.5.2 Narrowband Fabry Perot filter

The narrow band Fabry Perot (NBFP) is used to select one supermode. The strongest lasing mode is centered at a transmission peak of the NBFP by an electronic feedback circuit. If NBFP length is chosen to be cavity length divided by an integer N then the spacing between lasing mode equals the free spectral range of the NBFP(ω_{NB}). Each mode also centers under a transmission peak and the NBFP has no effect on the pulse spectrum In other words ω_{NB} equals an integral fundamental cavity frequency. $\omega_{NB} = N\omega_s$

The cavity frequency ω_s is determined by cavity length, which cannot be adjusted for many fiber lasers. If the laser cavity lengthy is fixed such that

$\omega_{NB} = N\omega_s$, conditional spectral filtering equivalent to an effective broadband Fabry Perot occurs. The results are pulse-bandwidth narrowing and pulse-width broadening

4.5.3 Effect of Offset

We have observed that the tuning of length of NOM is very critical to match the modulation frequency or bit rate to cavity mode spacing . We have tried to derive expressions to analyze the effect of offset in Fabry Perot and the cavity modes.Fig 4.11 shows the mismatch between narrow band Fabry Perot and the cavity Modes.Mode index is denoted by H

Electric field transfer function of NBFP

$$T_{BB}(\omega) = \frac{T_{BB}\exp\left(jl_{BB}\frac{\omega}{c}\right)}{1 - R_{BB}\exp\left(2jl_{BB}\frac{\omega}{c}\right)} \qquad (4.71)$$

The spectrum of the laser consists of discrete modes with frequency $\omega_{NB} = \omega_0 + H\omega_m$ where ω_m is the modulation frequency. $\omega_m = N\omega_s$, and $H = 0,\pm1,\pm2,..$ is the mode index denoting the supermodes.

Hence transmission coefficient for consecutive selected modes in the presence of cavity length mismatch is

$$T_{NB}(\omega) = \frac{T_{NB}\exp\left(jl_{BB}\frac{\omega}{c}\right)}{1 - R_{NB}\exp\left(2jl_{BB}\frac{\omega}{c}\right)} \text{ where } \delta\omega = \omega_{NB} - \omega_m$$

$$H = \frac{\omega - \omega_0}{\omega_m}$$

$$l_{NB}H\frac{\delta_\omega}{c} = \frac{l_{NB}\omega - \omega_0}{\omega_m}\frac{\delta_\omega}{c} = \frac{l_{BB1}\omega - \omega_0}{c}$$

$$l_{BB1} = \frac{l_{NB}\delta_\omega}{\omega_m} \Rightarrow x = \frac{\delta_\omega}{\omega_s}$$

$$l_{BB1} = \frac{l_{NB}\delta_\omega}{\omega_s}\frac{\omega_s}{\omega_m} = \frac{l_{NB}x}{N}, \text{ where } N = \frac{\omega_s}{\omega_m}$$

$$T_{BB1}(\omega) = \frac{T_{BB1}\exp\left(\frac{jl_{BB1}(\omega - \omega_0)}{c}\right)}{1 - R_{BB1}\exp\left(\frac{2jl_{BB1}(\omega - \omega_0)}{c}\right)} \qquad (4.72)$$

$$T_{BB1} = T_{NB}$$

$$R_{BB1} = R_{NB}$$

Hence equation for narrowband filter can be expressed as effective broadband Fabry Perot.

If there is no offset i.e. x=0 ,then $l_{BB1} = \frac{l_{NB}x}{N} = 0, T_{BB1} = 0$

NBFP transmission peaks coincide with one supermode . The presence of an offset gives rise to an effective broadband Fabry-Perot . Now T_{BB1} can be expressed in terms of Gaussian approximation

$$g_{BB1}(\omega) = \exp\left[-2\ln 2\left(\frac{\omega - \omega_0}{\Delta\omega_{BB}}\right)^2\right]\exp\left[2j\sqrt{2R_{BB1}\ln 2}\frac{\omega - \omega_0}{\Delta\omega_{BB1}}\right] \qquad (4.73)$$

$$\Delta\omega_{BB1} = \Delta\omega_{BB1}(1 + N/x)$$

We take an example to show the effect of filter

We have assumed following data

N=43000

fundamental laser cavity frequency =23.1 kHz

BBFP bandwidth=125 GHz

Worst case cavity length offset value x=0.5

$$\Delta\omega_{BB1} = 62.5x10^4(1 + 43000/0.5) = 53.8\,GHz$$

Hence pulse BW is limited to 49.41 GHz by using the expression

$$\text{where } \left(\frac{1}{\omega_e}\right)^2 = \left(\frac{1}{\Delta\omega_{BB}}\right)^2 + \left(\frac{1}{\Delta\omega_{BB1}}\right)^2$$

Hence cavity length mismatch limits the BW of the pulse.

The transfer function of the filter acquires a gaussian pulse shape and also a gaussian spectrum.

4.5.4 Effect of filter on output pulse parameters

We have derived expressions to show the effect of filter on spectral bandwidth and pulse width of extracted clock. The spectral width and pulse width of the pulse is limited by bandwidth of filter.

$$\frac{1}{4\gamma'} = P = \left\{\frac{1}{4\gamma} + \frac{4g_0}{\Delta\omega^2}\right\}$$

$$\frac{1}{\gamma'} - \frac{1}{\gamma} = \frac{16g_0}{\Delta\omega^2}$$

$$\gamma' - \gamma \approx \frac{16g_0\gamma^2}{\Delta\omega^2} \qquad (4.74)$$

We have assumed a gaussian pulse parameter γ of the pulse circulating inside cavity which changes on each successive round trip .The net change in the gaussian pulse parameter in each round trip as derived is given below:
From equation .Fourier transform of pulse coming out of EDFA has got modified gaussian parameter as
Because the gain function g is almost equal to unity and pulse spectral width is small compared to atomic linewidth $\Delta\omega$, the functional change in gaussian parameter on one pass will be small Net change in gaussian pulse parameter on passing through phase modulator

$$\gamma' - \gamma = \pm j\delta_\phi \omega_m^2$$

Total change $\gamma'' - \gamma$ in gaussian pulse parameter in one complete round trip the laser cavity
is given by

$$\left.\begin{aligned}\gamma' - \gamma &\approx \frac{-16g_0\gamma^2}{\Delta\omega^2} + \left\{\begin{matrix}1\\ \pm j\end{matrix}\right\}\delta_\phi \omega_m^2 \\ &= 0 \quad \text{for steady state}\end{aligned}\right\} \qquad (4.75)$$

1 –for amplitude modulator
$\pm j$ -for phase modulator

Because of filter present in cavity the term $\frac{g_0}{\Delta f^2}$ changes to $\left(\frac{g_0}{\Delta f^2}+\frac{1}{\Delta f_e^{\,2}}\right)$ the expressions of spectral width and pulse width in equation (4.68) change to expressions given below

$$\tau_S = \sqrt{\frac{2\ln 2}{a}} = \sqrt{2\ln 2}\,\frac{1}{\pi}\left(\frac{g_0}{MP_pL\sum x_n}\right)^{1/4}\left(\frac{g_0}{\Delta f^2}+\frac{1}{\Delta f_e^{\,2}}\right)^{1/2}$$

where ΔfEquivalent BW of filter

If $\frac{1}{\Delta f_e^{\,2}} > \frac{g_0}{\Delta f^2}$

$$\tau_S = \sqrt{\frac{2\ln 2}{a}} = \sqrt{2\ln 2}\,\frac{1}{\pi}\left(\frac{g_0}{MP_pL\sum x_n}\right)^{1/4}\left(\frac{1}{\Delta f_e^{\,2}}\right)^{1/2} \qquad (4.76)$$

$$\Delta f_s = \frac{1}{\pi}\sqrt{2\ln 2\left[\frac{a^2-b}{a}\right]}$$

$$= \sqrt{2\ln 2}\left(MP_pL\sum x_n\right)^{1/4}\left(f_m\Delta f_e\right)^{1/2}$$

We have seen that the pulse width and the spectral width of the mode locked pulses depend upon the combined action of modulator and filter. Though the above expression gives the variation of pulse width the steady state, there is requirement to know the pulse width before the steady state to correctly visualize the evolution of mode locked pulses We have tried to derive expression for variation of pulse width of mode locked pulses.

4.6 Variation of pulse width with number of round trips

Though variation of pulse width can be simulated on computer, we have tried to obtain analytical expression by assuming that after few trips the circulating signal in the cavity has reached steady state.

If we consider the steady state of laser cavity, steady state round trip solution is

$$\Delta\gamma = \gamma'' - \gamma \approx \frac{-16g_0\gamma^2}{\Delta\omega^2}\left(\gamma^2-\gamma_{ss}^{\,2}\right)$$

given by

Assuming fractional change in γ in one round to be small

$$\frac{d\gamma}{dt} \approx \frac{\Delta\gamma}{T} \approx \frac{(\gamma^2-\gamma_{ss}^{\,2})}{\gamma_{ss}T_{ss}}$$

T-cavity round time $\Rightarrow T_{ss} = \dfrac{\Delta\omega T}{16g_0\gamma_{ss}}$ (4.77)

We have assumed that laser starts off on its first round trip.
at t = 0 $\gamma(0) \approx 0$

$$\int_0^{\gamma} \frac{\gamma_{ss}\, d\gamma}{\gamma_{ss}^2 - \gamma^2} \approx \frac{1}{\gamma_{ss}} \int_0^t dt$$

$$\Rightarrow \gamma(t) = \gamma_{ss} \tanh\left(t / T_{ss}\right) \qquad (4.78)$$

The equation is valid for both AMor FMor harmonically mode locked solution.From equation

$$T_{ss} = \frac{\Delta\omega T}{16 g_0 \gamma_{ss}} = \frac{T_k}{a_{ss} + j b_{ss}} \Rightarrow \frac{t}{T_{ss}} = \frac{(a_{ss} + j b_{ss})t}{T_k}$$

We know that

$$\tanh z = \frac{\sinh 2x + j \sin 2y}{\cosh 2x + \cos 2y}$$

where $z = x + jy = \frac{t}{T_k} a_{ss} + j \frac{t}{T_k} b_{ss}$

$$\gamma(t) = (a_{ss} + j b_{ss}) \left[\frac{\sinh 2\frac{t}{T_k} a_{ss} + j \sin 2\frac{t}{T_k} b_{ss} y}{\cosh 2\frac{t}{T_k} a_{ss} + \cos 2\frac{t}{T_k} b_{ss}} \right]$$

For steady state

$$a_{ss} = b_{ss}$$

$$\frac{1}{T_{ss}} = \frac{a_{ss}(1 + j)}{T_k}$$

Taking real part $T_{ss} = \frac{T_k}{a_{ss}} \Rightarrow \tau_{ss} = \sqrt{\frac{2\ln 2}{a_{ss}}} \Rightarrow \tau_{ss}^2 = \frac{2\ln 2}{a_{ss}}$

$$T_{ss} = \frac{T_k}{2\ln 2\, \tau_{ss}} = \frac{\Delta\omega T}{2\ln 2\, \tau_{ss}} \Rightarrow \frac{T_{ss}}{T} = \frac{\Delta\omega}{2\ln 2\, \tau_{ss}^2}$$

$$\Rightarrow N_{ss} = \frac{T_{ss}}{T} = \frac{\Delta\omega}{2\ln 2\, \tau_{ss}^2}$$

$$\tau_{ss}^2 = \frac{\Delta\omega}{2\ln 2 N_{ss}}; \tau_{ss} - \text{static pulse width}$$

for N th round trip

$$a(NT) = \frac{a_{ss} \sinh \frac{2NT}{T_k} a_{ss} - b_{ss} \sin \frac{2NT}{T_k} b_{ss}}{\cosh \frac{2NT}{T_k} a_{ss} + \cos \frac{2NT}{T_k} b_{ss}}$$

since $a_{ss} = b_{ss}$

$$a(NT) = \frac{a_{ss}\left[\sinh\frac{2N16g_0}{\Delta\omega} - \sin\frac{2N16g_0}{\Delta\omega}\right]}{\cosh\frac{32N16g_0}{\Delta\omega}a_{ss} \div \cos\frac{32N16g_0}{\Delta\omega}a_{ss}} \qquad (4.79)$$

Similarily b(NT) can be calculated which will give γ(NT) which will calculate pulsewidth at N th roun trip till $N < N_{ss}$.

The above equation can be simulated on computer.

REFERENCES

4.1 E.J.Greer and K. Smith , "All optical FM mode –locking of fibre laser," Electron Lett.,28 (180,pp. 1741-1743, August 1992.

4.2 Nelson, B.P. Smith and Blow K.J, " Mode locked erbium fiber laser using all optical nonlinear loop modulator ", Elec. Lett., 28, pp. 656-657, 1992.

4.3 M. F. Becker, Kuizenga D.J and Seigman A.E, " Harmonic mode locking of the Nd:Yag laser", IEEE J. Quantum Electronics, Vol. QE-No. 8, August 1972.

4.4 Agarwal G. P, " Nonlinear fiber optics ", chapter 7., Academic Press Inc., 1989.

4.5 Joseph T. Verdeyn, " Laser Electronics", Prentice –Hall of India Private Limited, New Delhi, 1993.

4.6 Kuizenga D.J and Seigman A.E, " FM and AM mode locking of the homogeneous laser Part I: theory ", IEEE J. Quantum Electronics , QE-6, pp.674-708, 1970.

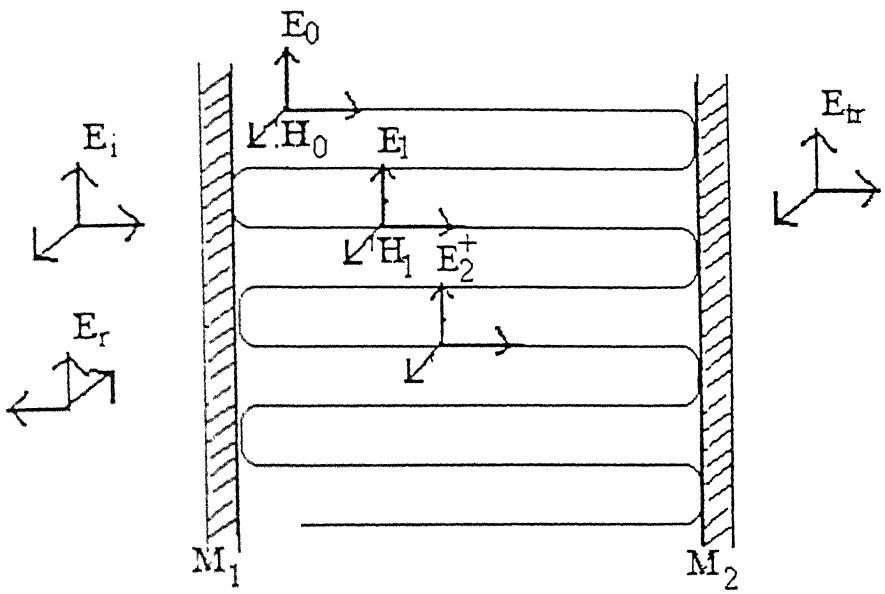

Fig 4.1 Optical cavity

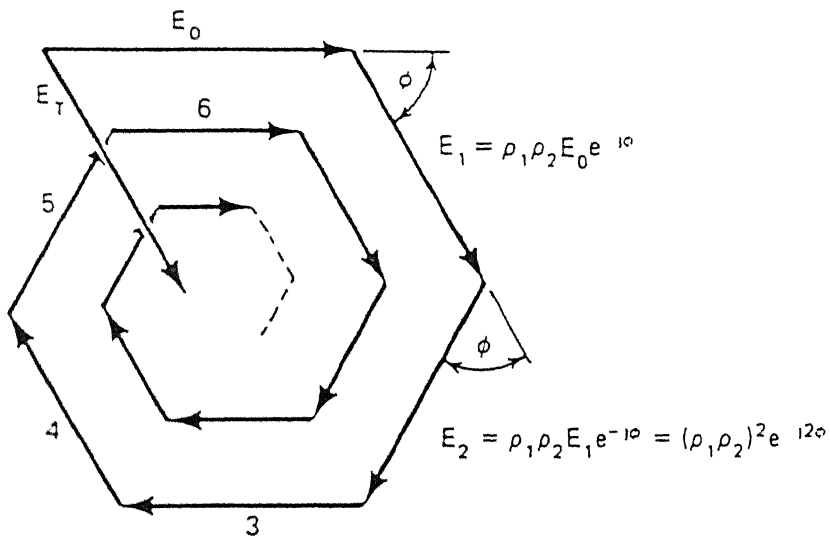

Fig 4.2 Phasor diagram

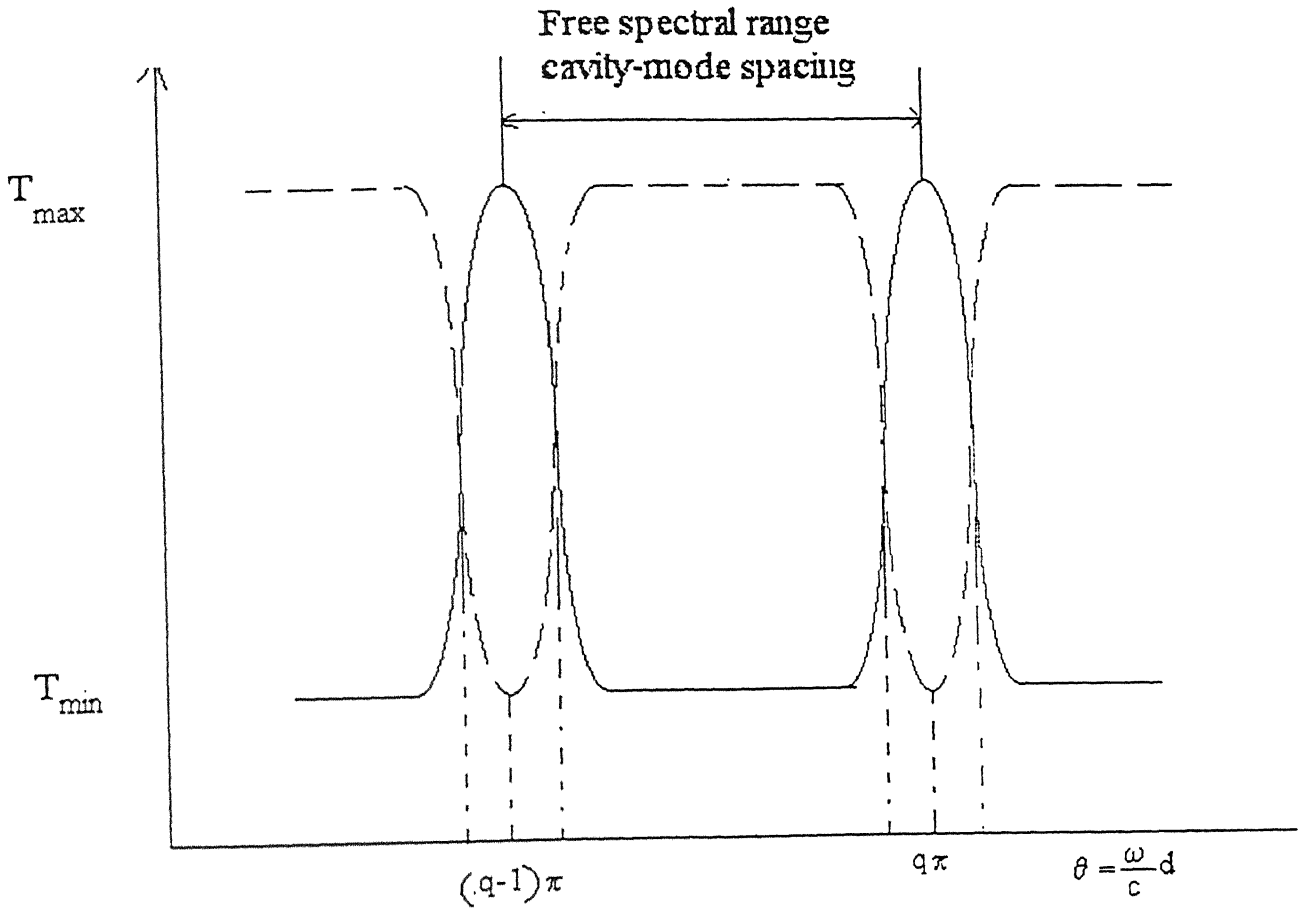

Fig 4.3 Transmission or bandpass characteristics of a Fabry-Perot cavity

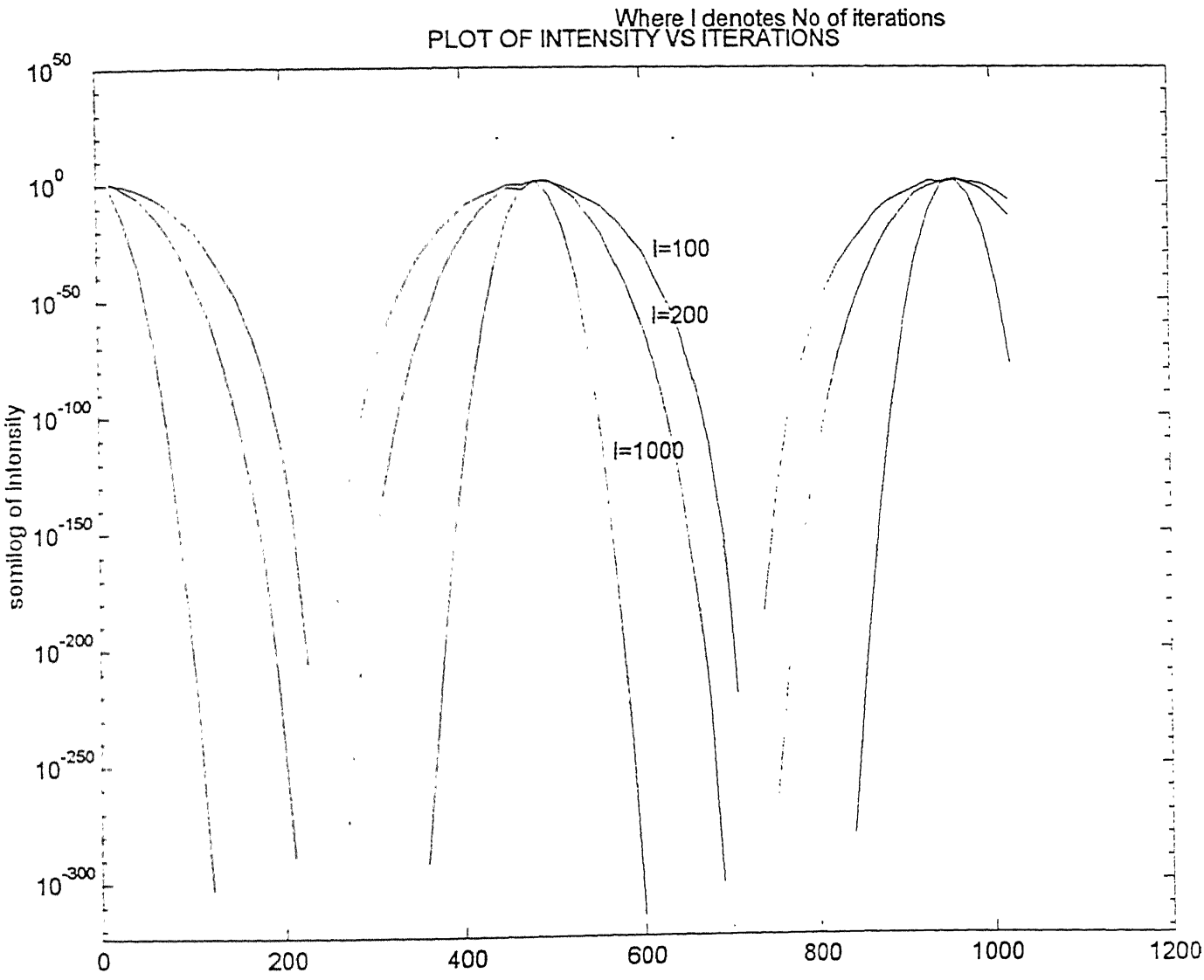

Fig 4.5 Plot of Intensity of mode locked pulses Vs Iteration

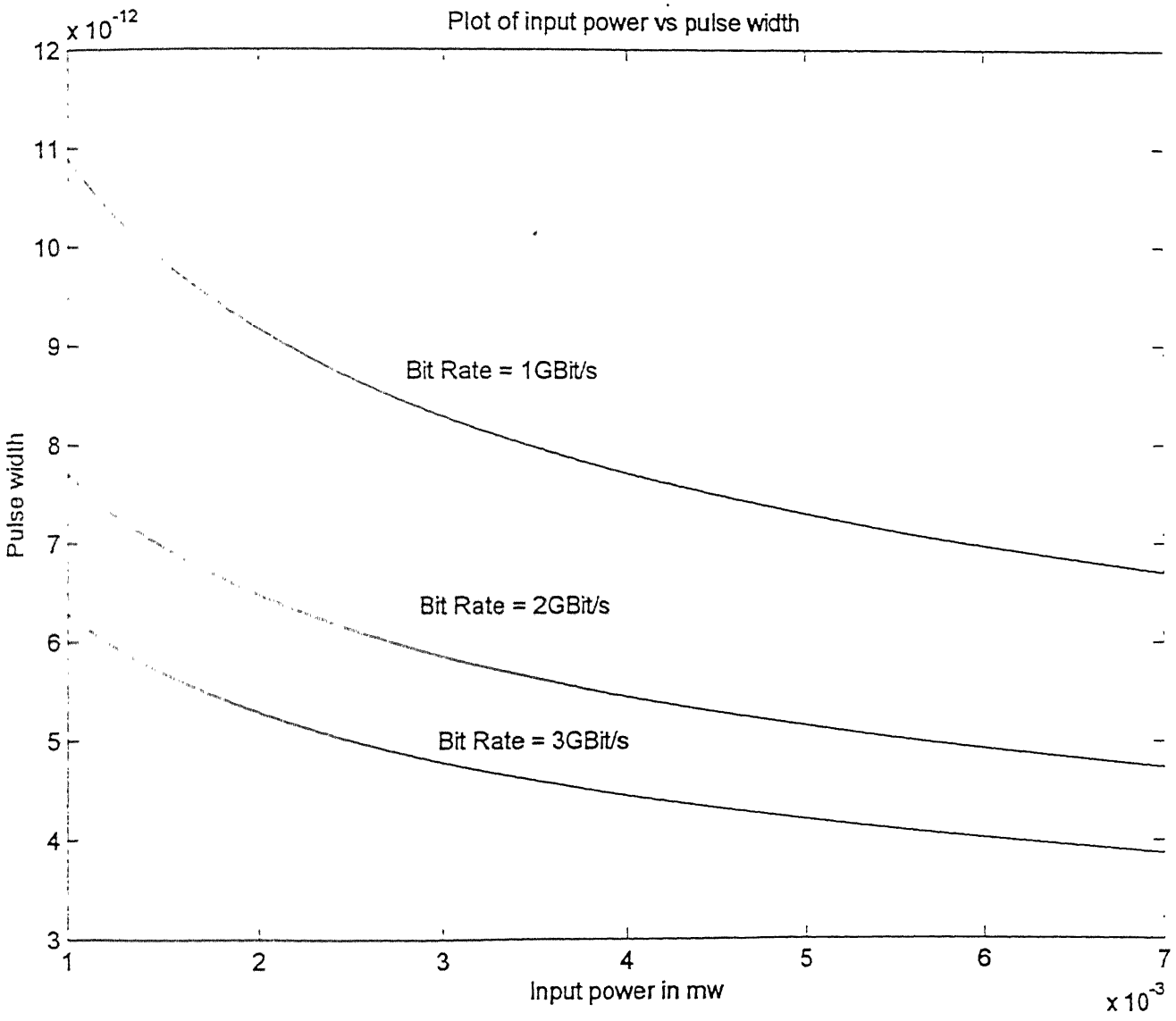

Fig 4.10 Plot of Input power Vs pulse width

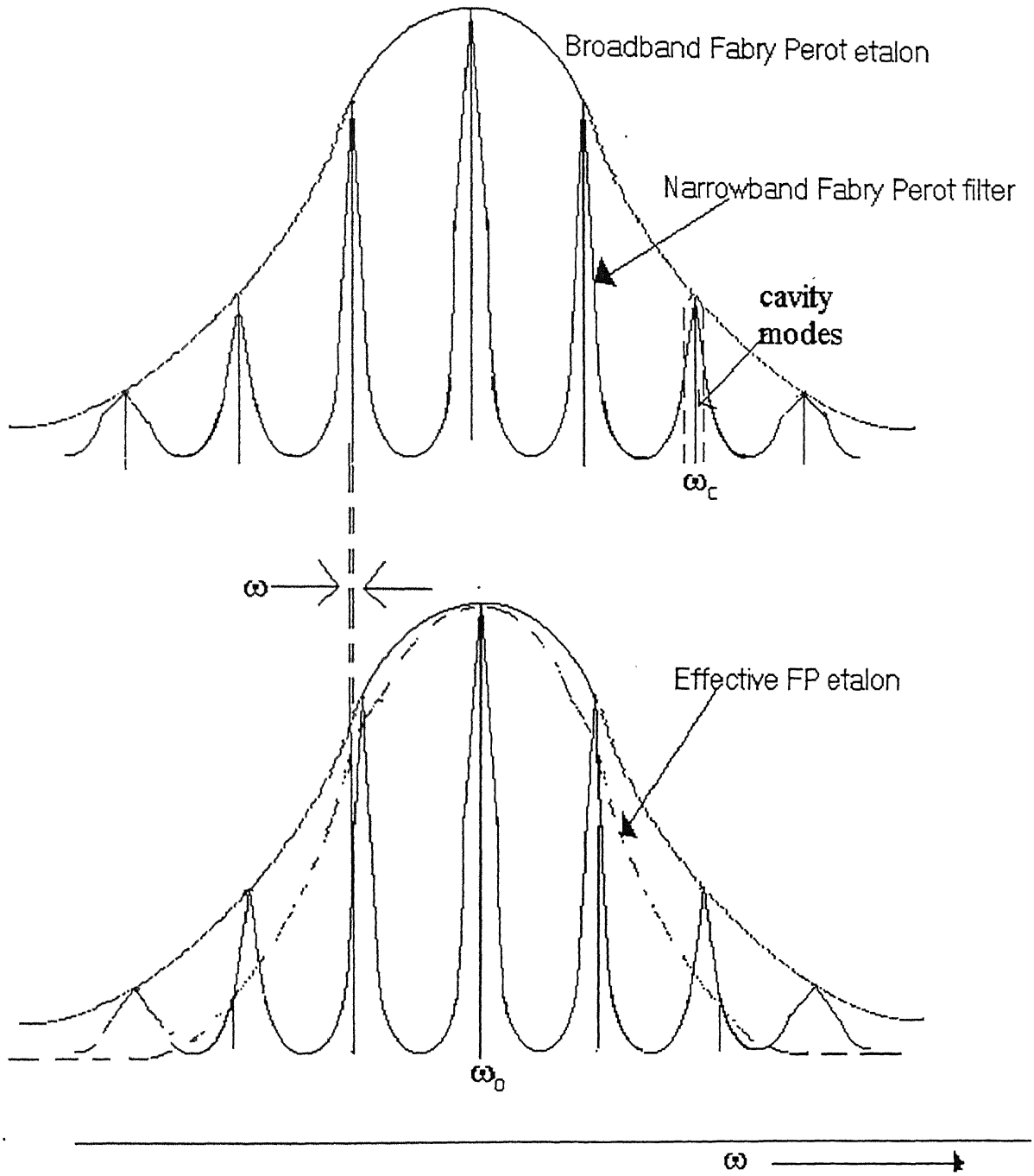

Fig 4.11Effect of offset

CHAPTER 6

CONCLUSION

In this thesis, we have investigated into an all optical clock recovery scheme in which an optical data stream is used to mode lock a fiber laser and hence clock is recovered. We have investigated the phenomenon due to which clock is recovered in the proposed clock recovery scheme and derived equations to validate the experimental result. We have observed that the proposed scheme by British Telecom is a novel all optical clock recovery scheme in which fiber laser has been actively mode locked using Nonlinear Optical loop mirror (NOLM). NOLM extends the range of repetition rate limited by modulation bandwidth of available modulators.

Based on study carried out future scope for studies are enumerated below: -

1. Polarization sensitivity :- Requirement of input power for mode lock has been calculated. But mechanical, thermal and acoustic disturbances cause the polarization state of pulses propagating in fiber to fluctuate with time. The requirement of power taking polarization into account can be further calculated.

2. Optically programmable mode locked laser: - We have observed that there exists a simple relationship between the repetition rate and cavity frequency for mode locking. The laser output forms a replica of nay driving pattern and is thus optically programmed .The theory can be extended to evaluate the performance of mode locked laser.
3. Dispersion: - Though British Telecom group has used the dispersion shifted fiber, but there is a requirement to take dispersion in account.

APPENDIX A

Multiplexed optical data stream is given by

$$P_s(t) = P_s \sum_{-\infty}^{\infty} x_n \exp\left\{-\left(\frac{t-nT}{t_s}\right)^2\right\} \qquad (A.1)$$

where $x_n = \{0,1\}$

T = slot width of the data stream

t_s = rms width of gaussian pulse

P_s = signal pulse peak power

Since $\kappa_1 = 0.5$ SPM and linear terms are same in both clockwise and anticlockwise rotating signals. Only cross phase modualtion term appear in difference between phase changes.

$$\phi_s(t) = \frac{2\pi n_2}{\lambda A_{eff}} \frac{2}{3} \int_0^L P_s(t + \frac{t_w l}{L}) dl \qquad (A.2)$$

$$\phi_s(t) = M \frac{2}{3} \int_0^L P_s(t + \frac{t_w l}{L}) dl \qquad (A.3)$$

$M = \frac{2\pi n_2}{\lambda A_{eff}}$

$\phi_c(t)$ = phase change of the clockwise rotating siganal

$t_w = \frac{L}{V_s} - \frac{L}{V_c}$ = amount of birefering ence present in the fiber i.e. time difference between two signals to travel the fiber loop. Assumption here is that clock pulse moves faster than signal pulse.

L = length of fiber loop

V_s = velocity of signal pulse

V_c = velocity of clock pulse

If $t_w = 0$

$$\phi_c(t) = M \frac{2}{3} \int_0^L P_s(t) dl$$

$$= M \frac{2}{3} P_s(t) L$$

$$= 2MP_s L \sum_{-\infty}^{\infty} x_n \exp\left\{-\left(\frac{t-nT}{t_s}\right)^2\right\} \qquad (A.4)$$

So $$\phi_c(t)\max = M \frac{2}{3} P_s(t) L$$

if $t_w \neq 0$ then

$$\phi_c(t) = M\frac{2}{3}\int_0^L P_s \sum_{-\infty}^{\infty} x_n \exp\left\{-\left(\frac{t+\frac{t_w l}{L}-nT}{t_s}\right)^2\right\}$$

$$\phi_c(t) = M\frac{2}{3}P_s \sum_{-\infty}^{\infty} x_n \int_0^L \exp\left\{-\left(\frac{t+\frac{t_w l}{L}-nT}{t_s}\right)^2\right\}$$

$$= M\frac{2}{3}P_s L\frac{t_s}{t_w}\sum_{-\infty}^{\infty} x_n \left\{erf\left(\frac{t+t_w-nT}{t_s}\right) - erf\left(\frac{t-nT}{t_s}\right)\right\}\frac{\sqrt{\pi}}{2} \qquad (A.5)$$

So

$$\phi_c(t)\max = M\frac{2}{3}\sqrt{\pi}P_s L\frac{t_s}{t_w} \qquad (A.6)$$

If slot width T is much smaller than twice the loop transit time ($T << \frac{2Ln}{c}$) the signal induced non - linear phase shift of anticlockwise rotating pulse is constant and given by

$$\phi_c(t)\max = M\frac{2}{3}\sqrt{\pi}P_s L\left(\frac{t_s}{T}\right) \qquad (A.7)$$

Electric field and power equation for regenerated signal pulse are given as

$$E_{reg}(t) = E_c(t)(1-\gamma_1)^{\frac{3}{2}}(1-\gamma_2)\sqrt{\kappa_1}\left[(1-\kappa_1)e^{j\phi_c} - \kappa_1 e^{j\phi_a}\right]$$

$$= \frac{E_c(t)}{\sqrt{2}}e^{\frac{j(\phi_c+\phi_a)}{2}}\sin\left(\frac{\phi_c-\phi_a}{2}\right)e^{j\left(\frac{\pi}{2}-\delta\right)} \qquad (A.8)$$

$$P_{reg}(t) = \frac{E_c(t)}{2}\left\{1-\cos^2\left(\frac{\phi_c-\phi_a}{2}\right)\right\} \qquad (A.9)$$

APPENDIX B

Mathematical Analysis for Amplitude Modulator

Real part of electric field of n^{th} mode is given by

$$E_n(t) = A_n(t) \cos(w_n t + \phi_n(t)) \quad \text{(B.1)}$$

The transmission chracteristics of an amplitude modulator is given by

$$\Gamma(t) = \cos(\beta \operatorname{Sin} w_m t) \quad \text{(B.2)}$$

Using trigonometric series

$$\cos x = 1 - \frac{x^2}{2!} + \frac{x^4}{4!} - \frac{x^6}{6!} + \ldots\ldots$$

$$\Gamma(t) = 1 - \frac{\beta^2 \sin^2 \omega_m(t)}{2} + \ldots..$$

We have assumed $\beta < 1$

Neglecting higher order terms

$$\Gamma(t) = 1 - \frac{\beta^2 \sin^2 \omega_m(t)}{2}$$

$$\cong 1 - \frac{\beta^2 \sin^2 \omega_m(t)}{2}$$

$$\cong 1 - \frac{\beta^2}{2}\left(\frac{1}{2} - \frac{1}{2}\cos \omega_m t\right) \quad (B.3)$$

$$\cong 1 - \frac{\beta^2}{4} + \frac{\beta^2}{4}\cos 2\omega_m t$$

$$\cong a + b\cos 2\omega_m t$$

$$\cong a + b\cos N\omega_s t \quad (B.4)$$

where $\omega_m = \frac{N}{2}\omega_s, a = 1 - b, b = \frac{\beta^2}{4}$

We have assumed that is carefully chosen so that to be equal to integral multiple of the difference between any two longitudinal cavity modes.

The electric field $E_n(t)$ is modified by transfer function of modulator and modified electric field is given as

$$E_n(t) = A_n(t)\cos(\omega_n t + \phi_n(t))(a + b\,Cos\,N\,\omega_s\,t) \quad \text{(B.5)}$$

Similarly the electric field of n-N mode and $n+N^{th}$ mode will be modified and modified electric field is given as

$$\left.\begin{aligned} E_{n-N}\Gamma(t) &= A_{n-N}(t)\ \mathrm{Cos}\,(w_{n-N}t + \phi_{n-N}(t))\,(a + b\,\mathrm{Cos}\,N w_s t) \\ E_{n+N}\Gamma(t) &= A_{n+N}(t)\ \mathrm{Cos}\,(w_{n+N}t + \phi_{n-N}(t))\,(a + b\,\mathrm{Cos}\,N w_s t) \\ E_n\Gamma(t) &= a\,A_n(t)\ \mathrm{Cos}\,(w_n t + \phi_n(t)) + \\ &\quad b\,A_n(t)\ \mathrm{Cos}\,(w_n t + \phi_n(t))\ \mathrm{Cos}\,N w_s t \end{aligned}\right\} \quad (B.6)$$

The side bands generated at ω_n due to $n-N^{th}$ and $n+N^{th}$ modify field at n^{th} mode.

From equation (*E*.6)

$$E_n(t) = a\,A_n(t)\ \mathrm{Cos}\,(w_n t + \phi_n(t)) + b\,a\,A_n(t)\ \mathrm{Cos}\,(w_n t + \phi_n(t))\,\mathrm{Cos}\,N w_s t \quad (B.7)$$

Expanding the two terms in equation series

$$E_n(t) = aA_n(t)\cos(\omega_n t + \phi_n(t)) + \tfrac{b}{2}A_n(t)\left(\cos(\omega_n + N\omega_s)t + \phi_n(t)\right) + \tfrac{b}{2}A_n(t)\left(\cos(\omega_n - N\omega_s)t + \phi_n(t)\right)$$

Substituting $\omega_n - N\omega_s = \omega_{n-N}$ and $\omega_n + N\omega_s = \omega_{n+N}$

$$E_n(t) = aA_n(t)\cos(\omega_n t + \phi_n(t)) + \tfrac{b}{2}A_n(t)\left(\cos(\omega_{n-N})t + \phi_n(t)\right) + \tfrac{b}{2}A_n(t)\left(\cos(\omega_{n+N})t + \phi_n(t)\right) \quad (B.8)$$

Similarily

$$E_{n-N}\Gamma(t) = aA_{n-N}(t)\cos(\omega_{n-n}t + \phi_{n-N}(t)) + \tfrac{b}{2}A_{n-n}(t)\cos(\omega_n t + \phi_{n-N}(t)) + \tfrac{b}{2}A_{n-N}(t)\cos(\omega_{n-2N}t + \phi_{n-N}(t)) \quad (B.9)$$

$$E_{n+N}\Gamma(t) = aA_{n+N}(t)\cos(\omega_{n+N}t + \phi_{n+N}(t)) + \tfrac{b}{2}A_{n+N}\cos(\omega_n t + \phi_{n+N}(t))) + \tfrac{b}{2}A_{n+N}\cos(\omega_{n+2N}t + \phi_{n+N}(t)) \quad (B.10)$$

Hence we observe that all the modes generate side-bands when modulated with modulation frequency $\omega_m = N\omega_s$. The n^{th} mode generates $n+N^{th}$ and $n-N^{th}$ modes as side bands. Similarly $n+N^{th}$ mode generates as n^{th} and $n+2N^{th}$ mode as side bands. The $n-N^{th}$ mode generates n and $n-2N^{th}$ mode side bands. Hence electric field of n^{th} mode is modified. The resultant electric field of n^{th} mode is given by field due to n^{th} mode and side bands generated due to $n-N^{th}$ mode and $n+N^{th}$ mode. We also observe that any other mode does not generate side band at mode, hence n^{th} mode is mode locked to $n-N^{th}$ mode and $n+N^{th}$ mode.

The resultant field of n^{th} mode is given by

$$E_n'(t) = aA_n(t)\cos(\omega_n t + \phi_n(t)) + \tfrac{b}{2}A_{n+N}(t)\cos(\omega_n t + \phi_{n+N}(t)) + \tfrac{b}{2}A_{n-N}(t)\cos(\omega_n t + \phi_{n-N}(t)) \quad (B.11)$$

Expanding equation (B.11)

$$E_n'(t) = aA_n(t)\left(\cos(\omega_n t)\cos\phi_n(t) - \sin(\omega_n t)\sin\phi_n(t)\right)$$
$$+ \tfrac{b}{2} A_{n+N}(t)\left(\cos(\omega_n t)\cos\phi_{n+N}(t) - \sin(\omega_n t)\sin\phi_{n+N}(t)\right)$$
$$+ \tfrac{b}{2} A_{n+N}(t)\left(\cos(\omega_n t)\cos\phi_{n-N}(t) - \sin(\omega_n t)\sin\phi_{n-N}(t)\right)$$
$$= \cos(\omega_n t)\left(aA_n(t)\cos\{\phi_n(t)\} + \frac{b}{2}A_{n+N}(t)\cos\{\phi_{n+N}(t)\} + \frac{b}{2}A_{n-N}(t)\cos\{\phi_{n-N}(t)\}\right)$$
$$- \sin(\omega_n t)\left(aA_n(t)\sin\{\phi_n(t)\} + \frac{b}{2}A_{n+N}(t)\sin\{\phi_{n+N}(t)\} + \frac{b}{2}A_{n-N}(t)\sin\{\phi_{n-N}(t)\}\right)$$

Taking

$$\left(aA_n(t)\cos\{\phi_n(t)\} + \frac{b}{2}A_{n+N}(t)\cos\{\phi_{n+N}(t)\} + \frac{b}{2}A_{n-N}(t)\cos\{\phi_{n-N}(t)\}\right) = A_n'(t)\cos\phi_n'(t)$$

$$\left(aA_n(t)\sin\{\phi_n(t)\} + \frac{b}{2}A_{n+N}(t)\sin\{\phi_{n+N}(t)\} + \frac{b}{2}A_{n-N}(t)\sin\{\phi_{n-N}(t)\}\right) = A_n'(t)\sin\phi_n'(t)$$

Hence the field of the n^{th} mode can be written as

$$E_n'(t) = A_n'(t)\cos(\omega_n t - \phi_n'(t)) \qquad (B.12)$$

$$A_n'(t) = \left[a^2 A_n^2(t) + \frac{b^2}{4}\left\{A_{n+N}^2(t) + A_{n-N}^2(t)\right\} + \frac{b^2}{4}A_n^2(t)A_n^2(t)\cos\{\phi_n(t) - \phi_{n+N}(t)\}\right.$$
$$\left. - abA_n(t)A_{n+N}(t)\cos\{\phi_n(t) - \phi_{n+N}(t)\} + abA_n(t)A_{n-N}(t)\cos\{\phi_n(t) - \phi_{n-N}(t)\}\right] \qquad (B.13)$$

and $$\phi_n' = \tan^{-1}\left[\frac{aA_n(t)\sin\{\phi_n(t)\} + \frac{b}{2}A_{n+N}(t)\sin\{\phi_{n+N}(t)\} + \frac{b}{2}A_{n-N}(t)\sin\{\phi_{n-N}(t)\}}{aA_n(t)\cos\{\phi_n(t)\} + \frac{b}{2}A_{n+N}(t)\cos\{\phi_{n+N}(t)\} + \frac{b}{2}A_{n-N}(t)\cos\{\phi_{n-N}(t)\}}\right] \qquad (B.14)$$

APPENDIX C

We have again investigated the effect of modulation on n^{th}, $n-N^{th}$ and $n+N^{th}$ modes for a phase modulator

The electric field of n^{th} mode is given by

$$E_n(t) = A_n'(t)\exp\left\{j(\omega_n t+\varphi_n'(t))\right\} \qquad (C.1)$$

The transmission chracteristics of the phase modulator.

$$\Gamma(t) = \exp\left\{j\delta_\phi \sin(\omega_m t)\right\}$$

After one pass through modulator, the electric field is given by

$$E_n(t)\Gamma(t) = A_n'(t)\exp\left\{j(\omega_n t+\varphi_n'(t))\right\}\exp\left\{j\delta_\varphi \sin(\omega_m t)\right\} \qquad (C.2)$$

We know that

$$\exp\left\{j\delta_\varphi \sin(\omega_m t)\right\} = \sum_{p=-\infty}^{\infty} J_p(\delta_\phi)e^{jp\omega_m t} \text{ where } J_p(\delta_\phi) \text{ is Bessel function of } 0^{\text{th}} \text{ order}$$

$$E_n'(t) = \sum_{p=-\infty}^{\infty} J_p(\delta_\phi)A_n(t)\exp\left\{j\left((\omega_n + p\omega_m)t-\varphi_n'(t)\right)\right\} \qquad (C.3)$$

We have assumed that $\beta < 1$ which is also valid assumption in our scheme of clock recovery circuit

$$J_{-n}(\beta) = J_n(\beta)$$

for $\beta < 1$

$$\left.\begin{aligned} J_0(\beta) &= 1 \\ J_1(\beta) &= \frac{\beta}{2} \\ J_n(\beta) &= 0 \qquad n >> 1 \end{aligned}\right\} \qquad (C.4)$$

$$E_n'(t) = A_n'(t)\exp\left\{j(\omega_n t+\varphi_n'(t))\right\} + \frac{A_n'(t)\delta_\phi}{2}\exp\left\{j(\omega_n+\omega_m)t+\varphi_n'(t))\right\} +$$

$$\frac{A_n'(t)\delta_\phi}{2}\exp\left\{j(\omega_n-\omega_m)t+\varphi_n'(t))\right\} \qquad (C.5)$$

Taking fourier transform

$$E_n'(t) = A_n'(t)\delta(\omega) + \frac{A_n'(t)\delta_\phi}{2}\delta(\omega-\omega_n-\omega_m)\frac{A_n'(t)\delta_\phi}{2}\delta(\omega-\omega_n+\omega_m) \quad (C.6)$$

Taking real part

$$E_n'(t) = A_n'(t)\cos\left\{j(\omega_n t+\varphi_n'(t))\right\}+\frac{A_n'(t)\delta_\varphi}{4}\cos\left\{j(\omega_n+\omega_m)t+\varphi_n'(t))\right\}+$$

$$\frac{A_n'(t)\delta_\phi}{4}\cos\left\{j(\omega_n-\omega_m)t+\varphi_n'(t))\right\}$$

If $\omega_m = N\omega_s i.e. B = N\omega_s$, then similar to the analysis of amplitude modulator, we get the field of the nth mode after modulation

$$\mathrm{E_n}'(t) = A_n'(t)\cos(\omega_n t-\phi_n'(t)) \quad (C.7)$$

where

$$A_n'(t) = \left[\begin{array}{l} A_n^2(t)+\frac{\delta_\phi^2}{16}\left\{A_{n+N}^2(t)+A_{n-N}^2(t)\right\}-\frac{\delta_\phi^2}{16}A_n^2(t)A_n^2(t)\cos\left\{\phi_n(t)-\phi_{n+N}(t)\right\}+ \\ \frac{\delta_\phi^2}{8}A_n(t)A_{n+N}(t)\cos\left\{\phi_n(t)-\phi_{n+N}(t)\right\}+\frac{\delta_\phi^2}{8}A_n(t)A_{n-N}(t)\cos\left\{\phi_n(t)-\phi_{n-N}(t)\right\} \end{array}\right] \quad (C.8)$$

$$and\ \phi_n' = \tan^{-1}\left[\frac{A_n(t)\sin\left\{\phi_n(t)\right\}+\frac{\delta_\phi}{8}A_{n+N}(t)\sin\left\{\phi_{n+N}(t)\right\}+\frac{\delta_\phi}{8}A_{n-N}(t)\sin\left\{\phi_{n-N}(t)\right\}}{A_n(t)\cos\left\{\phi_n(t)\right\}+\frac{\delta_\phi}{8}A_{n+N}(t)\cos\left\{\phi_{n+N}(t)\right\}+\frac{\delta_\phi}{8}A_{n-N}(t)\cos\left\{\phi_{n-N}(t)\right\}}\right] \quad (C.9)$$

APPENDIX D

We have considered periodic train of pulses

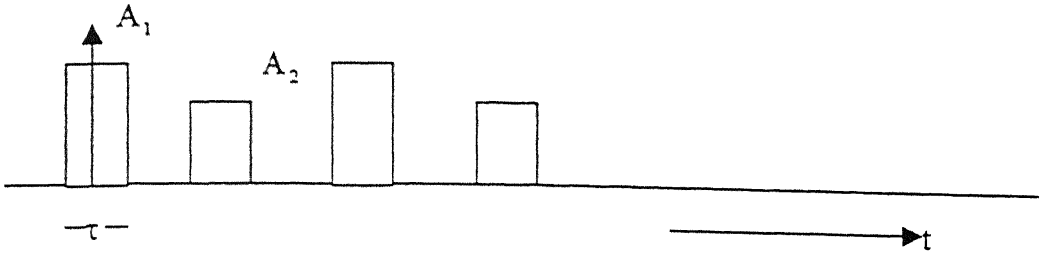

This can be represented as

$$g_p(t) = \begin{cases} A_1 & -\tau/2 \le t \le \tau/2 \\ 0 & -\tau/2 \le t \le (T-\tau)/2 \\ A_2 & (T-\tau)/2 \le t \le (T+\tau)/2 \\ 0 & elsewhere \end{cases} \qquad (D.1)$$

The periodic train of pulses consists of two pulses with a repetition frequency of 1/T.

The periodic pulse train can be represented as fourier series . The coefficients of fourier series can be given as

$$c_n = \frac{1}{T}\int_{-\frac{\tau}{2}}^{\frac{T+\tau}{2}} g_p(t)\exp\left(\frac{-j2\pi nt}{T}\right)dt$$

$$= \frac{1}{T}\left[\left\{\int_{-\frac{\tau}{2}}^{\frac{\tau}{2}} A_1 \exp\left(\frac{-j2\pi nt}{T}\right) + \int_{\frac{T-\tau}{2}}^{\frac{T+\tau}{2}} A_2 \exp\left(\frac{-j2\pi nt}{T}\right)\right\}dt\right]$$

$$= \frac{A_1}{T_0}\left[\frac{\exp\left(\frac{-j2\pi nt}{T}\right)}{\left(\frac{-j2\pi nt}{T}\right)}\right]_{-\frac{\tau}{2}}^{\frac{\tau}{2}} + \frac{A_2}{T_0}\left[\frac{\exp\left(\frac{-j2\pi nt}{T}\right)}{\left(\frac{-j2\pi nt}{T}\right)}\right]_{\frac{T-\tau}{2}}^{\frac{T+\tau}{2}}$$

$$C_n = \frac{A_1}{n\pi}\sin\left\{\frac{n\pi}{T}\right\} + \frac{A_2}{n\pi}\sin\left\{\frac{(T+\tau)n\pi}{T}\right\}$$

$$= \frac{A_1}{n\pi}\sin\left\{\frac{n\pi}{T}\right\} - \frac{A_2}{n\pi}\sin\left\{n\pi + \frac{n\pi\tau}{T}\right\}$$

$$= \frac{A_1}{n\pi}\sin\left\{\frac{n\pi}{T}\right\} - \frac{A_2}{n\pi}\left\{\sin n\pi\cos\frac{n\pi\tau}{T} + \sin\frac{n\pi\tau}{T}\cos n\pi\right\}$$

$$= \frac{A_1}{n\pi}\sin\left\{\frac{n\pi}{T}\right\} - \frac{A_2}{n\pi}\left\{\sin\frac{n\pi\tau}{T}\right\}\cos n\pi \qquad (D.2)$$

Now $\omega_n = \frac{2n\pi}{T}\cdot\frac{n\pi}{T} = \frac{\omega_n\tau}{2}$

$$\Rightarrow = A_1\tau\frac{\sin\left(\frac{\omega_n\tau}{2}\right)}{\left(\frac{\omega_n\tau}{2}\right)} + A_1\tau\frac{\sin\left(\frac{\omega_n\tau}{2}\right)}{\left(\frac{\omega_n\tau}{2}\right)}\cos n\pi \qquad (D.3)$$

Hence fourier series of $g_p(t)$ can be written as

$$g_p(t) = \sum_{n=-\infty}^{\infty}\left[A_1\tau\sin c\left(\frac{\omega_n\tau}{2}\right) + A_2\tau\sin c\left(\frac{\omega_n\tau}{2}\right)\cos n\pi\right]\exp(j\omega_n t) \qquad (D.4)$$

$$\omega_n = \frac{2\pi n}{T}; n = 0,1,2...$$

Hence the amplitude spectrum of the series is given by the fourier coefficient

$C_n = (A_1 + A_2)\tau$ n = 0 (D.5)

$= \frac{A_1 - A_2}{\pi}\sin\frac{n\tau}{T}$ n = 1,3,5,... (D.6)

The frequency spectrum of the periodic train of pulses is shown below.

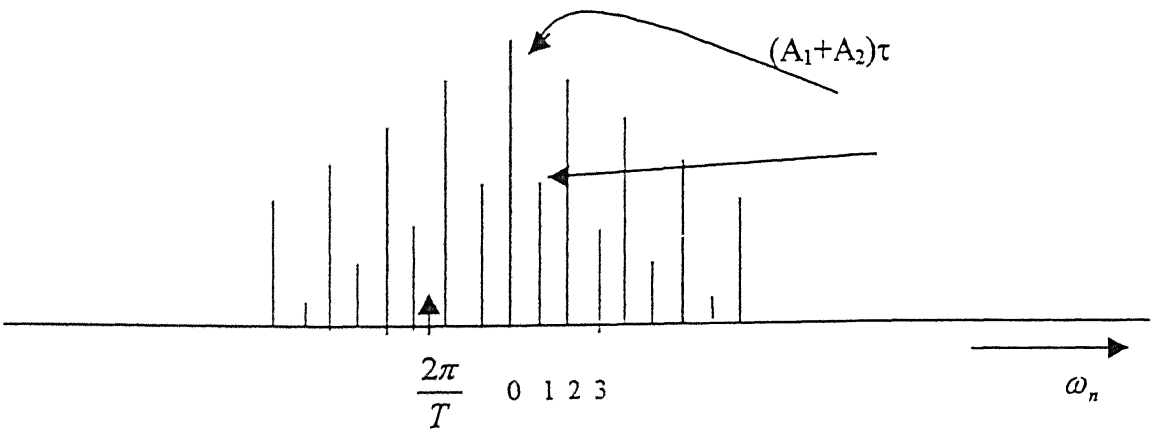

APPENDIX E

The gain coefficient of the EDFA is given by

$$g_E(\omega) = \left\{ \frac{g_0}{1 + j\left(\frac{\omega - \omega_E}{\nabla\omega_{.2}}\right)} \right\} \qquad \text{(E.1)}$$

On expanding

$$g_E(\omega) = G \exp\left[- jg_0\left(\frac{\omega - \omega_E}{\nabla\omega_{.2}}\right) - jg_0\left(\frac{\omega - \omega_E}{\nabla\omega_{.2}}\right)^2 \right]$$

$$\equiv \exp\left[g_0\left\{ 1 - j\left(\frac{\omega - \omega_E}{\nabla\omega_{.2}}\right) - j\left(\frac{\omega - \omega_E}{\nabla\omega_{.2}}\right)^2 \right\} \right]$$

Now $\left(\frac{\omega - \omega_E}{\nabla\omega}\right) << 1$

hence saturated line shape has become Gaussian shape and Gaussian pulse going through EDFA wil remain Gaussian. If pulse is on line centre i.e. $\omega_E = \omega_S$

$$g_E(\omega) \equiv \exp\left[g_0\left\{ 1 - j\left(\frac{\omega - \omega_E}{\nabla\omega_{.2}}\right) + j\left(\frac{\omega - \omega_E}{\nabla\omega_{.2}}\right)^2 \right\} \right] \qquad \text{(E.2)}$$

APPENDIX F

Self consistency requiement for mode locked pulses circulating in laser cavity is given by

$$E_1(t-T_m)e^{-j\phi} = E_3(t-\frac{L_F}{c}) \tag{F.1}$$

where ϕ is an additional phase factor

Substituting $E_1(t)$ and $E_3(t)$ from Equation (5.44) and (5.59)

$$\exp\left[-\gamma(t-T_m)^2\right]\exp\left[-j\omega_s(t-T_m)\right]e^{-j\phi}$$

$$= \frac{AG}{4\sqrt{\gamma P}}\exp\left[-\frac{(t-Q-\frac{L_F}{c})^2}{4P}\right]\exp\left[-j\delta_\phi\omega_m{}^2(t-Q-\frac{L_F}{c})^2\right]\exp\left[-j\omega_s(t-\frac{L_F}{c})\right]$$

$$= \frac{AG}{4\sqrt{\gamma P}}\exp\left[-\left(\frac{1}{4P}+\delta_\phi\omega_m{}^2\right)(t-Q-\frac{L_F}{c})^2\right]\exp\left[-j\omega_s(t-\frac{L_F}{c})\right]$$

Equating coefficient we get

$$T_m = Q - \frac{L_F}{c} \tag{F.2}$$

$$\gamma = \left(\frac{1}{4P} \pm j\delta_\phi\omega_m{}^2\right)$$

$$e^{-j\phi} = \frac{AG}{4\sqrt{\gamma P}}\exp\left[-j\omega_s(T_m-\frac{L_F}{c})\right] = \frac{AG}{4\sqrt{\gamma P}}\exp[-j\omega_s Q] \tag{F.3}$$

From equation (5.55)

$$P = \frac{1}{4\gamma} - \frac{4g_0}{\Delta\omega^2}$$

$$\Rightarrow \gamma = \frac{-j\delta_\phi\omega_m{}^2}{2} \pm \frac{1}{2}\sqrt{\left(\delta_\phi\omega_m{}^2\right)^2 \pm j\frac{\delta_\phi\omega_m{}^2\Delta\omega^2}{4g_0}} \tag{F.4}$$

The real part of γ must always be positive hence we retain positive sign

We have considered the term

$$\frac{\Delta\omega^2}{4g_0\delta_\phi\omega_m{}^2}$$

$$\frac{\Delta\omega^2}{4g_0\delta_\phi\omega_m{}^2} >> 1 \text{ since } \omega_m << \omega$$

$$\gamma = \frac{-j\delta_\phi\omega_m{}^2}{2} \pm \frac{1}{2}\delta_\phi\omega_m{}^2\left[\sqrt{1\pm\frac{\Delta\omega^2}{4g_0\delta_\phi\omega_m{}^2}}\right]; \text{neglecting 1 in square root}$$

$$\gamma = \frac{-j\delta_\phi \omega_m{}^2}{2} \pm j\frac{1}{2}\delta_\phi \omega_m{}^2 \frac{\Delta\omega}{2\sqrt{g_0 \delta_\phi \omega_m{}^2}}$$

$$= (1 \pm j)\frac{\omega_m \Delta\omega}{4}\sqrt{\frac{\delta_\phi}{2g_0}} = (a - jb) \qquad \text{(F.5)}$$

$$\Rightarrow b = \pm a = \frac{\omega_m \Delta\omega}{4}\sqrt{\frac{\delta_\phi}{2g_0}} = \pi^2 f_m \Delta\nu \sqrt{\frac{\delta_\phi}{2g_0}} \qquad \text{(F.6)}$$

From equation (5.55) the phase shift of the modulator is given by

$$\delta_\phi = 2MP_p L \sum x_n \qquad \text{(F.7)}$$

$$b = \pi^2 f_m \Delta\nu \sqrt{\frac{2MP_p L \sum x_n}{2g_0}} \qquad \text{(F.8)}$$

We know that from equation and

$$\tau_S = \sqrt{\frac{2\ln 2}{a}} = \sqrt{2\ln 2}\,\frac{1}{\pi}\left(\frac{g_0}{MP_p L \sum x_n}\right)^{1/4}\left(\frac{1}{f_m \Delta f}\right)^{1/2} \qquad \text{(F.9)}$$

$$\Delta f_s = \frac{1}{\pi}\sqrt{2\ln 2\left[\frac{a^2 + b^2}{a}\right]}$$

$$= \sqrt{2\ln 2}\left(\frac{MP_p L \sum x_n}{g_0}\right)^{1/4}(f_m \Delta f)^{1/2} \qquad \text{(F.10)}$$